UNIVERSITÀ DEGLI STUDI DI TRIESTE

XXXVI CICLO DEL DOTTORATO DI RICERCA IN
SCIENZE DELLA RIPRODUZIONE E DELLO SVILUPPO

A Novel Role for ACE2-TMEM16 Complexes in SARS-CoV-2 Infection

Settore scientifico-disciplinare: MED/07

DOTTORANDA
MARTINA VIDMAR

COORDINATORE
PROF. **PAOLO GASPARINI**

SUPERVISORE DI TESI
PROF. **MANOLA COMAR**

CO-SUPERVISORE DI TESI
PROF. **MAURO GIACCA**

ANNO ACCADEMICO 2022/2023

RIASSUNTO

COVID-19, acronimo di "Coronavirus Disease 2019," è una malattia causata dall'infezione del virus della sindrome respiratoria acuta grave 2 (SARS-CoV-2).
La severità dei sintomi può variare ampiamente di persona in persona e può portare a complicazioni come trombosi polmonari, sindrome da distress respiratorio acuto (ARDS), acuta ed eccessiva risposta infiammatoria (nota come tempesta citochinica) e un rapido peggioramento della funzione polmonare, con conseguente edema alveolare.
Ricerche precedenti hanno stabilito che il virus SARS-CoV-2 entra nelle cellule attraverso l'interazione tra la sua proteina spike (SPIKE) e l'enzima di conversione dell'angiotensina 2 (ACE2). Le cellule infette mostrano livelli ridotti di ACE2 sulla loro membrana cellulare poiché SPIKE provoca l'internalizzazione e degradazione di ACE2 nei lisosomi. Inoltre, le cellule infettate espongono SPIKE sulla loro superficie, diventando in grado di fondersi con le cellule vicine e formare cellule polinucleate chiamate sincizi. Questi sincizi agevolano la rapida diffusione del virus e consentono l'incorporazione di linfociti, contribuendo all'evasione delle cellule infettate dall'azione del sistema immunitario. È importante notare che è stata individuata una specifica sequenza amminoacidica di SPIKE, contenente un motivo a due arginine in R682 e R685 all'interno del sito di taglio polibasico S1/S2, come responsabile dell'abilità fusogena della proteina.
Uno studio condotto dal team del Professor Mauro Giacca ha evidenziato il potenziale uso della niclosamide come terapia nel COVID-19. L'abilità di questo farmaco, già in commercio come antielmintico orale, di bloccare la formazione di sincizi è attribuita alla sua capacità di inibire membri della famiglia delle TMEM16, in particolare TMEM16F, nota per la sua attività di scramblasi. Tuttavia, i dettagli dei processi molecolari alla base della formazione dei sincizi rimangono ancora largamente sconosciuti.

In questo studio, abbiamo esplorato le possibili interazioni tra ACE2 e TMEM16A e TMEM16F (TMEM16s), così come le interazioni tra TMEM16s e SPIKE, sfruttando tecniche come la proximity ligation assay (PLA), co-immunoprecipitazione (coIP) e il trasferimento energetico per risonanza di fluorescenza (FRET). Durante queste indagini, abbiamo notato che TMEM16A e, in misura minore, TMEM16F, erano associate a livelli ridotti di espressione di ACE2.

Trattamenti con Bafilomicina (un inibitore del flusso autofagico) hanno confermato che la degradazione di ACE2 causata dalle TMEM16s avviene nei lisosomi, come accade con SPIKE. Inoltre, abbiamo scoperto che sia il knockdown delle TMEM16s che il trattamento con niclosamide impediscono la degradazione di ACE2 indotta da SPIKE.

Questi risultati suggeriscono l'esistenza di un possibile complesso proteico che coinvolge ACE2, SPIKE e le due TMEM16, il quale gioca un ruolo cruciale nella degradazione di ACE2 e nel processo di formazione dei sincizi. È importante notare che la formazione di sincizi è una caratteristica condivisa da vari virus, e che ACE2 funge da recettore anche per altri coronavirus. Comprendere le intricate vie molecolari che governano queste interazioni è di grande rilevanza, non solo dal punto di vista fisiologico, data l'importanza centrale di ACE2 nel sistema renina-angiotensina-aldosterone (RAAS), ma anche nell'ottica di possibili infezioni virali future che utilizzano lo stesso recettore. Questo approfondimento apre nuove prospettive per l'individuazione di potenziali bersagli terapeutici che potrebbero contribuire a prevenire i sintomi gravi associati a tali patologie.

ABSTRACT

COVID-19, short for Coronavirus Disease 2019, is a disease caused by infection with the severe acute respiratory syndrome virus 2 (SARS-CoV-2). The severity of symptoms can vary, with potential complications including lung thrombosis, acute respiratory distress syndrome (ARDS), abnormal activation of the inflammatory response (cytokine storm), and rapid deterioration of lung function characterized by alveolar edema.

Prior research has established that SARS-CoV-2 enters the cells through the interaction between its spike protein (SPIKE) and the angiotensin-converting enzyme 2 (ACE2) receptor. These infected cells exhibit reduced levels of ACE2 on their cell membranes due to the internalization and lysosomal degradation driven by SPIKE. Furthermore, these cells display SPIKE on their surfaces, allowing them to fuse with neighboring cells, resulting in the formation of polynucleated cells known as syncytia. These syncytia facilitate the rapid spread of the virus and enable the incorporation of lymphocytes, thereby contributing to viral immune evasion. A specific amino acid sequence, containing a bi-arginine motif at R682 and R685 within the polybasic S1/S2 cleavage site, was identified as responsible for the fusogenic ability of SPIKE.

A study conducted by Professor Mauro Giacca's team has shed light on the potential therapeutic use of niclosamide in COVID-19. Niclosamide's ability to block the formation of syncytia is attributed to its inhibition of the TMEM16 family, in particular TMEM16F, known for its scramblase activity. However, the precise molecular processes leading to syncytia formation remain largely unknown.

Here, we have explored potential interactions between ACE2 and TMEM16A and TMEM16F (TMEM16s), as well as interactions between TMEM16s and SPIKE, using proximity ligation assays (PLA), co-immunoprecipitation (coIP), and fluorescence resonance energy transfer (FRET) techniques. During our investigation of these interactions, we observed that TMEM16A, and to a lesser extent, TMEM16F, were associated with reduced expression levels of ACE2.

Our experiments involving treatment with Bafilomycin (an inhibitor of auphagic flux) provided evidence that ACE2 degradation induced by TMEM16s occurs within lysosomes, as it occurs with SPIKE. Furthermore, we identified that both TMEM16s knockdown and treatment with niclosamide effectively prevented the SPIKE-driven ACE2 degradation.

These findings collectively suggest the possible formation of a protein complex involving ACE2, SPIKE, and TMEM16s, which plays a critical role in ACE2 degradation and the process of syncytia formation. It is important to note that syncytia formation is a shared feature among various viruses, and ACE2 serves as a receptor for other coronaviruses as well. Understanding the intricate molecular pathways underlying these interactions holds significant implications, not only from a physiological perspective, given the central role of ACE2 in the renin-angiotensin-aldosterone system (RAAS), but also in the context of potential future viral infections that utilize the same receptor. Unraveling these pathways opens up possibilities for new therapeutic targets that could aid in the prevention of severe symptoms associated with these pathologies.

TABLE OF CONTENTS

LIST OF FIGURES AND TABLES

ABBREVIATIONS

ABBREVIATION	MEANING
3	
3CLpro	3C-like protease
A	
ACE	angiotensin-converting enzyme
ACE2	angiotensin-converting enzyme 2
ADAM17	A disintegrin and metalloprotease 17
AIDS	acquired immunodeficiency syndrome
Ang	angiotensin
ANO	Anoctamin
ARDS	acute respiratory distress syndrome
Asn	asparagine
Atg5	autophagy-related protein 5
B	
BafA1	bafilomycin A1
C	
C-terminal	COOH terminus
CaCCs	Ca2+-activated chloride channels
Cdc2	cell dividion cycle protein 2
CHIKV	Chikungunya virus
CK1α	casein kinase 1α
coIP	co-immunoprecipitation
COVID-19	Coronavirus Disease 2019
CPs	clathrin-coated pits
D	
DCLK1-B	doublecortin-like kinase 1
DMV	double membrane vesicles
E	
E	Envelope
E1	ubiquitin-activating enzyme
E2	ubiquitin-conjugating enzyme
E3	ubiquitin ligase
EBOV	Ebola Virus
EBV	Epstein–Barr virus

EMA	European Medicines Agency
ER	Endoplasmic Reticulum
ERGIC	endoplasmic reticulum-Golgi intermediate compartmen
ESCRT	Endosomal Sorting Complex Required for Transport
EVs	extracellular vesicles

F

FDA	Food and Drug Administration
FRET	fluorescence resonance energy transfer

G

GAPs	GTPase-activating proteins
GEFs	guanine exchange factors

H

HADV	human adenovirus
HCV	hepatitis C virus
HDL	high density lipoprotein
HEV	Hepatitis E Virus
HIV	Human Immunodeficiency Virus
HLA	human leukocyte antigen
HR	heptapeptide repeats
HRV	human rhinovirus
HSV	Herpes Simplex Virus

I

IL6	interleukin 6
INF	Interferon

J

JEV	Japanese encephalitis virus

L

LC3	microtubule-associated protein 1A/1B-light chain 3
LEF1	lymphoid enhancer binding factor 1
LPS	lipopolysaccharides

M

M	Membrane
MAP4K3	mitogen-activated protein kinase 3, also known as GLK
MAPK	mitogen-activated protein kinase
MERS-CoV	Middle East respiratory syndrome coronavirus
mRNA	messanger RNA

N

N	Nucleocapsid
N-terminal	NH2 terminus
nAbs	neutralizing antibodies
NF-κB	nuclear factor κB
Niclo	niclosamide
NSP	non-structural proteins
NTD	N-terminal domain
NUAK2	NUAK family kinase 2

P

PAH	pulmonary arterial hypertension
PASMC	pulmonary artery smooth muscle cells
PE	phosphatidylethanolamine
PIKFYVE	1-phosphatidylinositol 3-phosphate 5-kinase
PIP2	phosphatidylinositol 4,5-bisphosphate
PLA	Proximity Ligation Assay
PLP	papain-like-protease
PPCA	Pro-Xaa Carboxypeptidase
PS	phosphatidylserine
PTM	post-translational modifications

R

R0	primary reproduction number
RAAS	renin-angiotensin-aldosterone system
RBD	receptor binding domain
RdRp	RNA-dependent RNA polymerase
ROS	reactive oxygen species
RSV	Respiratory Syncytial Virus
RTC	replication trascriptase complex

S

sACE2	soluble ACE2
SARS-CoV	severe acute respiratory syndrome coronavirus
SARS-CoV-2	severe acute respiratory syndrome coronavirus 2
SCARB1	Scavenger receptor class B member 1
Ser	serine
Sph	sphingomyelin
SRP	signal recognition particle

T

TFRC	Transferrin receptor protein 1
TGF-β	transforming growth factor-β

Thr	threonine
TMDs	transmembrane domains
TMEM16	Transmembrane 16 family, also known as Anoctamines
TMEM16s	TMEM16A and TMEM16F
TMPRSS2	transmembrane protease serine 2
TMs	transmembrane α-helices
TNFα	tumor necrosis factor-α
TNG	trans-Golgi network

U

UPS	ubiquitin-proteasome system
UTRs	untranslated regions

V

VOCs	variants of concern
VOIs	variants of interest

W

WHO	World Health Organization

Z

ZIKV	Zika virus

INTRODUCTION

COVID-19

COVID-19, short for Coronavirus Disease 2019, is an illness caused by the infection of the severe acute respiratory syndrome coronavirus 2 (SARS-CoV-2). This virus was initially identified in November 2019 in Wuhan, Hubei Province, China, and subsequently spread worldwide, leading the World Health Organization (WHO) to declare it a global pandemic on March 11, 2020. COVID-19 exhibits a high transmission rate, with nearly 770 million confirmed infections, almost 7 million deaths and 13.5 million vaccinations recorded to date, 19th September 2023 (Chauhan et al, 2020; WHO).

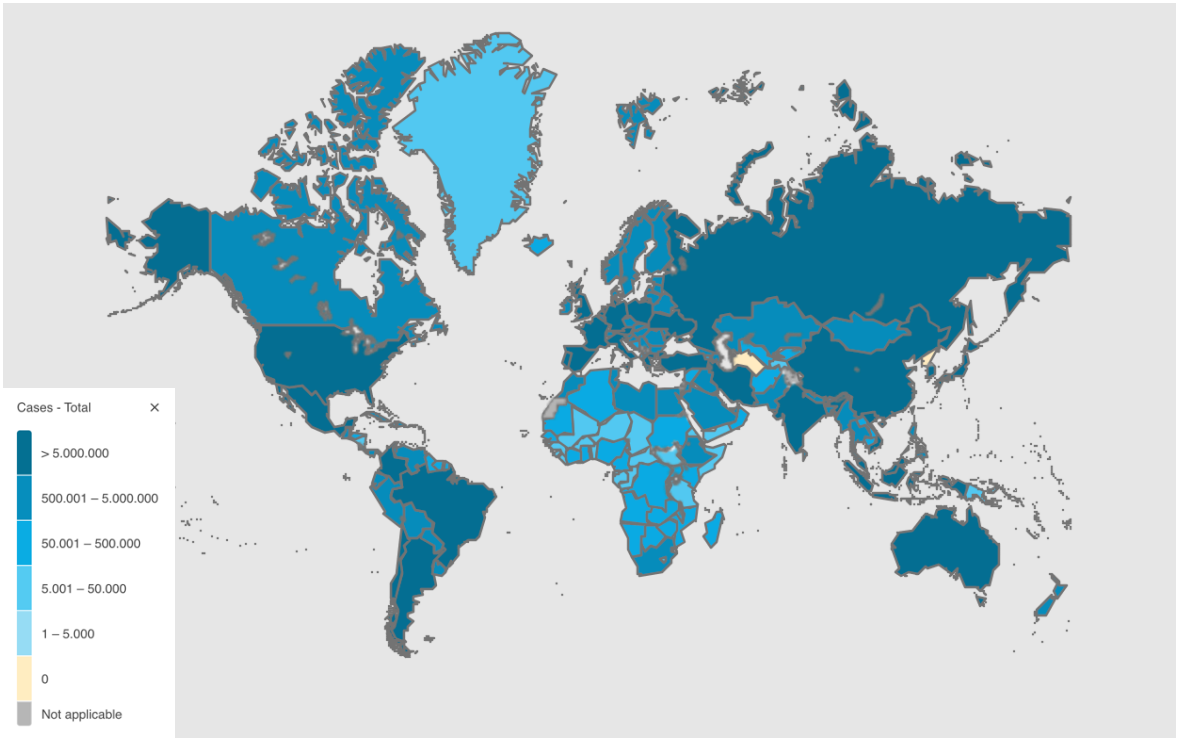

Figure 1: SARS-CoV-2 worldwide spread since the beginning of the pandemic. This map shows SARS-CoV-2 worldwide spread since the beginning of the pandemic. Countries are colored as described by the scale bar on the left side of the image, the darker blue the higher number of cases (WHO dashboard).

SARS-CoV-2, as other members of its family such as SARS-CoV and MERS-CoV, is transmitted through respiratory droplets, commonly resulting from close contact with infected individuals. The primary reproduction number (R0) of the person-to-person spread of the original virus strain was about 2.6, meaning that the infection rate was growing at an

exponential rate. It is worth noting that SARS-CoV-2 exhibits an 82% sequence similarity with both SARS-CoV and MERS-CoV, sharing over 90% identity in essential enzymes and structural proteins (Naqvi et al. 2020). This similarity suggests a common pathogenic mechanism, which in turn could guide therapeutic targeting. SARS-CoV-2 demonstrates a broad tissue tropism, but its most severe symptoms manifest in the lungs (WHO COVID19 Dashboard). Common COVID-19 symptoms include fever, cough, shortness of breath, fatigue, muscle or body aches, headache, sore throat, loss of taste or smell, congestion or runny nose, nausea or vomiting, and diarrhea (Goyal et al. 2020). The severity of symptoms can vary, with potential complications including lung thrombosis (Levi et al. 2020), acute respiratory distress syndrome (ARDS) (Xu et al. 2020), abnormal activation of the inflammatory response (cytokine storm) and rapid deterioration of lung function characterized by alveolar edema (Edler et al. 2020; Jose et al., 2020). Other complications include blood clotting alterations, heart disease, acute kidney injury, neurological complications, and long-term symptoms such as fatigue, cognitive difficulties (referred to as brain fog), and breathing problems (termed long COVID) (Davis et al., 2023).

The wide variation in COVID-19 symptoms can be attributed to a combination of genetic factors and immune responses. Genetic characteristics, including human leukocyte antigen (HLA) variations, genes involved in inflammation like interleukin 6 (IL6) and tumor necrosis factor-α (TNFα), as well as blood type, may influence an individual's susceptibility to the virus and their inflammatory response (Pereira et al. 2021).

SARS COV 2

SARS-CoV-2 belongs to the Coronaviridae virus family, order of Nidovirales, characterized by its spherical envelope derived from the host cell membrane. It houses a single-stranded, positive-sense RNA genome, approximately 30,000 bases long. Coronaviridae, in fact, have the largest RNA genome usually ranging from 26 to 32 kb. Coronaviruses are categorized into four genera: Alpha (α), Beta (β), Gamma (ɣ), and Delta (**δ**)-coronavirus and SARS-CoV-2 falls within the β-coronavirus genus (Wu et al. 2020). α-coronavirus and β-coronavirus primarily infect mammals, while ɣ-coronavirus target avian species. **δ**-coronavirus, on the other hand, can infect both mammals and birds. The family name is inspired by the crown-like appearance of the virus, featuring protrusions of about 20 nm on the envelope, formed by the glycoprotein S or spike (from now on: spike) (Neuman et al. 2006; Yao et al. 2020).

Spike plays a pivotal role in receptor attachment and host cell penetration binding angiotensin-converting enzyme 2 (ACE2) (Satarker and Nampoothiri 2020) leading to its tropism for tissues found primarily in the lungs, heart, blood vessels, small intestine, thymus, kidney, pancreas, testis, gallbladder, oral and nasal cavities, and the central nervous system—sites where SARS-CoV-2 infection occurs, as well as its associated complications (Gkogkou et al. 2020; Hikmet et al. 2020).
ACE2 was already known to be one of the key players in the renin-angiotensin-aldosterone system (RAAS) as well as the receptor for other viruses causing mild upper respiratory tract infections such as the α-coronavirus HCoV-NL63 and the SARS-CoV-2 precursor SARS-CoV (Hoffmann et al. 2005; Jackson et al. 2022; Li et al. 2003).

Of note, if ACE2 is fundamental at early stages of viral entry, other proteins play a key role in the SARS-Cov-2 infection like Rab-7a, the loss of which has been associated with ACE2 sequestration and consequent reduced viral entry (Daniloski et al. 2021), Transferrin receptor protein 1 (TFRC) which could act as an alternative receptor for SARS-CoV-2 (Tang et al. n.d.), Scavenger receptor class B member 1 (SCARB1) which facilitates viral entry acting as a co-factor binding high density lipoprotein (HDL) (Wei C et al. 2020), and 1-phosphatidylinositol 3-phosphate 5-kinase (PIKFYVE) necessary for viral endocytosis and, more specifically, essential for early endosomes maturation in late endosomes, phagosomes, and lysosomes

(Baranov et al. 2019). PIKFYVE has been widely studied as a potential universal drug target for viral infections that are endocytosis dependent.

SARS-CoV-2 encodes 29 proteins in total, 16 of which are non-structural proteins (NSP1-16) which are required for viral replication and pathogenesis (Chan et al. 2020; Fehr and Perlman 2015; F. Wu et al. 2020), nine are auxiliary proteins (open reading frame (ORF) 3a, 3b, 6, 7a, 7b, 8, 9b, 9c/14, and 10) (Chan et al. 2020; Wu et al. 2020) and four are structural proteins, a category that includes spike, Envelope (E), Membrane (M), and Nucleocapsid (N) (Naqvi et al. 2020). spike, E and M are embedded in the bilayer envelope on the virus surface, while the N proteins bind the RNA genome in a spiral symmetric manner at the core of the virion (Feng Wei et al. 2020; Liu et al. 2021; Satarker and Nampoothiri 2020; Yao et al. 2020).

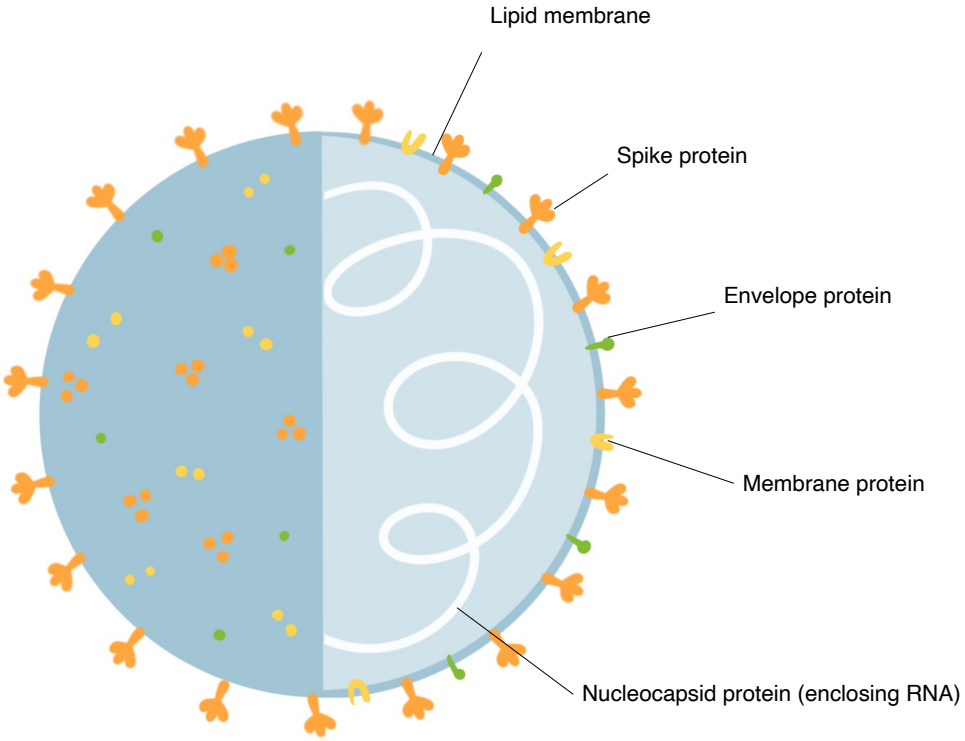

Figure 2: **Structure of SARS-CoV-2.** This image is representing the structure of the coronavirus: it has a crown-like shape with proteins embedded in its membrane (M, E and spike proteins), while its capsid contains the viral genome and the associated proteins (credits to abcam website https://www.abcam.com/content/structural-and-functional-mechanism-of-sars-cov-2-cell-entry)

E protein participates in the assembly, budding, envelope formation, and pathogenesis of the virus (Schoeman and Fielding 2019). The M protein is an N-linked glycosylated protein and has the highest level of expression comparing all proteins in coronaviruses (Alsaadi and Jones

2019). It helps to bend the membrane to create a spherical structure encircling the ribonucleoprotein and serves as a scaffold for viral assembly (Satarker and Nampoothiri 2020). Notably, the generation of infectious spherical particles is promoted by co-expression of the E and M proteins (Schoeman and Fielding 2019). The N proteins predominantly participate in viral RNA synthesis and attach the viral genome to replication transcriptase complex (RTC), thus in charge of viral replication (Zhai et al. 2005).

Relevant nsp proteins:

NSP	FUNCTION
nsp1	suppression of host gene expression and inhibiting the INF signalling
nsp2	probably involved in replication and modulation of host immune responses
nsp3	papain-like protease (PLP), protease activity and cleaves the viral polyproteins
nsp4	membrane-associated, key factor of viral RNA replication and double membrane vescicles (DMV) formation
nsp5	or 3C-like protease (3CLpro), key enzyme responsible for cleaving the viral polyproteins. Inhibiting INF signalling.
nsp6	transmembrane protein involved in the rearrangement of intracellular membranes for the formation of the replication organelles required for viral RNA synthesis
nsp7 and nsp8	Co-factors of nsp12, they form a complex that acts as a primer RNA-dependent RNA polymerase (RdRp). They are critical for viral replication, as they catalyze the synthesis of the viral RNA genome
nsp9	RNA binding protein, probably involved in viral RNA replication and stabilization
nsp10	scaffold protein for nsp14, exonuclease involved in viral RNA proofreading and replication fidelity
nsp11	Unkown
nsp12	RNA-dependent RNA polymerase (RdRp) responsible for the viral RNA replication.
nsp13	RNA helicase 5' triphosphate
nsp14	Exoribonuclease N7 MTase
nsp15	Endoribonuclease, evasion of dsRNA sensors
nsp16	2'-O-MTase, avoiding MDA5 recognition, negatively regulation innate immunities

Table 1: **Nsps SARS CoV 2 proteins.** Table describing the functions of the different nsps of SARS-CoV-2 (Naqvi et al. 2020).

SARS-CoV-2 virus infects cells and hijacks the host cell mechanisms for self-replication. These viral proteins are located in diverse positions in the cell (Liu et al. 2021), working as bait and

prey proteins, leading to several virus-host proteins interactions (Laurent et al. 2020; Samavarchi-Tehrani et al. 2020; Stukalov et al. 2021).

The virus effectively hijacks the endoplasmic reticulum (ER) system, for example through Sec61, an ER membrane translocon required for secretory protein transport and processing (Haßdenteufel et al. 2018; Lee et al. 2021:2; Liu et al. 2021). Additionally, it interferes with phagocytosis to evade the primary mechanism of innate immune defense (Baranov et al. 2019; Schubert et al. 2018), disrupts the oxidative phosphorylation energy pathway, potentially resulting in mitochondrial dysfunction (Stukalov et al. 2021), and modulates host translation processes. Additional interactions occur between some viral proteins and host proteins related to tight junctions maintenance in epithelial cells in the lungs, intestines, kidney, and brain (Zhang et al. 2021), or proteins involved in cholesterol metabolic process and cardiac muscle contraction (Chen et al. 2021; Y. Chen et al. 2022; Tian et al. 2020).

ANGIOTENSIN CONVERTING ENZYME 2

ACE2 is a type I integral membrane protein with a single transmembrane domain. It belongs to the peptidase M2 family and functions as a carboxypeptidase. As already mentioned, ACE2 is predominantly found in the lungs, heart, kidneys, intestines, and blood vessels. Structurally, ACE2 is a heterodimer that further forms dimers through ACE2 mediated dimerization interfaces. It has its N-terminal domain located outside the cell, while the C-terminal is situated inside.

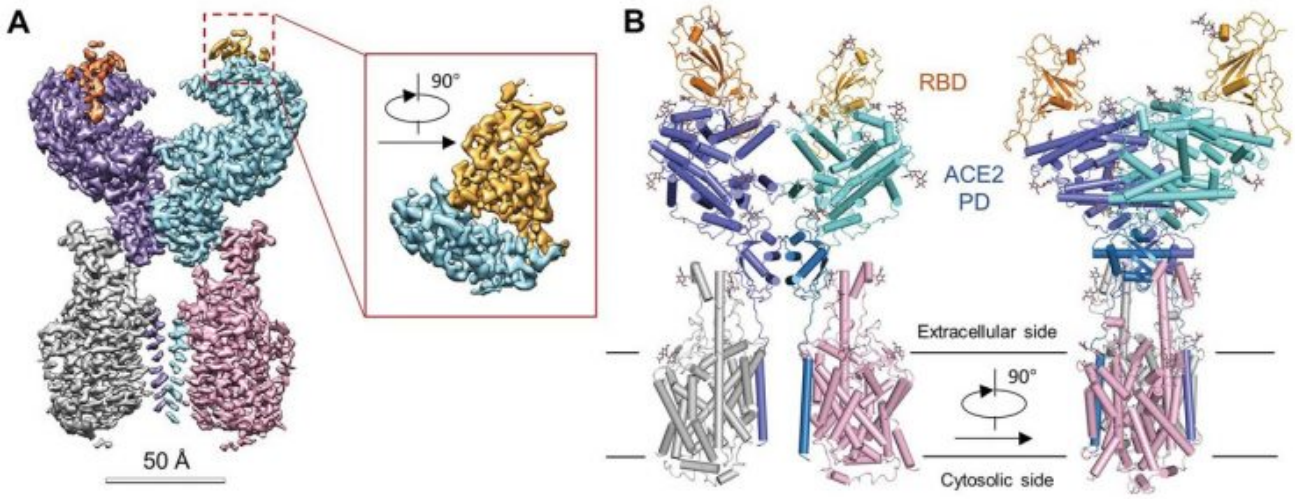

Figure 3: Structure of ACE2. This image represents the 3D structure of ACE2 and its interactions with RBD of spike (yellow) and B0AT1 (gray and pink) (Yan et al. 2020).

ACE2 was identified in 2000 (Donoghue et al. 2000; Tipnis et al. 2000) as an ACE homolog. It provides protection against several chronic conditions, including cardiovascular diseases, lung injury, and diabetes (Bader 2013). The ACE2 N-terminal domain, which is exterior to the cell, is responsible for its catalytic function, displaying peptidase activity and playing a crucial role in converting angiotensin 2 to angiotensin-(1-7) leading to vasodilation (Wiese et al., 2021). Furthermore, this domain is essential for the interaction with the spike protein of SARS-CoV-2 due to the presence of the RBD site, which also interacts with other ligands (Hoffmann et al. 2020; Li et al. 2003). Additionally, the N-terminal region features a short sequence of peptides acting as a signal peptide for transport to the cell surface. ACE2 is composed of 1100 amino acids and has a molecular mass ranging from 110 to 130 kDa, while its soluble form (sACE2) has a mass of 75-90 kDa (Xiao et al. 2014).

The C-terminal domain, located intracellularly, is involved in various cellular processes, including signal transduction and receptor trafficking. ACE2 also possesses a binding site for

an interaction with the Amino Acid Transporter B0AT1, also known as SLC6A19. This interaction is vital for regulating amino acid transport in the intestine and kidneys. In this context, ACE2 functions as a chaperone protein for B0AT1 aiding in its proper folding and trafficking to the cell membrane. Hence an hypothesis suggesting that the interaction between intestinal ACE2 and spike could downregulate the absorption of neutral amino acids in the small intestine of COVID-19 patients, potentially causing symptoms such as diarrhea and intestinal inflammation (Zhang, Yan, and Zhou 2022).

As previously mentioned, ACE2 is well-known for its role in RAAS, which plays a crucial function in regulating blood pressure and fluid balance in the body. While ACE (angiotensin-converting enzyme) cleaves angiotensin I to form angiotensin II, a potent vasoconstrictor, ACE2 counterbalances this effect by cleaving angiotensin (Ang) II to Ang 1-7, which exerts different physiological effects (Fountain, Kaur, and Lappin 2023).

Key components of the RAAS system include Renin, Ang, and Aldosterone. Renin is a proteolytic enzyme produced in juxtaglomerular cells in the kidney and is released into the bloodstream in response to changes in renal perfusion. Renin cleaves Angiotensinogen, synthesized in the liver, to form Ang I. ACE then converts Ang I into angiotensin II, leading to various effects, including vasoconstriction, aldosterone secretion, and vasopressin release. It is worth noting that Ang II can have pathological implications in conditions such as hypertension, atherosclerosis, heart failure, and kidney disease, which is why a category of drugs known as ACE inhibitors can be prescribed to prevent cardiovascular complications. Ang II also plays a role in regulating aldosterone synthesis in the adrenal cortex, affecting electrolyte balance by increasing sodium reabsorption in renal collecting ducts (Fountain et al. 2023).

On the other hand, ACE2 cleaves Ang II to Ang (1-7), which has anti-inflammatory and vasodilatory effects (Wiese et al. 2021).

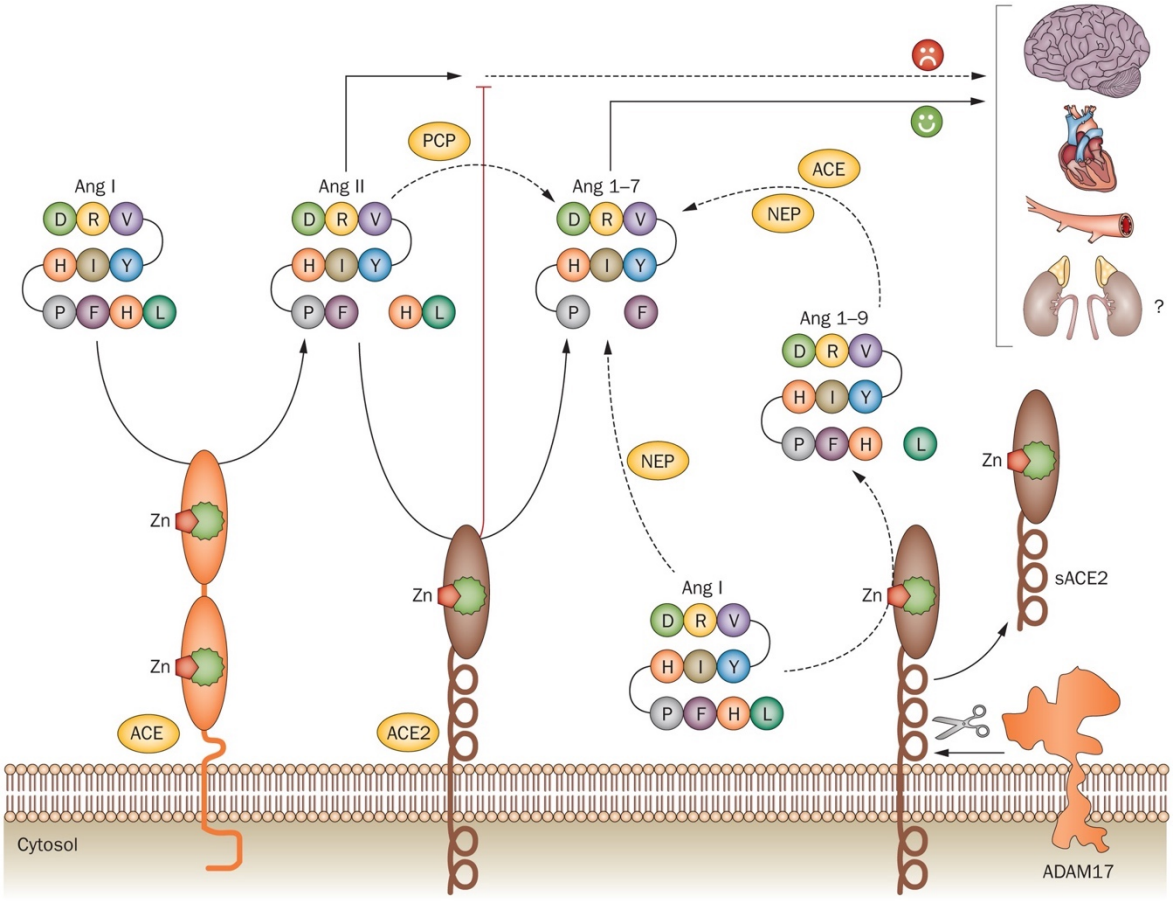

Figure 4 **Ang1-7 pathway in RAAS.** Scheme representing the role of ACE2 in RAAS. ACE transforms Ang I in Ang II while ACE2 is processing Ang II In Ang 1-7, which has opposite effects of its precursor **(**Jiang et al. 2014**).**

During the SARS-CoV-2 pandemic, ACE2 received widespread attention due to its role as a receptor for the coronavirus entry. The spike protein binds ACE2 at the receptor binding domain (RBD), and following this binding, the virus enters the cell through membrane fusion. It has been observed that viral entry is followed by internalization of ACE2 through the endocytic pathway, involving processes such as clathrin-mediated endocytosis or alternative mechanisms like macropinocytosis (Jackson et al. 2022).

It is important to note that reduced ACE2 expression may disrupt the physiological regulation of RAAS, contributing to the side effects of COVID-19. Furthermore, once SARS-CoV-2 starts replicating, the cells themselves begin to express spike on their membrane, allowing them to fuse with neighboring cells (Cattin-Ortolá et al. 2021; Jennings et al., 2021).

In addition to its known functions, ACE2 serves as a multifaceted player in physiology, influencing the regulation of glucose and lipid metabolism (Chen et al. 2022). Studies on ACE2-deficient mice have revealed impaired glucose tolerance and insulin sensitivity, suggesting a

potential role for ACE2 in modulating glucose homeostasis (Ma et al. 2020). Furthermore, ACE2 regulates lipid metabolism by enhancing fatty acid uptake and promoting lipid oxidation. Notably, evidence indicates that ACE2 expression in adipose tissue tends to decrease in obesity, a phenomenon linked to heightened inflammation and insulin resistance.

Moreover, recent studies have also suggested that ACE2 may have additional anti-inflammatory effects due to its capacity to neutralize lipopolysaccharides (LPS) (Ye and Liu 2020) or activate the PI3K/Akt pathway (Zhang et al. 2019). Moreover, ACE2 has been implicated in regulating oxidative stress. Not only angiotensin II is a pro-oxidant molecule, but ACE2 reduces the expression of NADPH oxidase, one of the major sources of reactive oxygen species (ROS) production (Wysocki et al. 2014). Oxidative stress is another side effect of COVID-19, contributing to the development of acute respiratory damage. Therefore, upregulation of ACE2 could potentially be beneficial for managing the disease.

It is important to note that ACE2 is degraded by the spike protein of SARS-CoV-2 and more broadly through lysosomes (Yi et al. 2022). In addition, there are already other examples of proteins that regulate ACE2 expression. These include:

1) casein kinase 1α (CK1α), which phosphorylates ACE2 by inducing its binding to SPOP and leading to a stabilization of the protein that prevents its E3 ligase mediated protein degradation (Su et al. 2021);

2) NUAK family kinase 2 (NUAK2), which is known to increase after SARS-CoV-2 infection; being required for ACE2 maintenance on the cell surface and consequently for the infection (Prasad et al. 2023), higher levels of NUAK2 increase ACE2 levels;

3) MAP4K3 (GLK), the levels of which are increased after infection; this kinase induces ACE2 phosphorylation and inhibits ACE2 ubiquitination (Chuang et al. 2022).

ACE2 ECTODOMAIN SHEDDING

ACE2 has been observed to undergo protease cleavage, resulting in the release of sACE2 into the extracellular space and blood stream, where it can still act as AngII converter. A disintegrin and metalloprotease 17 (ADAM17), a metalloprotease enzyme, is well-known for cleaving the ACE2 extracellular domain (Lambert et al. 2005:17). Recent studies have highlighted that the transmembrane protease serine 2 (TMPRSS2), a transmembrane protease responsible for cleaving and activating the SARS-CoV-2 spike, can also cleave ACE2 (Hoffmann et al. 2020). Interestingly, TMPRSS2 competes with ADAM17 for ACE2 processing, with TMPRSS2 cleavage appearing to enhance SARS-CoV-2 infection levels (Heurich et. al, 2014).

There is some inconsistency in findings regarding the role of sACE2 in the SARS-CoV-2 infection process. On the one hand, sACE2 binds to the spike protein, facilitating viral entry via vasopressin receptor-mediated endocytosis. Studies have shown that inhibiting ACE2 sheddase or using ADAM17 siRNA knockdown can block live SARS-CoV-2 infection (Yeung et al. 2021). On the other hand, sACE2 appears to reduce cell susceptibility to infection while increasing viral binding, effectively acting as a decoy for the virus (Sokolowska 2020). Notably, treatment of pre-mixed SARS-CoV-2 pseudovirus (spike) with recombinant sACE2 could reduce the cell entry of spike protein in human A549 lung epithelial cells (Jocher et al. 2022).

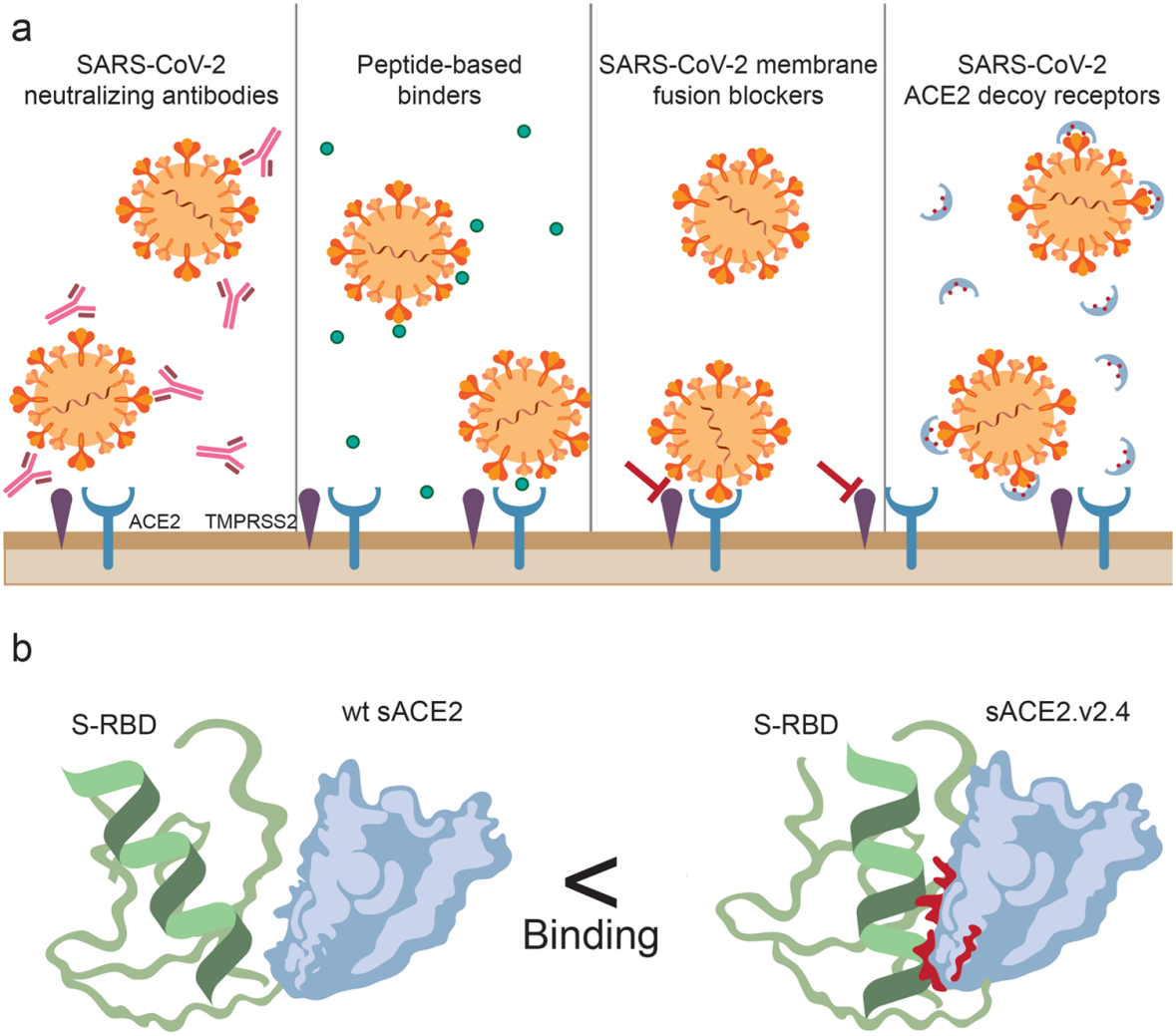

Figure 5: Soluble ACE2 could act as a decoy for SARS-CoV-2. This image is showing four different neutralising approaches for SARS-CoV-2. In particular, the top right image is showing how analogs of sACE2 could act as a decoy for SARS-CoV-2 binding the virus before its attachment to host cells. b is showing the interaction between sACE2 and spike RBD in case of wt sACE2 or sACE2 v2.4, a variant engineered by Chan and colleagues to enhance its binding with spike **(**Sokolowska 2020**).**

Spike is a homotrimeric class I transmembrane fusion protein, consisting of approximately 1,273 amino acids in each subunit. It has a molecular weight of 600 kDa and is divided into two functional subunits: S1 and S2 (Bagdonaite et al. 2021; Tian et al. 2021; Walls et al. 2020). Glycans attached to spike can shield certain regions from immune recognition, blocking antibody binding and enabling the virus to evade innate and adaptive immune responses (Bagdonaite et al. 2021; Shajahan et al. 2020).

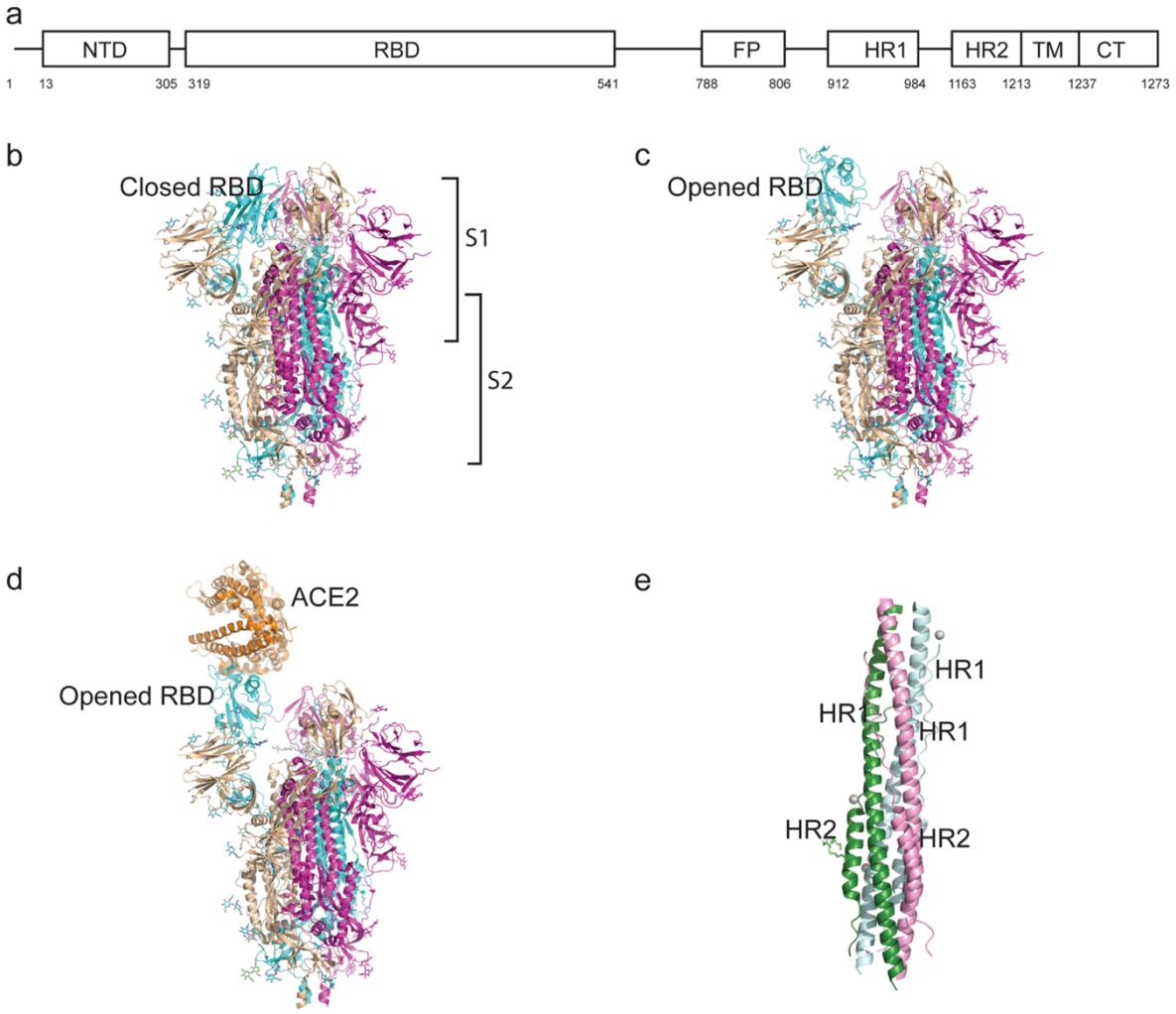

Figure 6: Structure of spike. Images representing the structure of spike and its different conformation during the infection process, from the closed RBD state to the open one that allows its binding to ACE2. e is showing the structure of the heptapeptide repeats domains. (Huang et al. 2020)

S1 comprises a RBD, N-terminal domain (NTD), and a signal peptide (Watanabe et al. 2020; Yao et al. 2020). The RBD is involved in the receptor interaction, while the NTD plays a role in co-receptor binding, which are mainly sugars (B et al. 2020; Premkumar et al. 2020).

S2 includes a conserved fusion peptide, heptapeptide repeats HR1 and HR2, a transmembrane domain, and a cytoplasmic domain and it is involved in membrane fusion (Shah et al. 2021; Yao et al. 2020).

Coronaviruses enter host cells through their spike glycoprotein, which is initially synthesized as an inactive precursor requiring cleavage to mediate membrane fusion. Cleavage can occur:

- During trafficking within the producer cell by host furin-like enzymes.
- At the cell surface during attachment by serine proteases like TMPRSS2 or extracellular furin.
- Within the late endosome/endolysosome by cathepsin proteases (Benton et al. 2020; Belouzard et al., 2009).

Following the initial S1/S2 cleavage and binding of the spike receptor binding domain to ACE2, a second cleavage site (S2′) within the S2 domain becomes exposed (Benton et al. 2020; Matsuyama et al. 2010). Cleavage of S2′ by serine proteases or cathepsins triggers the release of the S2 fusion peptide, initiating the fusion of viral and host cell membranes (Hoffmann et al. 2020).

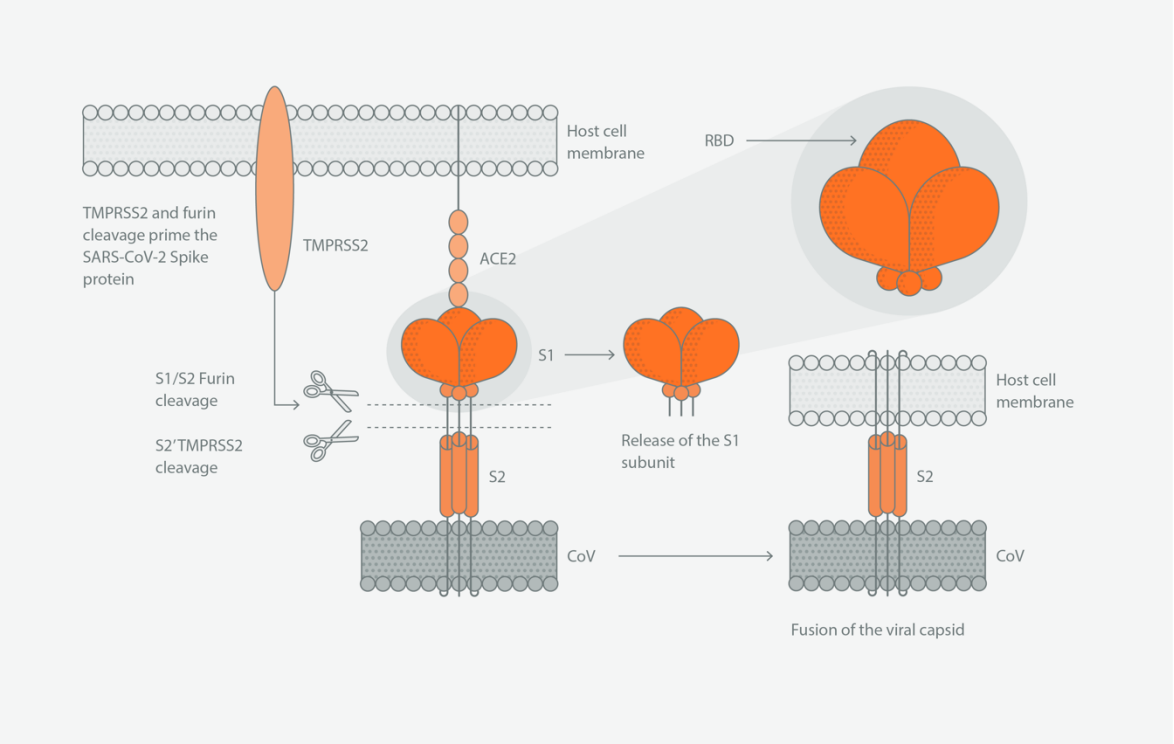

Figure 7: ACE2-spike interaction. This scheme represents the interaction between ACE2 and spike, after TMPRSS2 and furin cleavage priming**.** Credits to the abcam website.

Summarizing the first steps of the infection process: as already mentioned, SARS-CoV-2 primarily utilizes ACE2 as its primary receptor for cellular entry through endocytosis or direct fusion at the plasma membrane (Jackson et al. 2022). Initially, the RBD of the S1 unit binds the ACE2 receptor. Subsequently, a furin-like protease cleaves the site between the S1/S2 subunits, activating the conformational change of the spike protein to expose the S2 subunit. The S2 subunit facilitates virion fusion with the cell membrane and initiates virus entry (Chan et al. 2020; Sanda, Morrison, and Goldman 2021; Watanabe et al. 2020). Two cleavage sites exist in the spike protein: the multibasic S1/S2 furin cleavage site and the S2′ cleavage site, which can be cleaved either by TMPRSS2 at the cell membrane or cathepsins in the endosome (WHO COVID19 Dashboard).

To note, spike surface is highly glycosylated, featuring 22 N-linked glycans and 17 O-glycans, which significantly influence the host immune response (Tian et al. 2021; Watanabe et al. 2020).

Importantly, the spike protein has undergone multiple mutations during the course of the SARS-CoV-2 pandemic, affecting receptor binding affinity, virus transmissibility, and immune system evasion.
Over the course of 2020, SARS-CoV-2 gained only few amino acid substitutions, however, by late 2020, new variants began to emerge (B et al. 2020; Jr et al. 2020). The World Health Organization (WHO) termed these newly emerging variants as variants of concern (VOCs) or variants of interest (VOIs) depending on increased transmission, pathogenesis, and immune escape.

Variants of Interest (VOI)

WHO label	Lineage + additional mutations	Country first detected (community)	Spike mutations of interest	Year and month first detected	Impact on transmissibility	Impact on immunity	Impact on severity	Transmiss in EU/EEA
Omicron	BA.2.75 (x)	India	(y)	May 2022	Unclear (1)	Similar to Baseline (2-4)	No evidence	Communit
Omicron	XBB.1.5-like (a)	United States	N460K, S486P, F490S	n/a	Baseline (5, 6)	Baseline (v) (5, 7)	Baseline (8)	Communit
Omicron	XBB.1.5-like + F456L (b) (e.g. **EG.5, FL.1.5.1, XBB.1.16.6**, and **FE.1**)	n/a	**F456L**, N460K, S486P, F490S	n/a	Similar to Baseline	Increased (9)	Similar to Baseline	Communit

Variants under monitoring

WHO label	Lineage + additional mutations	Country first detected (community)	Spike mutations of interest	Year and month first detected	Impact on transmissibility	Impact on immunity	Impact on severity	Transmissio in EU/EEA
Omicron	XBB.1.16	n/a	E180V, T478R, F486P	n/a	No evidence	No evidence	No evidence	Detected (a)
Omicron	BA.2.86	n/a	I332V, D339H, R403K, V445H, G446S, N450D, L452W, N481K, 483del, E484K, F486P	n/a	No evidence	No evidence	No evidence	Detected (a)
Omicron	DV.7.1	n/a	K444T, L452R, L455F	n/a	No evidence	No evidence	No evidence	Detected (a)
Omicron	XBB.1.5-like + L455F + F456L (b)	n/a	**L455F**, **F456L**, N460K, S486P, F490S	n/a	No evidence	No evidence	No evidence	Detected (a)

Figure 8: **SARS-CoV-2 variants of interest.** List of SARS-COV-2 variants of interest and under monitoring for WHO.

The Alpha, Beta, and Gamma variants emerged in September, October, and November of 2020, respectively, followed by the Delta variant in December 2020, which became dominant globally by mid-2021 (Drew Weissman et al. 2021; Liu et al. 2022; F. Tian et al. 2021; Zhang et al. 2020). In November 2021, the Omicron VOC emerged and since then, multiple Omicron subvariants have been globally dominant. Amino acid substitutions, insertions, and deletions (indels) have arisen in both subunits of spike, however, those in the RBD, which is the primary target of neutralizing antibodies (nAbs), had the largest impact on immune escape. The RBD is also the most variable among coronaviruses, mutating rapidly, resulting in immune escape (Laurent et al. 2020). Substitutions and indels in the NTD and the S2 have also been implicated in nAbs escape, although to a much lesser extent than those in the RBD (Heald-Sargent and Gallagher 2012; Sun et al. 2022; WI et al. 2022).

The S2, in fact, is highly conserved among coronaviruses and this makes S2 an appealing target for developing cross-neutralising antibodies (Premkumar et al. 2020). While these

antibodies may not block receptor binding, they can still hinder the fusion of the viral envelope with the target cell plasma membrane. Additionally, they can exert their effects through Fc-mediated effector functions. (Chen et al. 2023; Pinto et al. 2021; Wl et al. 2022). To note, substitutions and indels that occur in the S2 subunit may impact the fusogenic function of spike or the interaction of S2 with S1, altering the protein structure and stability (Satarker and Nampoothiri 2020).

Moreover, considering that S1/S2 cleavage primes spike, substitutions and indels in this region likely alter protease usage and therefore tropism, infectivity, and fusogenicity. Interestingly, increased infectivity and spread through cell–cell fusion may also act as an alternative antibody escape route by the virus (Jackson et al. 2021; Zeng et al. 2022).

The molecular process underlying SARS-CoV-2 cell infection follows specific steps:

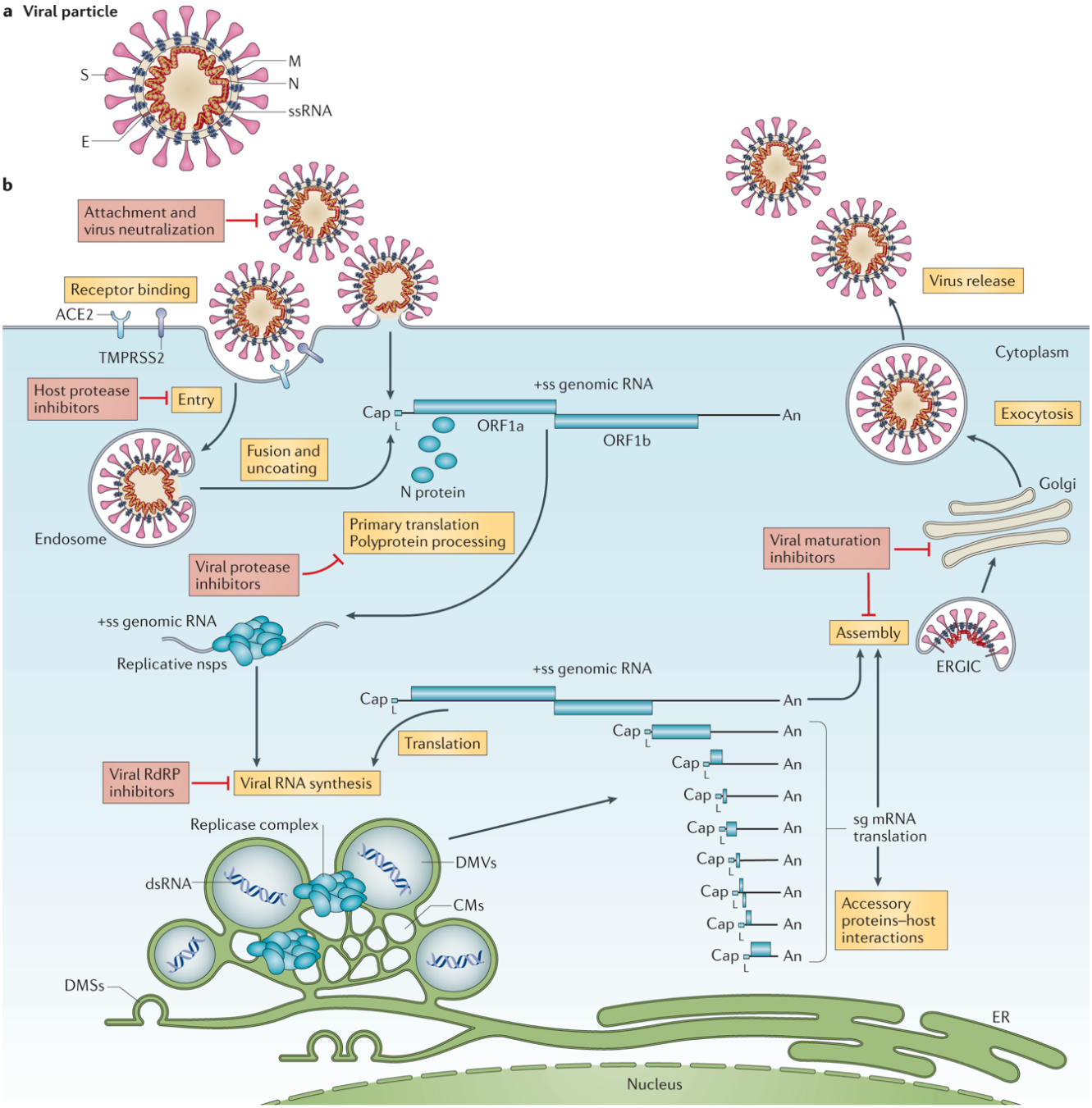

Figure 9: SARS-CoV-2 infection process. Image summarizing the entry of SARS-CoV-2 into an host cell through endosome pathway or membrane fusions, its replication and, eventually, its release through exocytosis (V'kovski et al. 2021).

1. Viral Recognition and Attachment: The spike protein initially interacts non-specifically with various regions of ACE2 on the host cell surface. This interaction triggers conformational changes in spike, including an upward transition of the RBD, exposing it to ACE2 for a more specific binding that stabilizes the receptor interaction (Jackson et al. 2022).

2. Viral Entry: Following binding, other conformational changes occur, and the S protein is cleaved by host proteases such as TMPRSS2 or cathepsin L, typically at the S1/S2 cleavage site located between the two subunits. Removal of the S1 domain enables further conformational changes, priming the fusion machinery (Simmons et al. 2005). The S2 peptide inserts into the host cell membrane, forming a six-helix bundle structure called the fusion core. HR1 and HR2 undergo a zipper-like interaction, bringing the viral membrane closer to the host cell membrane until fusion occurs. Once HR1 and HR2 fuse, they create a fusion pore in the host cell membrane, allowing viral entry. This process is referred to as "uncoating" (V'kovski et al. 2021).

3. Translation: The viral RNA binds to ribosomes at the 5' and 3' untranslated regions (UTRs). Ribosomes identify the start codon (typically AUG) and initiate the translation process. This process includes initiation, elongation, and eventually, the synthesis of a polypeptide chain that folds into a functional shape. Some viral proteins undergo post-transcriptional modifications in the Golgi apparatus, involving the addition of chemical groups such as phosphorylation and glycosylation, as well as cleavage by specific enzymes or proteases to generate mature, functional viral proteins (V'kovski et al. 2021), which, as mentioned before, they are divided in structural (S, E, M, and N proteins) and NSP.

5. RNA Replication: After translation, the viral RNA undergoes a replication process facilitated by certain NSPs functioning as RdRp.

6. Virion Assembly: In this phase, viral genomic RNAs and structural proteins come together to form new viral particles within the host cell. N proteins exhibit a high affinity for binding to the viral RNA genome, forming oligomers. The interaction between the viral genome and N proteins results in the formation of a helical nucleocapsid structure that encapsulates the viral RNA, protecting it from degradation. The nucleocapsid structure interacts with other viral proteins, particularly M proteins, anchoring them to the membrane of the endoplasmic reticulum-Golgi intermediate compartment (ERGIC), where virion assembly takes place. M protein also associates with E proteins for envelope formation. Once the envelope is fully

formed, the budding process commences. Notably, the SARS-CoV-2 envelope is formed using the host cell membrane. Various molecular processes facilitate the detachment of N and M proteins from ERGIC, allowing virion formation (V'kovski et al. 2021).

7. Budding: Mature virions bud from host cells, acquiring their envelope and becoming infectious.

To note, in the SARS COV 2 infection process it could be important to consider the role of extracellular vesicles (EVs), which are reported to participate in several physiological and pathological processes (Doyle and Wang 2019). Exosomes are one of the extracellular vesicle subtypes with the size around 30 to 150 nm in diameter (Doyle and Wang 2019). A model was proposed to describe the mechanism of extracellular vesicles uptake: first, the extracellular vesicle-carried protein binds to the proteoglycan on the cell surface. Next, the interacting protein of the extracellular vesicle-carried protein on the cell surface binds the proteoglycan, promoting the extracellular vesicle uptake (Mulcahy, Pink, and Carter 2014). Several viruses take advantage of the exosome machinery for transporting viral and cellular elements that are beneficial for viral infections (Saad et al. 2021).

SYNCYTIA FORMATION

The spike protein of SARS-CoV-2 possesses the remarkable ability to induce the formation of multinucleated giant cells known as syncytia, both in vitro and in vivo (Braga et al., 2021). Syncytia are cellular structures highly conserved in animals, formed by the fusion of multiple mononucleated cells, resulting in a single cell with multiple nuclei. This process, known as syncytia formation, is not unique to SARS-CoV-2 but is a feature shared with various viral infections, including those caused by Human Immunodeficiency Virus (HIV) (Nardacci et al. 2015a), Respiratory Syncytial Virus (RSV) (Battles and McLellan 2019), and Herpes Simplex Virus (HSV) (Weed and Nicola 2017).

Syncytia formation offers several advantages to viruses. Firstly, it enables them to spread more rapidly within the host. Furthermore, syncytia can incorporate immune cells, a phenomenon observed in conditions like acquired immunodeficiency syndrome (AIDS), where fusion with immune cells can lead to the depletion of CD4+ T cells, weakening the host's immune response (Battles and McLellan 2019; Nardacci et al. 2015b).

The expression of the spike protein alone is sufficient to induce rapid (~45.1 nm/s) membrane fusion. Histopathological examination of lung sections from COVID-19 patients has revealed the presence of atypical cells containing 2-20 nuclei. This membrane fusion process is governed by a bi-arginine motif containing R682 and R685 within the polybasic S1/S2 cleavage site, a characteristic shared by the surface glycoproteins of many highly contagious viruses (Zhang et al., 2021).

These syncytia can readily internalize multiple lines of lymphocytes, forming typical cell-in-cell structures and ultimately leading to the death of internalized cells: a recent research by Sun et al. for example, identified a type of CD45 positive cell structure within the syncytia of COVID-19 patients, which were not present in mononucleated cells.

The Giacca group conducted extensive screenings of 3049 FDA/EMA-approved drugs, using an in vitro cell fusion system based on SARS-CoV-2 spike protein-expressing Vero cells, to identify drugs that can block syncytia formation. Intriguingly, these syncytia-blocking drugs were found to have the common capability of regulating intracellular Ca2+ levels. One of the most promising drugs, niclosamide an oral antihelminthic agent, effectively blocked syncytia formation at a relatively low dose (IC50 = 0.34 μM) and prevented cell death induced by the virus. Niclosamide acts as a potent antagonist of Ca2+-activated transmembrane 16 family

(TMEM16) of chloride channels, and its effectiveness is noteworthy (Braga et al., 2021 - Cattin-Ortolá et al., 2021).

It has been established that cells infected by SARS-CoV-2 express the spike protein on their cell membrane following viral replication. Spike exhibits interactions with COPI and COPII vesicle coats (Cattin-Ortolá et al. 2021), ERM family actin regulators (Millet et al. 2012), and the WIPI3 autophagy component (Cattin-Ortolá et al. 2021). While the COPII binding site promotes exit from the ER, an imperfect histidine residue recognition motif allows spike to escape retention by COPI, resulting in its accumulation on the cell surface. Here, it plays a crucial role in directing the formation of multinucleated syncytia, in addition to its incorporation on new virions (Nardacci et al. 2015).

PROTEIN TRAFFICKING AND DEGRADATION

Proteins are synthesized from messenger RNAs (mRNA), and then translated into a specific sequence of amino acids into the ribosomes. Ribosomes are found in the cytoplasm or on the ER membrane depending on the localisation of the future protein. If the protein is not a cytoplasmic protein and needs to be trafficked somewhere, mRNAs could have a signal peptide which is recognized by a signal recognition particle (SRP), a ribonucleoprotein complex that binds to the signal peptide as it emerges from the ribosome during translation (Neuhof et al. 1998). The SRP-ribosome complex then binds to the SRP receptor on the ER membrane, targeting the ribosome-mRNA complex to the ER. In that location, ribosomes resume translation on the ER membrane, and the nascent protein is translocated across the ER membrane into the ER lumen or embedded within the ER membrane itself (Neuhof et al. 1998).

Newly synthesized proteins undergo folding and post-translational modifications (PTM) in both ER and Golgi apparatus. Glycosylation is one of the most prominent PTMs that takes place. During glycosylation, carbohydrate chains are added to proteins or lipids (Reily et al. 2019). This process involves the modification and maturation of N-linked and O-linked glycosylation, which can impact protein stability, localization, and function. In N-glycosylation, which occurs in the ER, the carbohydrate chain is attached to the nitrogen (N) atom of asparagine (Asn) residues within the protein's amino acid sequence (Reily et al. 2019). The attachment occurs at the consensus sequence Asn-X-Ser/Thr, where X can be any amino acid except proline, while in the n O-glycosylation, occurring in the Golgi apparatus, the carbohydrate chain is attached to the oxygen (O) atom of serine (Ser) or threonine (Thr) residues within the protein amino acid sequence (Breitling and Aebi 2013). Properly folded proteins are transported from the Golgi apparatus to their final destination, such as the plasma membrane, lysosomes, or secretory vesicles.

Vesicle trafficking

For the trafficking of vesicles, and consequently their cargo, at the beginning they form at the donor membrane (ER, Golgi apparatus or plasma membrane) thanks to the recruitment of coat protein complexes (Gomez-Navarro and Miller 2016). There are different types of proteins involved in their formation and addressing based on the donor membrane and their destination:

- For the budding and transport from the ER to the Golgi apparatus and from the Golgi to the ER there are two classes of proteins called COPI and COPII. COPI is responsible for the vesicle transport from the Golgi apparatus directed to the ER, while COPII is involved in the formation of transport vesicles that bud from the ER and transport proteins to the Golgi apparatus (Gomez-Navarro and Miller 2016).
- Clathrin is associated with clathrin-coated vesicles involved in endocytosis (receptor-mediated and non-specific) and transport between the trans-Golgi network (TGN) and endosomes (Mayor and Pagano 2007); this molecular process will be deepened in the next chapter.
- Dynamin is a GTPase protein involved in membrane scission during endocytosis, particularly in the formation of clathrin-coated vesicles (Moreno-Layseca et al. 2021).
- Proteins like adaptins and AP-2 are involved in cargo recognition and vesicle formation during endocytosis (Casler et al. 2019; Gomez-Navarro and Miller 2016).
- Rab Effectors and Motor Proteins: These proteins link Rab GTPases, which is regulated by GTPase-activating proteins (GAPs) and guanine exchange factors (GEFs), to vesicle transport processes. Motor proteins, such as kinesins and dyneins, move vesicles along microtubules (Gennerich and Vale 2009).
- Exocyst Complex: Involved in targeting secretory vesicles to specific sites on the plasma membrane for exocytosis (Wu and Guo 2015).
- ESCRT Complexes: Endosomal Sorting Complex Required for Transport (ESCRT) proteins are involved in sorting cargo into intraluminal vesicles within late endosomes for eventual lysosomal degradation (Hurley 2010; Schmidt and Teis 2012).
- Syntaxins, SNAPs and SNAREs are involved in vesicle fusion and membrane docking (Teng, Wang, and Tang 2001).

Clathrin-mediated endocytosis

Clathrin-mediated endocytosis is one of the major endocytosis pathways in mammalian cells (Mettlen et al. 2018). The process follows several steps: the initial steps in the formation of clathrin-coated pits (CPs) at the plasma membrane and trans-Golgi network (TGN) involve the recruitment to the membrane of clathrin and either adaptor protein complex 2 (AP2 - at the plasma membrane) or AP1 (in the TGN) (Santini et al., 1998). AP2 binds the endocytic sorting motifs AP2-targeting motif (781YASI784) of the target proteins and triggers clathrin-mediated endocytosis (Takei et al. 1999). Clathrin molecules assemble into a lattice-like structure, forming a coat around the pit. To note, clathrin is a protein complex made up of three heavy chains and three light chains that self-assemble into a polyhedral structure. Adaptor proteins (AP1 and AP2) are then recruited to the clathrin-coated pit. These adaptor proteins connect the cargo receptors to the clathrin coat, allowing the recognition and internalization of various cargo molecules, including receptors and signaling proteins (Santini et al., 1998).

The clathrin-coated pit begins to invaginate, forming a vesicle as the clathrin lattice continues to assemble. This invagination is driven by the bending of the plasma membrane. Dynamin, a GTPase protein, plays a crucial role in pinching off the newly formed vesicle from the plasma membrane. It forms a ring around the neck of the vesicle and, with the help of GTP hydrolysis, constricts and severs the vesicle from the membrane. After scission, the clathrin-coated vesicle loses its clathrin coat, allowing it to become a clathrin-free vesicle and maturate into an endosome. This step is essential for the vesicle to fuse with other cellular compartments or undergo further processing (Takei et al. 1999).

Endosomes can fuse with other vesicles or cellular compartments, depending on the cargo it contains. It can eventually fuse with lysosomes for degradation or with other organelles for transport and sorting. Interestingly, in some cases, vesicles can be targeted for recycling. Cargo molecules and receptors may be sorted and returned to the cell surface to be reused (Casler et al. 2019).

If the vesicle contains a cargo destined for degradation, it may fuse with a late endosome or lysosome, where the cargo is broken down by acidic enzymes.

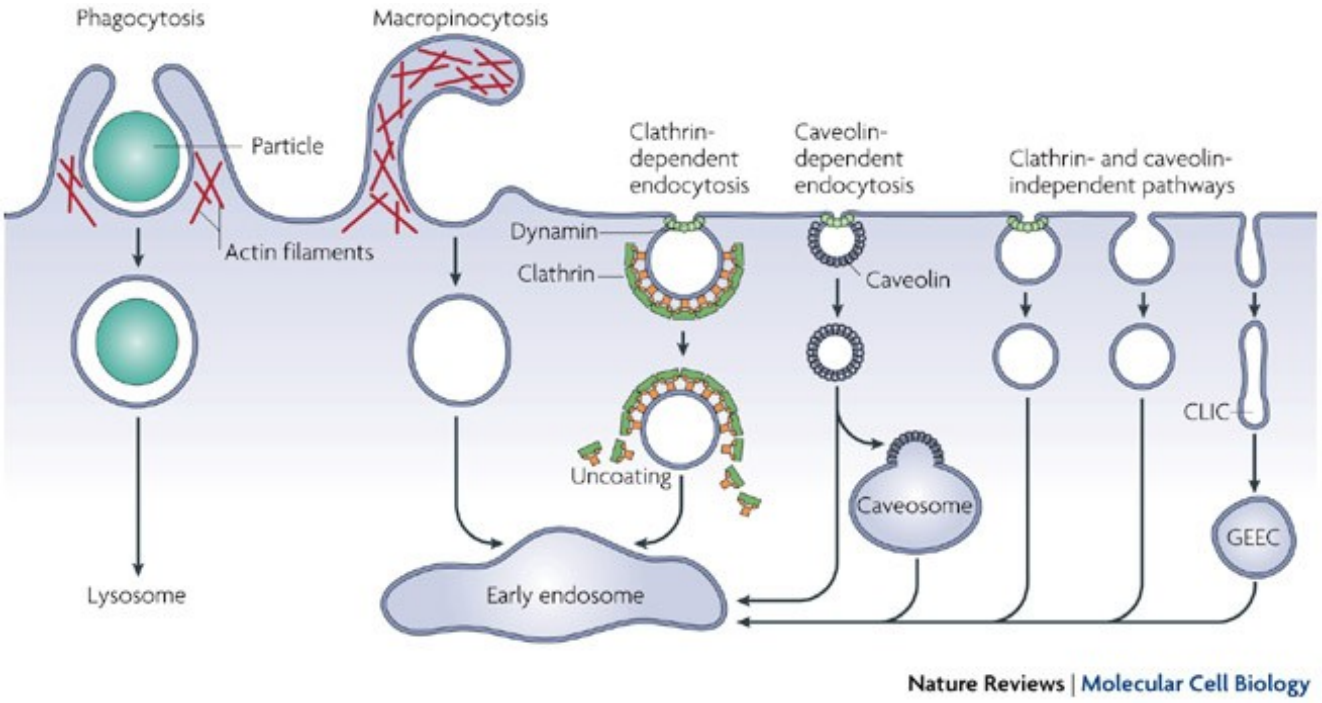

Figure 10: Different internalization pathways. This scheme represents the different ways in which a molecules could be internalized into a cell (Mayor and Pagano 2007).

Numerous studies have revealed a reduction in ACE2 levels within the lung tissues of SARS-CoV-2-infected patients, as well as in virus-infected cells in general (Lu et al. 2022). This phenomenon appears to be linked to the binding of the spike protein to ACE2, which triggers its internalization through clathrin-mediated endocytosis and subsequent degradation within lysosomes (Lu et al. 2022), as well as a possible downregulation at a transcriptional level (Gao et al. 2022). Supporting evidence of the lysosomal degradation can be found in studies where ACE2 levels were restored by either the use of a lysosome blocker, bafilomycin A1 (BafA1) or the mutation in the ACE2 AP2-targeting motif (Lu et al. 2022).

Interestingly, it is highly possible that SARS-CoV-2 virions can enter the cells by endocytosis with one or more of the three proteins nsp6, ORF3a, and ORF7 because TFRC mainly acts as an adaptor protein in the endocytosis biological pathway (Bayati et al. 2021).

Aiming at keeping cellular homeostasis, proteins are constantly degraded and recycled. There are two main pathways for protein degradation in cells: the ubiquitin-proteasome system (UPS) and autophagy-lysosomal pathway. The UPS, which involves the attachment of ubiquitin molecules to the target protein, is responsible for the degradation of short-lived or misfolded proteins, while autophagy, involving the formation of double-membraned vesicles, is responsible for the degradation of long-lived proteins and organelles (Cooper 2000).

- The Ubiquitin-Proteasome Pathway

The primary pathway for selective protein degradation in eukaryotic cells relies on ubiquitin as a marker to target cytosolic and nuclear proteins for rapid proteolysis. Ubiquitin owes its name to the fact that it is a highly conserved 76-amino-acid polypeptide found in all eukaryotes, including yeasts, animals, and plants (Dikic, Wakatsuki, and Walters 2009). The process involves marking proteins for degradation through the attachment of ubiquitin to a lysine residue amino group. Additional ubiquitin molecules are subsequently added, forming a multiubiquitin chain. These polyubiquitinated proteins are then recognized and degraded by a large, multi-subunit protease complex known as the proteasome (Dikic et al. 2009). Importantly, ubiquitin is released during this process, making it available for reuse in subsequent cycles. It is worth noting that both the attachment of ubiquitin and the degradation of marked proteins require energy in the form of ATP (Yaqin et al. 2012).

The stability of many proteins hinges on whether they undergo ubiquitination, a multi-step process. First, ubiquitin is activated by binding to the ubiquitin-activating enzyme, E1 (Yang et al. 2021). It is then transferred to a second enzyme, known as the ubiquitin-conjugating enzyme (E2). The final transfer of ubiquitin to the target protein is mediated by a third enzyme called ubiquitin ligase or E3. E3 is responsible for selectively recognizing appropriate substrate proteins. In some instances, ubiquitin is initially transferred from E2 to E3 and then to the target protein. In others, ubiquitin may be directly transferred from E2 to the target protein within a complex involving E3. While most cells have a single E1, they possess numerous E2s and multiple families of E3 enzymes. Different members of the E2 and E3 families recognize

distinct substrate proteins, thereby conferring specificity to the ubiquitin-proteasome degradation pathway (Callis 2014).

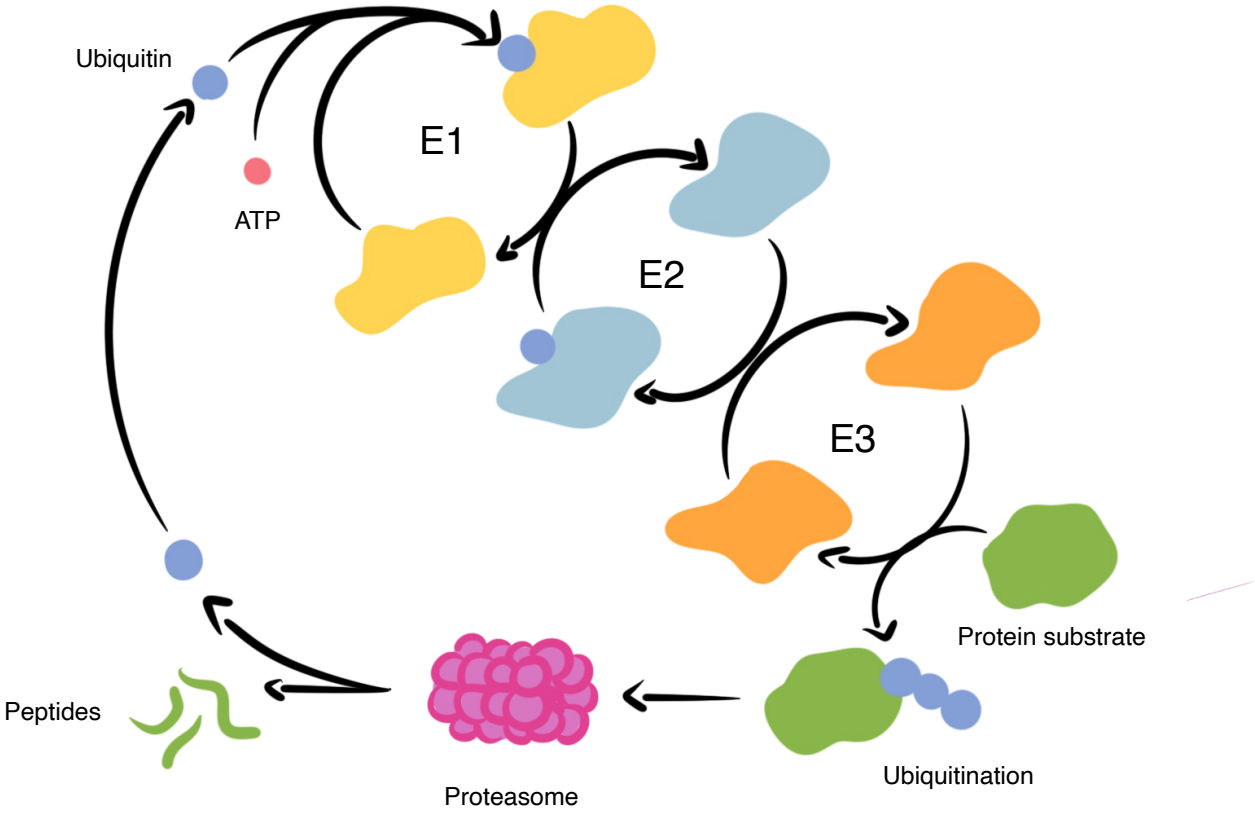

Figura 11: **The ubiquitin-proteosome degradation.** Ubiquitin is activated by E1. It is then transferred to E2 and finally transferred to E3. E3 is responsible for selectively recognizing appropriate substrate proteins and leading to their degradation into the proteasome. Ubiquitin is then recycled (Callis 2014).

Many proteins that govern critical cellular processes, such as gene expression and cell proliferation, are subject to regulated ubiquitination and proteolysis. A compelling example is presented by proteins known as cyclins, which regulate the progression through the cell division cycle in eukaryotic cells (Yaqin et al. 2012). The initiation of mitosis in all eukaryotic cells is partially controlled by cyclin B, a regulatory subunit of the protein kinase Cdc2. The interaction of cyclin B with Cdc2 is essential for activating the Cdc2 kinase, which leads to mitotic events, including chromosome condensation and nuclear envelope breakdown, through the phosphorylation of various cellular proteins. Additionally, Cdc2 triggers a ubiquitin-mediated proteolysis mechanism that degrades cyclin B toward the end of mitosis (Yaqin et al. 2012). This degradation of cyclin B leads to the inactivation of Cdc2, permitting the cell to

exit mitosis and progress to the interphase of the subsequent cell cycle. The ubiquitination of cyclin B is a highly specific process, directed by a 9-amino-acid cyclin B sequence known as the destruction box (Yaqin et al. 2012). Mutations in this sequence prevent cyclin B proteolysis and result in the arrest of dividing cells in mitosis, underscoring the pivotal role of regulated protein degradation in governing the fundamental process of cell division (Yaqin et al. 2012).

- **Lysosomal Proteolysis**

On the other hand, the lysosomal proteolysis pathway in eukaryotic cells involves the degradation of proteins within lysosomes. Lysosomes are membrane-enclosed organelles equipped with a variety of digestive enzymes, including several proteases like Cathepsins. Cathepsins are a family of lysosomal proteases that includes several members, among which lysosomal Pro-Xaa Carboxypeptidase (PPCA), Neuraminidase and other cysteine proteases (Turk et al. 2012; Yadati et al. 2020). They serve multiple roles in cell metabolism, including the breakdown of extracellular proteins acquired through endocytosis and the gradual renewal of cytoplasmic organelles and cytosolic proteins.

The primary mechanism for the internalization of molecules that need to be degraded into the lysosomes is known as autophagy. It involves the formation of vesicles called autophagosomes, within which small regions of cytoplasm or cytoplasmic organelles are enclosed by membranes derived from the ER (Yim and Mizushima 2020). These vesicles subsequently merge with lysosomes, allowing the lysosomal enzymes to break down their contents. A key element during autophagy is LC3 (microtubule-associated protein 1A/1B-light chain 3). It exists in two forms: LC3I and LC3II and it is used as a marker for macroautophagy (Tanida et al., 2008; Runwal et al. 2019). LC3 is synthesized as an inactive precursor of LC3II (LC3I or pro-LC3). It is then conjugated to phosphatidylethanolamine (PE) on the membrane of new vesicles (autophagosomes) and processed into LC3 II. It plays a role in cargo recognition interacting with specific receptors and helps the maturation of autophagosomes first, and the fusion process by interacting with lysosomal proteins later. LC3-II on the autolysosomal membrane may be released and recycled for future autophagic events (Tanida et al. 2008).

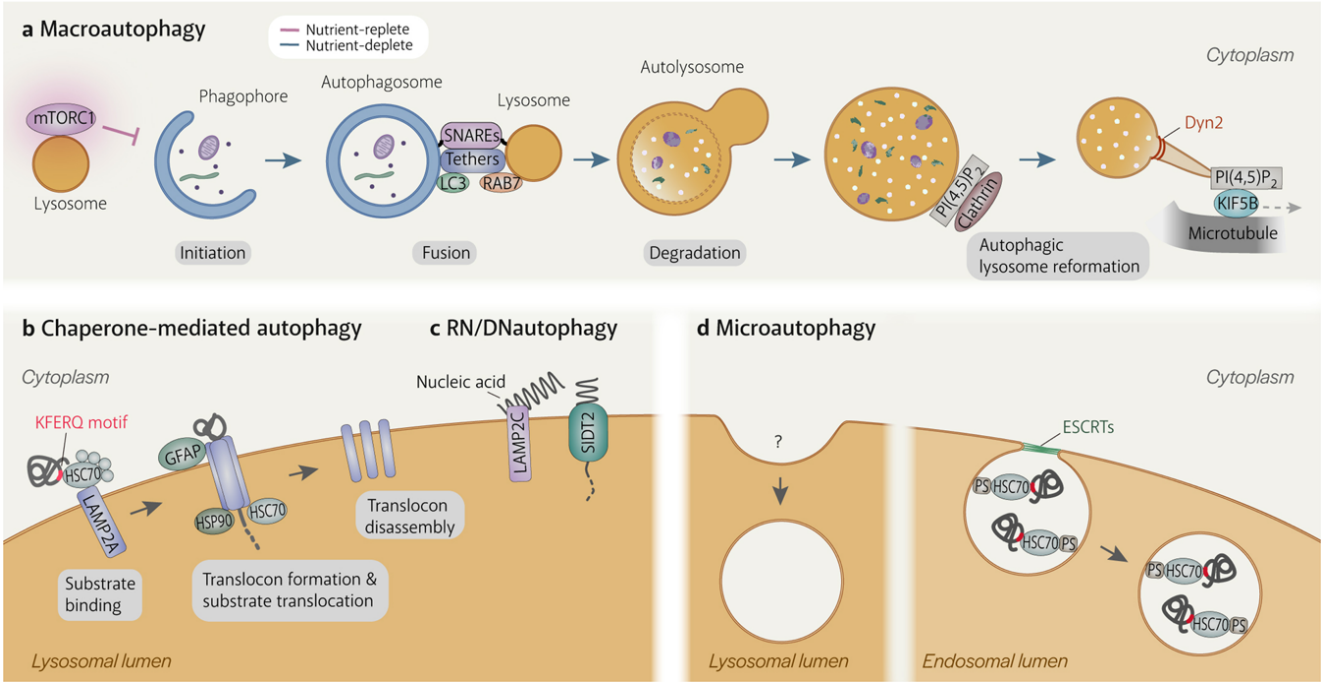

Figura 12: Lysosomal degradation pathways. Image showing the different types of autophagy and fusion with lysosomes (Yim and Mizushima 2020).

The process of protein uptake into autophagosomes is generally nonselective, leading to the gradual degradation of long-lived cytoplasmic proteins over time. However, then lack of selectivity is not universal for all proteins. For instance, some proteins contain amino acid sequences resembling the consensus sequence Lys-Phe-Glu-Arg-Gln, which likely serves as a targeting signal for lysosomal degradation (Chiang and Dice, 1988). This process requires the involvement of a member of the Hsp70 family of molecular chaperones, as this assists in unfolding the polypeptide chains during their transport across the lysosomal membrane. The proteins susceptible to degradation through this pathway are typically long-lived but dispensable proteins (Nylandsted et al. 2004). During periods of cellular starvation, these proteins are sacrificed to provide amino acids and energy, enabling essential metabolic processes to continue functioning.

TRANSMEMBRANE 16 PROTEIN FAMILY

In the context of this project, understanding the role of the transmembrane protein 16 (TMEM16) family in association with SARS CoV 2 infection is crucial. This family comprises calcium-dependent chloride channels and, in some cases, lipid scramblases. This study delves into the roles of two of these proteins and their potential interactions with ACE2 and SARS-CoV-2 spike.

TMEM16s are also known as Anoctamins because these proteins were first identified as anion channels (an) and thought to have eight transmembrane helices (8=octa). They are part of a larger group of proteins called Ca2+-activated chloride channels (CaCCs). The CaCCs are found in almost all species ranging from invertebrates to mammals, and the ubiquitous expression of CaCCs indicates a variety of functions important for physiology, including regulation of epithelial Cl– secretion, excitability of neuronal and cardiac cells, smooth muscle contraction and nociception (Hartzell et al. 2005; Ji et al. 2019; Oh and Jung 2016).
TMEM16s, despite the anoctamin name, contain ten transmembrane domains with two large intracellular loops. They are approximately 1100 amino acids long and have a molecular weight of about 100-110 kDa. Notably, both the N-terminus and C-terminus are intracellular and, in contrast to other membrane proteins like ACE2, TMEM16 family members are synthesized and integrated directly into the membrane through a process involving transmembrane domains (TMDs), which facilitate their insertion into the lipid bilayer (Feng et al. 2023).

TMEM16 proteins form dimeric structures, where each subunit consists of 10 transmembrane α-helices (TMs) (Brunner et al. 2014) and possesses an individual ion conduction pore specialized for chloride ions (Cl-) surrounded by TM3-TM7. Activation dependent on calcium involves the direct binding of calcium ions to two adjacent calcium-binding sites created by TM6-TM8. This structure also confirmed biochemical results suggesting that a critical sequence of 78 amino acids in the NH2-terminal region are necessary for dimerization. In fact, the dimerization interface is formed in part by interaction between the NH2 terminus of one chain and the COOH terminus of the other (as well as interactions between transmembrane domains in the hydrophobic core of the bilayer) (Feng et al. 2023).

Among the ten homologous proteins within this family, TMEM16A (also known as anoctamin 1 or ANO1) and TMEM16F (or anoctamin 6 or ANO6) have received more comprehensive investigation due to their physiological functions and pathological implications.

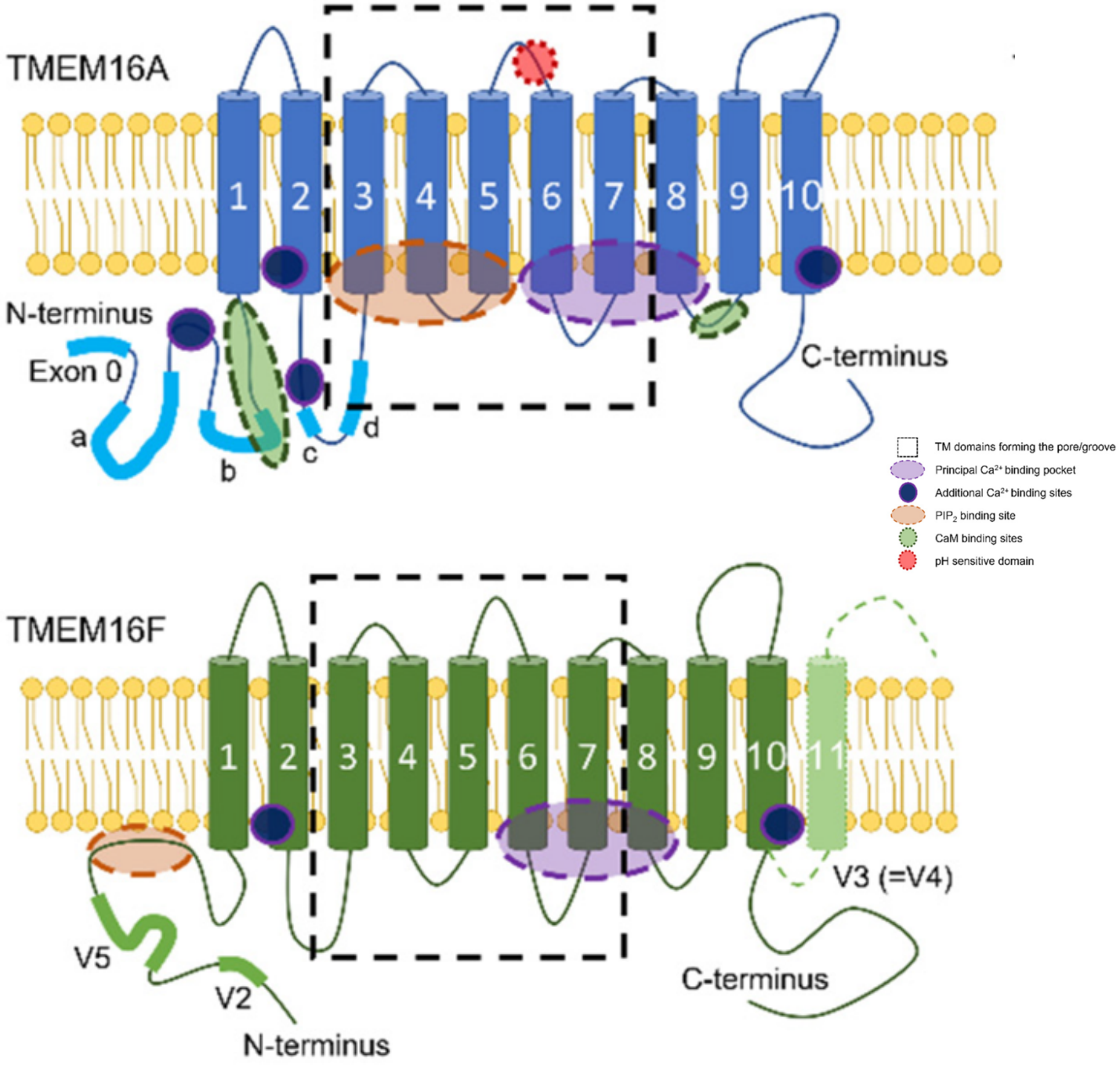

Figura 13: **Molecular structure of TMEM16A and TMEM16F.** This figure represents the structure of TMEM16A and TMEM16F. They have 10 transmembrane domains, the site surrounded by TM6. TM7 and TM8 is the Ca2+ binding domain, while TM 3-7 are forming the pore for Cl- exchange (Agostinelli and Tammaro 2022).

Structural examinations of both calcium-free and calcium-bound states of the calcium-activated chloride channels TMEM16A and TMEM16F reveal significant conformational changes in TM6 that are driven by calcium ions. TMEM16F and TMEM16A share similar structural features, characterized by protein-enclosed pores that facilitate ion permeation. TMEM16F, in addition to its channel function, works as a scramblase, exposing phosphatidylserine (PS) on the external side of the cell membranes.

- **TMEM16A**

The Ca2+-gated Cl– channel TMEM16A (ANO1), was initially discovered in Xenopus oocytes nearly four decades ago. Over the years, it has emerged as a pivotal regulator of essential physiological functions, including the control of vascular tone, local blood flow regulation, and epithelial solute transport (Yang et al. 2008). This channel has garnered attention as a potential target for various diseases, such as hypertension, stroke, cancer, and cystic fibrosis (CF) (Benedetto et al. 2017; Crottès and Jan 2019; Danielsson et al. 2015).

Recent studies have shed light on TMEM16A inner workings, revealing the presence of two Ca2+ binding sites within the pore inner vestibule. Binding of Ca2+ triggers conformational changes in an α-helix, rendering the pore conductive (Dang et al. 2017). Furthermore, TMEM16A activation can be regulated by factors such as calmodulin, protons, cell volume, and thermal stimuli (Herrero, Sanchez, and Lorente 2018). Additionally, phosphatidylinositol 4,5-bisphosphate (PIP2) plays a role in modulating the activation and desensitization of TMEM16A (Le et al. 2019; Yu et al. 2019).

TMEM16A exhibits a preference for activation in response to local increases in intracellular Ca2+ released from the ER, which may represent a common mechanism for TMEM16A activation (Jin et al. 2016). Its expression is subject to regulation by multiple signaling pathways, including mitogen-activated protein kinase (MAPK), nuclear factor κB (NF-κB), and transforming growth factor-β (TGF-β) in pathological contexts (Crottès and Jan 2019).

Recent advancements in understanding the structure and gating mechanisms of TMEM16A have opened avenues for rational drug design, potentially expediting the discovery of novel drug-like modulators.

As a promising drug target, TMEM16A has garnered significant attention, resulting in the identification of various inhibitors. Among these, several drugs are of particular interest, including clarithromycin, benzbromarone, niclosamide, nitazoxanide, and avermectins

(Danielsson et al. 2015; Li et al. 2019; Shang et al. 2013). Notably, niclosamide and nitazoxamide, originally clinical anthelmintics, have been identified as potent TMEM16A inhibitors capable of blocking airway smooth muscle (ASM) depolarization and contraction (Miner et al. 2019). Intriguingly, recent research indicates that the upregulation of TMEM16A depolarizes the membrane potential of pulmonary artery smooth muscle cells (PASMC), contributing to vasoconstriction and increased pulmonary vascular resistance in pulmonary arterial hypertension (PAH) rats (Papp et al. 2019). Furthermore, studies have shown that Ang II significantly enhances TMEM16A expression in human umbilical vein endothelial cells, and endothelial-specific TMEM16A knockout significantly reduces Ang II-induced hypertension through the ROS signaling pathway (Ma et al. 2017).

- **TMEM16F**

TMEM16F (ANO6) plays a multifaceted role as both a calcium-activated ion channel and a calcium-activated lipid scramblase. Its functions are integral to critical cellular processes, including membrane fusion, membrane budding, blood coagulation, extracellular vesicle generation, protection against arthritis, and membrane repair (N et al. 2020).

The asymmetrical distribution of various phospholipids within the mammalian cell plasma membrane has long been recognized. This asymmetry is typically described for major phospholipids: PS and phosphatidylethanolamine (PE) are predominantly found in the inner leaflet, while phosphatidylcholine (PC) and sphingomyelin (Sph) on the outer surface. PS distribution is the one that is more often studied because of the specific proteins that bind this phospholipid (Bretscher 1972).

The enzymes responsible for establishing and maintaining lipid asymmetry belong to the P4 subfamily of P-type ATPases and use ATP to transport phospholipids against concentration gradients. These enzymes typically form heterodimers with members of the TMEM30 family of membrane proteins. Lipid asymmetry is crucial for various cellular processes, including signaling, apoptotic pathways, and membrane fusion (Wu et al. 2020).

The regulated scrambling of bilayer phospholipids is a process influenced by proteins but can also occur independently of protein catalysis. Scrambling agents include chemical compounds, organic molecules, peptides, and proteins (Arndt et al. 2022).

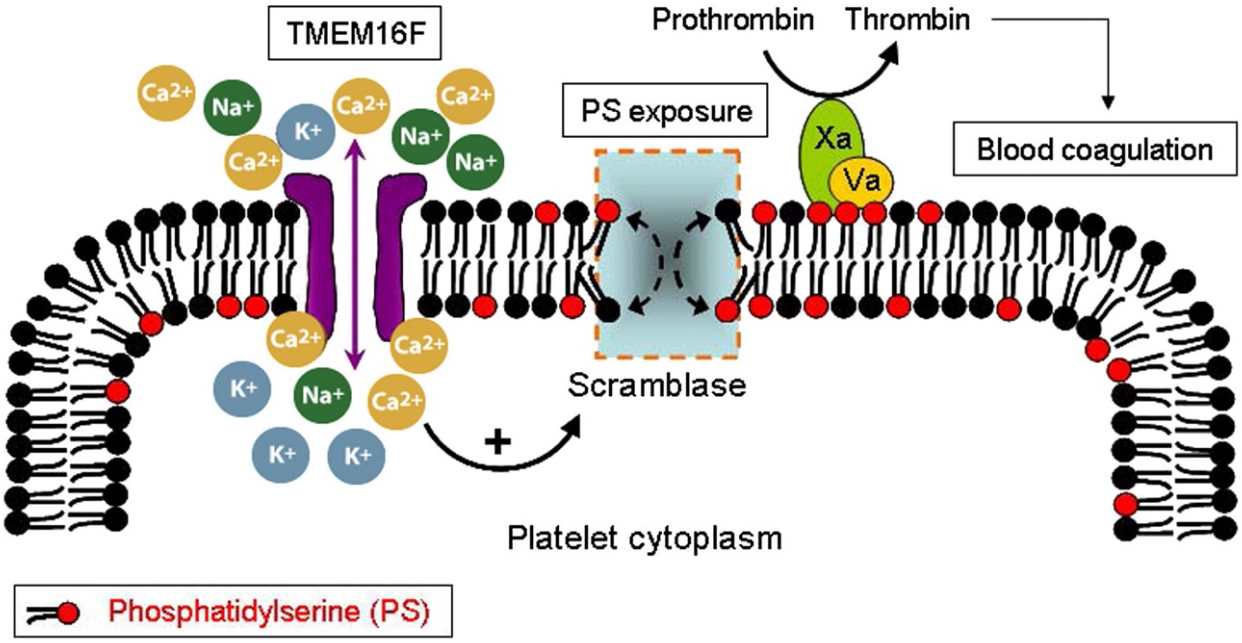

Figura 14: **Scramblase function of TMEM16F.** Image representing the scramblase activity of TMEM16F: thanks to its activity, phosphatidylserine is exposed on the membrane external layer, starting a molecular signalling (Yang et al. 2012).

TMEM16F-mediated PS exposure plays a key role in cell fusion and the entry of enveloped viruses. Modulators of TMEM16F can inhibit SARS-CoV-2 virus entry and the formation of syncytia induced by interactions between the spike protein and its ACE2 receptor on adjacent cells (Bricogne et al. 2019). In platelets, Ca2+-activated PS exposure is a crucial step in blood coagulation, and mutations in TMEM16F are associated with a bleeding disorder known as Scott Syndrome (Yang et al. 2012). However, it is important to note that PS exposure during apoptosis, which marks cells for phagocytosis, does not depend on TMEM16F (Bricogne et al. 2019).

Recent investigations suggest that the TMEM16F protein-enclosed open pore, stabilized by activating mutations, encompasses roughly half the thickness of the lipid bilayer, thus supporting the idea of a distinct route for lipid translocation across the bilayer. The redistribution of lipids appears to be facilitated by membrane distortion and thinning, which can be influenced by specific conformations of the TMEM16F protein. These conformations can be stabilized by factors such as the presence of PIP2 or activating mutations. Notably, certain mutations in residues responsible for lipid coordination and charged residues near membrane

distortion have been observed to affect the timing of lipid exposure, without interfering with calcium influx. In addition, alanine substitutions of K370 and F374 on TM2, residues lining the lipid trail specifically altered TMEM16F-mediated PS exposure only, while both niclosamide and the pore blocker 1PBC demonstrated dose-dependent inhibition of TMEM16F-mediated Ca2+ influx and PS exposure (Wu et al. 2020). These findings collectively provide evidence for a separate lipid scrambling pathway outside the ion conduction pore of TMEM16F.

NICLOSAMIDE

Niclosamide (5-chloro-salicyl-(2-chloro-4-nitro) anilide) is synthesized through the condensation of 2-chloro-4-nitrobenzenamine with 5-chloro-2-hydroxybenzoyl chloride. The latter compound is prepared by chlorinating 5-chloro salicylic acid using thionyl chloride. It is a small molecule with an average weight of 327.12 and its chemical formula is C13H8Cl2N2O4. It was originally developed and marketed as a molluscicide by Bayer in the late 1950s, and approved by the US Food and Drug Administration (FDA) as an effective anthelmintic drug for the treatment of tapeworm infections in 1982 (Andrews et al., 1982; Wang et al. 2022). It may act by uncoupling the electron transport chain of the oxidative phosphorylation pathway preventing ATP synthase in worms on contact. niclosamide is minimally absorbed from the gastrointestinal tract and rapidly eliminated by kidneys making it safe for human health upon oral administration for tapeworm infection, with minimal toxicity (Wilkie et al. 2019).

Recent studies highlighted the existence of interactions between niclosamide and several molecular pathways, describing this molecule as a promising candidate for the treatment of different diseases such as metabolic diseases (Chen et al. 2018), immune system diseases like rheumatoid arthritis (Huang et al. 2016), systemic sclerosis (Morin et al. 2016) and systemic lupus erythematosus (Han et al. 2020), asthma, arterial constriction, myopia, cancer and bacterial and viral infections (Yavuz and Çelikyurt 2021; Wang et al. 2022).
It has been shown that niclosamide is able to induce apoptosis in cancer through mechanisms that mainly involve the mitochondrial pathway, the ER pathway, and death receptor pathway. It was reported that niclosamide blocks DCLK1-B transcription by disrupting the binding between lymphoid enhancer binding factor 1 (LEF1) to the doublecortin-like kinase 1 (DCLK1-B) promoter, leading to increased apoptosis (Park et al. 2019). In addition, niclosamide activates caspases that induce apoptosis as well and elevates ROS level via ER stress and mitochondrial potential loss. More specifically, niclosamide inhibits the Notch pathway (Suliman et al. 2016), regulates AMPK-mTOR (Figarola et al. 2018) and inhibits Wnt/β-catenin (Lee et al. 2020) signaling pathways. Furthermore, the drug also plays a role in modulating STAT3 and NF-κB, especially in a cancer context (Wang et al. 2022). Finally, niclosamide promotes mTORC1-dependent autophagy and cell death by targeting pGSK3β-mediated non-canonical Hedgehog signaling, thereby promoting apoptosis (Kaushal et al. 2021).

Niclosamide has broad-spectrum antiviral activities against SARS (J. Xu et al. 2020), MERS-CoV (Mostafa et al. 2020), Zika virus (ZIKV) (Li et al. 2020), Japanese encephalitis virus (JEV) (Fang et al. 2013), hepatitis C virus (HCV) (Xu et al. 2020), Ebola virus (EBOV) (Herring et al. 2021), human rhinovirus (HRV) (Jurgeit et al. 2012), Chikungunya virus (CHIKV) (Wang et al. 2016), human adenovirus (HADV) (Xu et al. 2021), and Epstein–Barr virus (EBV) (Huang et al. 2017). In particular, it was reported that niclosamide can inhibit the replication and cytopathic effect of SARS coronavirus at low concentrations of 1 M and eliminate viral antigen synthesis at 1.56 M (Wu et al. 2004) as well as can inhibit MERS-CoV replication by 1000-fold, even if the specific mechanism has not been clarified (Brunaugh et al. 2021). As already mentioned, the Giacca group has proposed the potential use of niclosamide in SARS-CoV-2 infection as an inhibitor of syncytia formation, due to its ability of blocking TMEM16F.

In literature, there are different studies highlighting how niclosamide can block TMEM16A as well, resembling the action of its pore blocker 1PBC. The structures of TMEM16A and TMEM16F, as defined by cryo-electron microscopy, are very similar. A study of Chai and colleagues showed that these proteins exhibit a lipid trail within a groove flanked by TM1 and TM6 which is positioned outside TMEM16s pore. When cells are treated with niclosamide or 1PBC, the lipid trail is not visible anymore in cryo-electron microscopy, suggesting that those molecules are binding a pocked located near the extracellular end of the groove between TM1 and TM6 (Chai et al. 2020).
Niclosamide triggers a time-dependent elevation in the levels of LC3 II and autophagy-related protein 5 (Atg5). This effect becomes evident just 24 hours after treatment, signifying that its actions include the enhancement of autophagy (Chai et al., 2020). It's worth noting that inhibiting autophagy amplifies the apoptotic cell death induced by niclosamide.

For all the above reasons, niclosamide is regarded as a low-cost drug with extensive antiviral properties that show very promising potential for clinical development.

AIM

OVERALL AIM

This study aims to understand whether an interaction between ACE2 and TMEM16A as well as ACE2 and TMEM16F occurs in the cells. In particular, a computational prediction by Dr. Sergio Pantano (Pasteur Institute, Montevideo, Uruguay) (Fig. A) suggested that the transmembrane helix of ACE2 can interact with TMEM16A on the TM6 pore, possibly through Gly747 and Gly751. This possibility is explored in this Thesis work.

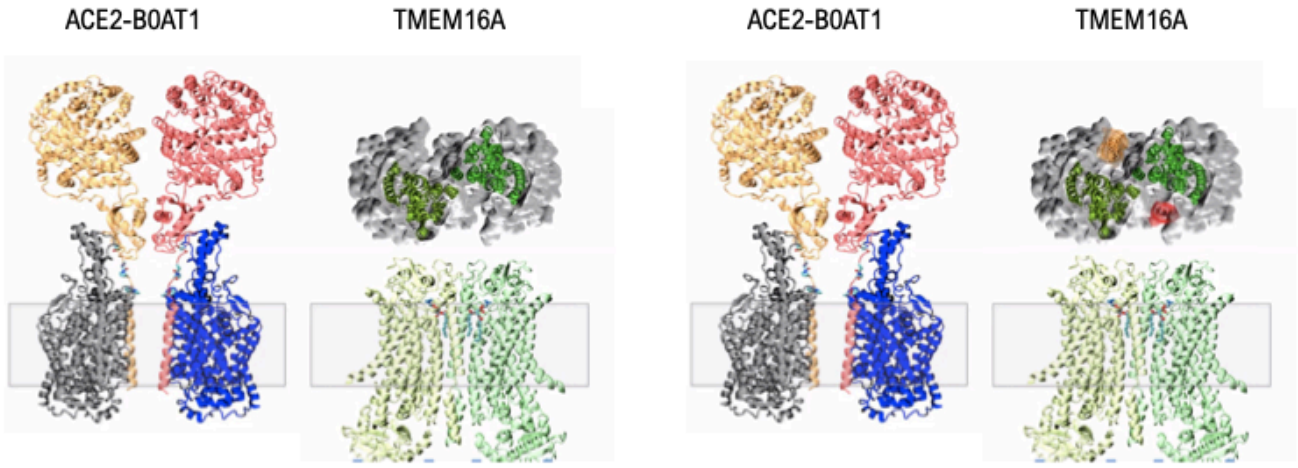

Figure A: Computational prediction of ACE2-TMEM16A interaction. On the left side of every image (1a and 2a) there is the representation of ACE2 and TMEM16A structures. ACE2 dimer (yellow and red) binds B0AT1 (gray and blue) with its transmembrane helixes. On the right side of both images (1b and 2b) there is TMEM16A (light green and green), 1b and 2b show TMEM16A from a top view, while 1c and 2c show a frontal view. The image on the right (2, 2b) is showing how ACE2 is supposed to interact with TMEM16A, inserting its helixes (red and yellow) into TMEM16A pores. The hypothesis is that ACE2 needs its Gly747 and Gly751 for this interaction.

SPECIFIC AIMS

While investigating the interaction between ACE2 and TMEM16s, we wanted to provide answers to the following specific questions:

- Do TMEM16A and TMEM16F (TMEM16s) interact with spike?
- Does niclosamide block the interaction between ACE2 and TMEM16s or between spike and TMEM16s?
- Are the TMEM16s involved in spike-driven lysosomal ACE2 degradation?
- Do the TMEM16s lead to ACE2 lysosomal degradation?

MATERIALS AND METHODS

Cells

Vero (WHO) clone 118 cells (ECACC 88020401), U-2 OS (U2OS; ATCC HTB-96), HEK293T (ATCC CRL-3216) were cultured in DMEM with 1 g l^{-1} glucose (Gibco) supplemented with 10% heat-inactivated fetal bovine serum (FBS) (Life Technologies), without antibiotics. Cells were incubated at 37 °C, 5% CO2.

All cell lines were negative for mycoplasma contamination. Cell lines were not authenticated.

Stable Cell Line Generation

HEK293T stabling expressing ACE2 have been used, this cell line has been kindly provided by Prof. Giacca's lab.

U2OS and Vero cell lines stably expressing ACE2-eGFP were obtained through the Transgene Knockin via CRISPR at AAVS1 and ROSA26 Loci Kit (GE100027 Origene). We used ACE2eGFP (154962 AddGene) for the insert, while the pAAVS1-Puro-DNR (GE100024) was the donor. To note, two primers were ordered to insert restriction enzymes sites on ACE2-eGFP: AATGTCGACAATtttaaacgggccctctagaccat for SalI and attGCGGCCGCattaacgcggatccaagcttaagt for NotI. Once obtained the plasmid through cloning, we followed the manufacturer's instruction transfecting 1ug of donor and 1ug of GE100023 pCas-Guide-AAVS1 diluting them in Opti-MEM (Life Technologies), mixed with the transfection reagent (FuGENE HD, Promega). Cells were then splitted 10 times 1:10 and puromycin (2ug/mL or 3ug/mL) selection for 3 weeks. Cells were then diluted in order to get a single cell clone in a 96 wells plate well and then expanded.

Antibodies

Antibodies against the following proteins were used: TMEM16A (Abcam, ab64085), TMEM16F (Abcam ab234422 and Sigma-Aldrich HPA038958-100UL), FLAG(F3165 Sigma-Aldrich), ACE2 (Abcam ab87436 and ab15348), V5 (Thermo Fisher Scientific R96025), Goat anti-Mouse: Alexa Fluor 594 (A32742, Thermo Scientific), Alexa Fluor 647 (a32728, Thermo Fisher) Alexa Fluor 488 (A32723, Thermo Scientific); Goat anti-Rabbit: Alexa Fluor 594 (A32740, Thermo Scientific), Alexa Fluor 647 (A32733, Thermo Scientific), Alexa Fluor 488

(A32731, Thermo Scientific), Alexa Fluor 488 (# A32742, Thermo Fisher), Goat anti-Rat Alexa Fluor 647 (A48265; Thermo Scientific) mouse-HRP (Abcam ab6789), rabbit-HRP (Abcam ab205718), SARS-CoV-2 spike protein (GeneTex GTX632604), anti Sodium Potassium ATPase (MA5-32184, Thermo Scientific), anti LC3 (2775S Cell Signaling Technology).

Plasmids

The expression plasmid pEC117- spike -V5 was generated as follows: the SARS-CoV-2 wild-type protein (NCBI accession number NC_045512.2, position 21563-25384) was codon-optimized and synthesized in two fragments of approximately 2 kb each as gBlock DNA fragments (IDT Integrated DNA Technologies) with the in-frame addition of the V5 tag at the C terminus, and then cloned into the pZac 2.1 backbone under the control of the cytomegalovirus (CMV) IE promoter. The construct DNA sequences were verified by Sanger sequencing. The following expression vectors were used: hTMEM16A (GenScript OHu26085D), hTMEM16F (GenScript OHu26351D), hACE2 (Addgene 1786), pCMV-eGFP (obtained from L. Zentilin), mSCARLET (AddGene 85042), ACE2eGFP (AddGene 154962), TMEM16AmSCRLET (from Prof. Giacca's lab), TMEM16FmSCARLET (from Prof. Giacca's lab).

Small Interfering RNAs (siRNA) knockdown

For TMEM16A and TMEM16F knockdown, siRNAs (Dharmacon siGENOME SMARTpools, four siRNAs per gene target) targeting TMEM16A (also known as ANO1) (M-027200-00-0005), TMEM16F(ANO6) (M-003867-01-0005) were used, siRNA buffer and a non-targeting siRNA were used as controls.

Basing on the type of analysis needed: IF, qPCR or WB, plates of 96 wells (CellCarrierUltra 96, PerkinElmer), 12 wells (10253041 Thermo Fisher Scientific) or 6 wells (10578911 Thermo Fisher Scientific) were respectively used.

In brief, the transfection reagent (Lipofectamine RNAiMAX, Life Technologies) was diluted in Opti-MEM (Life Technologies) and incubated for 30 minutes with siRNAs, aiming at a final concentration of 25 nm once in cell medium.

Cells were seeded as reported in table 2, following the reverse transfection protocol.

Twenty-four hours after siRNA transfection, cells were transfected with expression plasmids (see table for the amount) following a standard forward transfection protocol.

After 48 h from siRNA transfection, cells were fixed and stained for IF or cell lysates were analyzed by qPCR and/or western blotting, as detailed later.

Forward

Cell line	10cm Petri	6-well plate	12-well	8-well slide	96-well plate
U2OS	1,5 M	300.000	175.000	32.000	10.000
VERO	1 M	150.000	87.500	15.000	5.000
HEK293T	1,7 M	320.000	190.000	37.000	12.000

Reverse

Cell line	10cm Petri	6-well plate	12-well	8-well slide	96-well plate
U2OS	3 M	480.000	260.000	50.000	14.000
VERO	2 M	240.000	130.000	25.000	8.000
HEK293T	3,2 M	500.000	285.000	60.000	16.000

Table 2: **Number of cells seeded for transfection.** The table show the number of cells seeded basing on the cell line and the type of plate used. With “forward” we mean a protocol where cells are seeded on day 0 and transfection occurs on day 1 (after 24H), while “reverse” means that the transfection occurs while cells are seeded.

Plasmid Transfection

In brief, pDNA was diluted in Opti-MEM (Life Technologies), mixed with the transfection reagent (FuGENE HD, Promega) using the following ratios: 1 µg pDNA:3µl FugeneHD. The mix was incubated for 20 min at room temperature and added to the siRNA-transfected plates. After 24 h or 48h, cells were fixed in 4% paraformaldehyde and processed for immunofluorescence.

Drugs

Cells were treated 24h after transfection with niclosamide (N0560000 Sigma Aldrich) 5uM for 24h or 10uM for 6h, cyclohexamyde (01810-1G Merck Life Science Ltd) 100nm for 24h, or pre-treated with bafilomycin (ab120497 abcam) 100nm, MG132 (M7449-200UL Merck Life Science Ltd) 10 µg for 4 hours, followed by transfection, cells were treated in total for 24 hours.

Fractionation Assay

For the fractionation of cell lysate we used the Pierce Subcellular Protein Fractionation Kit, Thermo Scientific. Cells were grown on 10cm dishes and then collected harvesting samples with trypsin-EDTA and then centrifuged. Cells were then resuspended in ice-cold PBS. 10

million cells are needed for the assay. We then followed the manufacturer's instruction, adding different buffers and using different incubation and centrifugation timings to separate proteins from different cell compartments. All protein samples were conserved at -80°C.

RNA extraction and qPCR

Total mRNA was isolated from U2OS, HEK293T or Vero cells 48 h after siRNA transfection or 24/48h after plasmid transfection using Trizol as lysing reagent and the miRNAeasy kit (217004 Qiagen) for the extraction. The RNA obtained (0.5–1 µg) was reverse-transcribed using iSript kit (1725035BUN Bio-Rad) with random hexameric primers (10 µM) in a 20-µl reaction following the manufacturer's instructions. Quantification of the gene expression of ACE2 (Hs01085333_m1), TMEM16A (Hs00216121_m1), and TMEM16F (Hs03805835_m1) was performed by quantitative PCR (qPCR) using Taqman probes. Expression of the housekeeping gene GAPDH(Hs02786624_g1) was used for normalization.

Amplifications were performed using a QuantStudio3 machine using TaqMan Gene Expression Master Mix (Applied Biosystems 4369016). The qPCR profile was programmed with a standard protocol, according to the manufacturer's instructions.

Immunofluorescence

After fixation in 4% PFA for 10 min at room temperature, cells were washed three times in 100 µl per well of PBS and then permeabilized in same volumes of 0.1% Triton X-100 (Sigma-Aldrich 1086431000) for 10 min at room temperature. Cells were then washed three times in PBS and blocked in 10% Goat Serum for 1 h at room temperature. After blocking, the supernatant was removed, and cells were stained according to type of staining, as follows.

Primary antibodies were diluted 1:500 into Goat Serum 10% and let overnight (ON) at 4 degrees. On the second day, primary antibodies were tapped off and cells were washed three times in PBS. Cells were incubated 1h with secondary antibody diluted 1:500 in PBS at RT and then washed in PBS 3X again. Finally, 100 µl of Hoechst (H3570) diluted 1:5000 in PBS was added in every well.

Image acquisition was performed using the Operetta CLS high content screening microscope (Perkin Elmer) with a Zeiss 20× (NA 0.80) objective. A total of 25 fields per well were imaged at three different wavelengths: (1) excitation 365–385 nm, emission 430–500 nm (nucleus 'blue'); (2) excitation 460–490 nm, emission 500–550 nm ('green'); (3) excitation 615–645 nm

emission 655–750 nm (‘red’) (4) excitation 561–594 nm emission 618-700 nm (‘red’). Images were subsequently analyzed, using the Harmony software (PerkinElmer).

Proximity Ligation Assay

The proximity ligation assay (PLA) is a technique that allows detection of protein interaction. It could be direct or indirect, basing on the fact that, respectively, the primary or secondary antibodies are conjugated with PLA probes. In this study we used the indirect PLA, where we choose pairs of antibodies raised in different species to detect the target proteins (Fig. 15-2). Then, a pair of oligonucleotide-labels secondary antibodies (PLA probes) binds the primary antibodies (Fig.15-3). Next, hybridizing connector oligos join the PLA probes only if they are in close proximity to each other (closer than 40 nm) and a ligase forms a closed, circle DNA template that is required for rolling-circle amplification (RCA). The PLA probe then acts as a primer for a DNA polymerase, which generates concatemeric sequences during RCA (Fig. 15-4). This allows up to 1000-fold amplified signal, allowing localization of the signal. In our case, the signal is red and detectable at an emission wavelength of 595 nm.

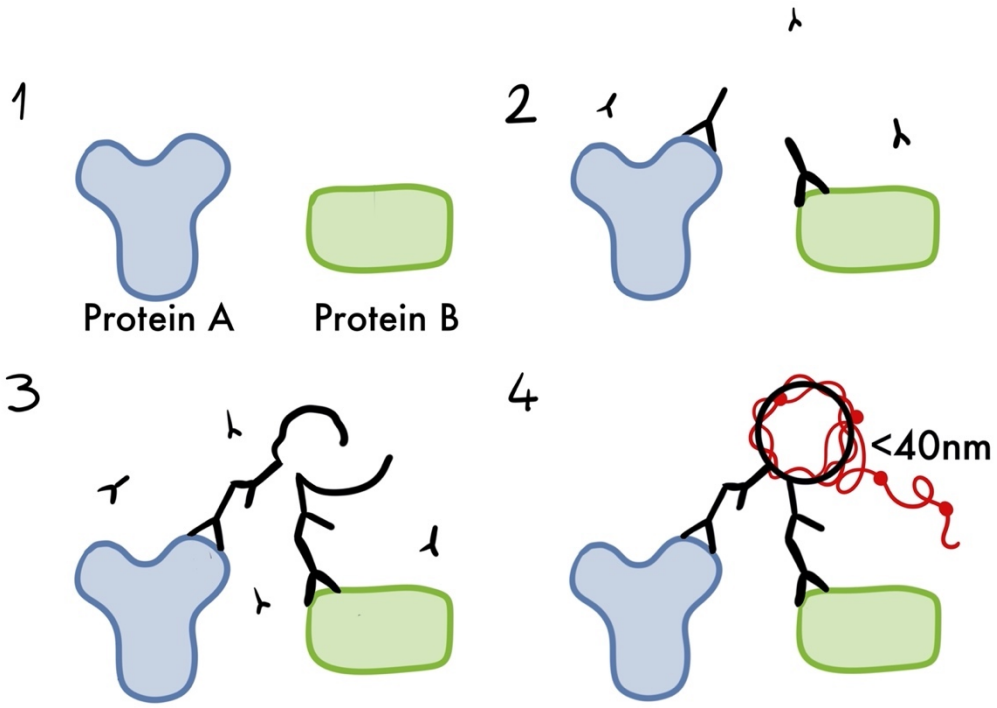

Figure 15: Proximity ligation assay. Two target proteins are bound by primary antibodies raised in different species. Secondary antibodies, linked to pairs of oligonucleotides, bind the primary antibodies and, if the target proteins are closer than 40 nm, a ligase joins the oligos into a circular DNA. This is amplified by a DNA polymerase and gives a red fluorescent signal in correspondence of the protein interaction.

The protocol, more in detail is: after fixation in 4% PFA for 10 min at room temperature, cells were washed two times in 100 µl per well (96-well plate) of PBS and then permeabilized in same volumes of 0.1% Triton X-100 (Sigma-Aldrich 1086431000) for 10 min at room temperature. Cells were then washed three times in PBS and blocked in blocking reagent following the manufacturer's instruction of the Proximity Ligation Assay Kit (DUO92008 Detection Reagents Kit) at room temperature. After blocking, the supernatant was removed, and primary antibodies were added ON 1:500. The following day, samples were washed in buffer A, Probe anti-Rabbit PLUS (DUO92002-100RXN, Sigma-Aldrich), and Probe anti-Mouse (DUO92004-100RXN, Sigma-Aldrich) were added and instructions for detection were followed as described in the manufacturer's kit.

Image acquisition was performed using the Operetta CLS high content screening microscope (Perkin Elmer) with a Zeiss 20× (NA 0.80) objective. A total of 25 fields per well were imaged at three different wavelengths: (1) excitation 365–385 nm, emission 430–500 nm (nucleus 'blue'); (2) excitation 460–490 nm, emission 500–550 nm ('green'); (3) excitation 615–645 nm emission 655–750 nm ('red') (4) excitation 561–594 nm emission 618-700 nm ('red'). Images were subsequently analyzed, using the Harmony software (PerkinElmer).

Fluorescence Resonance Energy Transfer

Fluorescence resonance energy transfer (FRET) is a technique which uses pairs of fluorescent proteins which are acting as donor and acceptor in case they are in close proximity (less than 10 nm). In this study we used spectral FRET, which principle is that, given two target proteins A, B which interaction is unknown, a pair of fluorescent proteins are cohen to be fused to A and B in order to get a couple of fluorophores in which the donor could excite di acceptor with its emission wavelength. We choose the pair eGFP (ex: 488 nm, em 500-550) - mScarlet (ex: 561, em 594). Again, only if the target proteins are closer than 40nm, eGFP could transfer energy to mScarlet which could fluoresce.

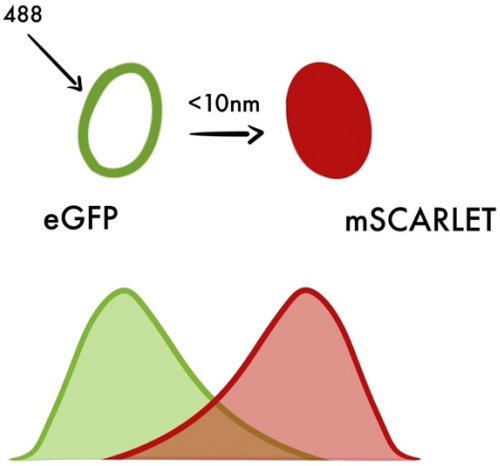

Figure 16: **Fluorescence resonance energy transfer.** In FRET, pairs of fluorophores are choose in order to obtain one that acts as a donor and the other as an acceptor. In this image the couple eGFP-mScarlet is represented: eGFP is excited at 488 nm and, given the fact its emission wavelength could excite mScarlet, if the two proteins are in close proximity (10 nm), eGFP donates energy to mScarlet which fluoresces and its red signal is detected at 594 nm.

U2OS cells were grown on 8 wells slides and transiently co-transfected with the appropriate EGFP- and mScarlet fusion plasmids: eGFP-ACE2 or eGFP- spike and TMEM16A- mScarlet or TMEM16F- mScarlet. After 48 h, cell imaging was conducted by Nikon AR1 HD25 confocal microscope. The excitations used were 488 and 561, where: 488 - eGFP was the Donor- Donor channel, 561 - mScarlet the Acceptor - Acceptor channel; 488 - mScarlet the Donor - Acceptor (FRET) and 561 - eGFP the Acceptor- Donor.

All the analyses were performed through the Nikon software, NIS element. Calibration was calculated on the Donor only and Acceptor only images, taking into account the bleedthrough and using the sensitized emission method.

Normalised FRET analysis were performed using the ImageJ pixFRET plugin, developed by Laurent Gelman group, University of Lausanne. In this case the normalized FRET images were calculated on the following formula:

$$N_{FRET} = \frac{I_{FRET} - BT_{DONOR} \times I_{DONOR} - BT_{ACCEPTOR} \times I_{ACCEPTOR}}{N}$$

where:

I_{FRET} = intensity of fluorescence of the FRET image (signal detected exciting at 488 nm and acquiring mScarlet emission wavelenght)

BT_{DONOR} = Donor Bleedthrough

I_{DONOR} = Fluorescence intensity of Donor

$BT_{ACCEPTOR}$ = Bleedthrough of the acceptor

$I_{ACCEPTOR}$= Fluorescence intensity of the acceptor

N = normalizer… in this case we used the squared product of IDonor and IAcceptor

Western blotting

After siRNA transfections for 48–72 h, HEK293 cells were collected and homogenized in RIPA lysis buffer (20 mM Tris-HCl, pH 7.4, 1 mM EDTA, 150 mM NaCl, 0.5% Nonidet P-40, 0.1% SDS, 0.5% sodium deoxycholate supplemented with protease inhibitors (Roche)) for 10 min at 4 °C and sonicated by using Bioruptor (Diagenode) for 10 min. Equal amounts of total cellular proteins (10–20 µg), as measured with the BSA reagent (Biorad), were resolved by electrophoresis in 4–20% gradient polyacrylamide gels (Mini-PROTEAN, Biorad) and transferred to nitrocellulose/PVDF membranes (GE Healthcare). Membranes were blocked at room temperature for 60 min with PBST (PBS + 0.1% Tween-20) with 5% skim milk powder (Cell Signaling, 9999). Blots were then incubated (4 °C, overnight) with primary antibodies against ACE2 (diluted 1:1,000), TMEM16A (1:500), TMEM16F (1:500), β-actin-HRP (diluted 1:10,000), V5 (diluted 1:5,000) or FLAG (diluted 1:1000). Blots were washed three times (5 min each) with PBST. For standard western blotting detection, blots were incubated with either anti-rabbit HRP-conjugated antibody (1:5,000) or anti-mouse HRP-conjugated antibody (1:10,000) for 1 h at room temperature. After washing three times at room temperature with PBST (10 min each), blots were developed with ECL (Amersham) and images were acquired with ChemiDoc.

Co-Immunoprecipitation

Cell lysates were collected using an in-house lysis buffer (for 50 mL of solution: 1% (0.5% w/v) of Triton X-100, 1 ml of IM Tris-HCL pH 7.6 or pH 8; 1.3 ml of 5M NaCl; 1 cocktail tablet or 5 mini cocktail tablets for 50 ml; 50 μl of 1M DTT; 47.7 ml of sterile water) was used to collect cells. Lysates were then sonicated for 10 minutes and spinned down at maximum speed for 15 minutes at 4 degrees. Then proteins were purified moving the supernatant into a new tube and quantified with the Pierce BCA kit (23209, Thermo Scientific).

Anti-Flag coated beads (ANTI-FLAG M2 Affinity Gel, A2220) were pre-cleaned with 3X washes in lysis buffer and then 20µl were added to 800 µl of proteins for a 4h incubation at 4°C.

Beads were then boiled at 95 degrees for 5 minutes with loading buffer and DTT (reducing agent) to elute with heating.
Samples were then run on a Western Blot.

Live Cell Imaging

Live cell imaging was performed 6 h after transfection in DMEM with 1 g l–1 glucose (Gibco) supplemented with 10% heat-inactivated fetal bovine serum (FBS) (Life Technologies).
Cells were transfected with fluorescent proteins, in particular: eGFP-ACE2, TMEM16A-mScarlet, TMEM16F-mScarket, and eGFP-spike. 6H after transfections cells were treated with drugs (niclosamide and bafilomycin) and stained with LysoTracker (L12492, Thermo Fisher Scientific) and Hoechst 33342 (1:100000).
Image acquisition was performed using the Operetta CLS high content screening microscope (Perkin Elmer) with a Zeiss 20× (NA 0.80) objective for 18 hours, setting the temperature at 37°C and 5% of CO2. A total of 25 fields per well were imaged at three different wavelengths: (1) excitation 365–385 nm, emission 430–500 nm (nucleus ‘blue’); (2) excitation 460–490 nm, emission 500–550 nm (‘green’); (3) excitation 615–645 nm emission 655–750 nm (‘red’) (4) excitation 561–594 nm emission 618-700 nm (‘red’). Images were subsequently analyzed, using the Harmony software (PerkinElmer).

RESULTS and DISCUSSION

ACE2 interacts with TMEM16A and TMEM16F

We first wanted to assess whether ACE2 and TMEM16A/TMEM16F interact inside the cells. We decided to use three different techniques, aiming at confirming and supporting the results: Proximity Ligation Assay (PLA); co-immunoprecipitation (co-IP) and fluorescence resonance energy transfer (FRET).
The indirect PLA, the mechanism of which is better explained in the Materials and Methods chapter, relies on the fact that, after adding primary antibodies for a given target protein, secondary antibodies conjugated to oligos PLUS and MINUS bind the respective primary antibodies. In this way, only if the target proteins are closer than 40 nm, the fluorescent signal is generated and amplified in situ through the use of rolling-circle amplification and fluorescently labelled oligonucleotides. The optimization of this assay was challenging: the overexpression of both proteins potentially involved in the interaction combined with the usage of indirect PLA, rather than direct PLA (which involves primary antibodies conjugated to the oligos) presented several hurdles, occasionally yielding false positive signals.

To address this issue, we relied on endogenous ACE2 expression to limit the background and any false-positive signal and enhance the reliability of our results. Of note, it was impossible for us to detect any signal using both endogenous ACE2 and TMEM16A/TMEM16F.

For the PLA (Fig. 1a), Vero cells were transfected in triplicates in a 96 well plate with TMEM16A, TMEM16F or spike, while we used the interaction between ACE2 and spike as a positive control and the interaction between TMEM16A and Na^+/K^- ATPase as a negative control (Fig. 1b). We also used U2OS cells as negative controls (Fig. 1c), given the fact that this cell line does not show detectable ACE2 levels (Fig. 1d).
The PLA was performed 24H after transfection. When assessing the PLA between ACE2 and either TMEM16A or TMEM16F, we detected a positive signal, that was instead absent in U2OS cells, leading us to conclude that indeed there is an interaction between ACE2 and

TMEM16A/TMEM16F in the cells. Of note, most of the interaction does not occur on the cell membrane, but in some intracellular compartments (most likely, the ER or Golgi)

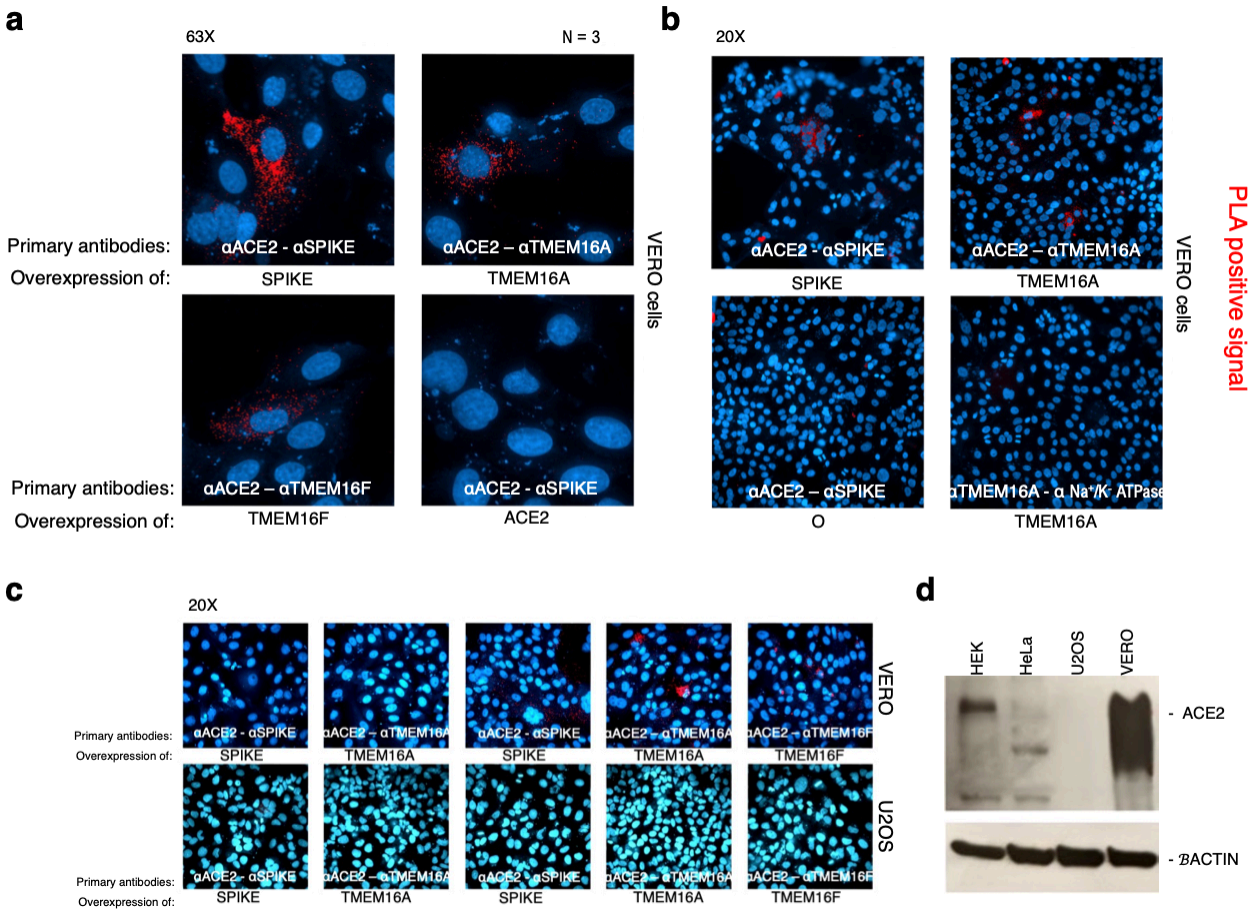

Figure 1: **Assessing ACE2-TMEM16A/TMEM16F interaction in PLA. a:** Vero cells were transfected in a 96-well plate with the indicated plasmid. PLA was performed 24H post-transfection: antibodies against ACE2 and, respectively, Flag (for TMEM16A and TMEM16F that are Flag tagged), or spike were used. Secondary antibodies anti-rabbit PLUS and anti- mouse MINUS were added to detect the PLA signal (in red). As CTR cells transfected with ACE2 were used as well as in **b** we used the interaction between TMEM16A and Na^+/K^- ATPase. **c**: The same conditions were reproduced in Vero and U2OS cells, the latter, as already mentioned above, do not show detectable levels of ACE2, as shown in **d**. The WB shows ACE2 levels in HEK293T, Hela, U2OS and VERO E6 cells.

The interaction between ACE2 and the TMEM16s was further assessed in co-IP experiments. Vero (Fig. 2a) and U2OS cells (Fig. 2b) were transiently co-transfected in duplicates with ACE2 and either TMEM16A, or TMEM16F. 24H post-transfection, samples were eventually treated with niclosamide 5 μM for another 24H. 48H after transfection co-IP was performed with αFlag agarose beads, targeting TMEM16A and TMEM16F. We assessed the flag-immunoprecipitate for the presence of ACE2 and detected it in the samples overexpressing both ACE2 and TMEM16A/TMEM16F.

Niclosamide consistently reduced the interaction in all the tested conditions, despite the higher levels of ACE2 in input niclosamide treated samples. The reduction and the increase in ACE2 levels due to the co-transfection with TMEM16s, spike or niclosamide treatment will be discussed in the following paragraphs.

Considering that niclosamide is a small molecule which blocks the TMEM16 pore, it is reasonable to think that the potential interaction site between ACE2 and TMEM16A/TMEM16F would involve the TMEM16 TM1 and TM6 sites (Feng et al. 2023).

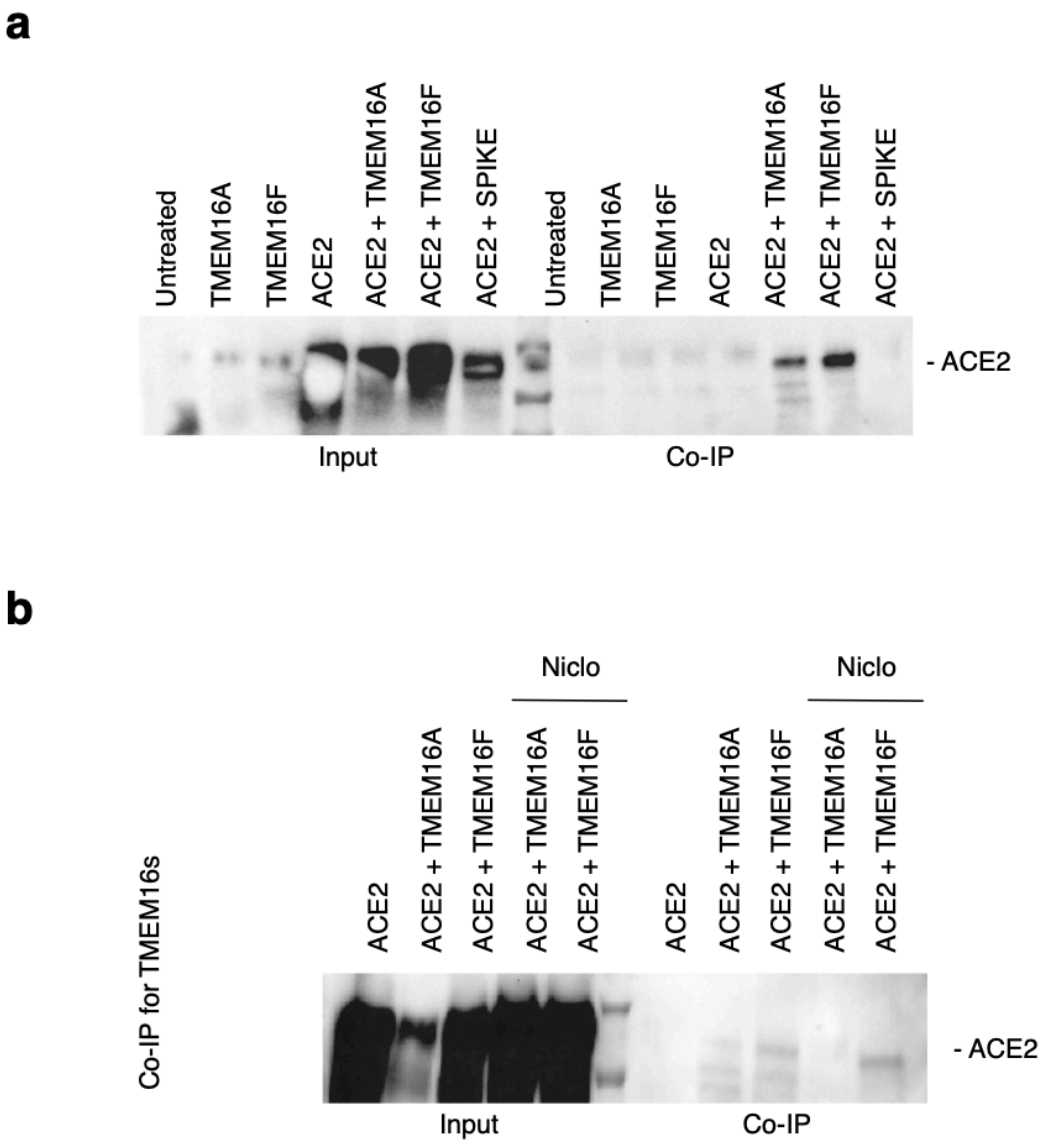

Figure 2: Assessing ACE2-TMEM16A/TMEM16F interaction in coIP. a,b: Samples were transiently transfected with the indicated plasmids. Niclosamide treatment used a concentration 5 μM for 24H, added 24H post-transfection.
48H cells were collected and coIP was performed on 800 μg of proteins with α-flag agarose beads (TMEM16s are flag tagged). Samples were blotted for ACE2. Input samples are on the left side of the membrane while the flag-immunoprecipitates are on the right side of the marker.

Finally, we wanted to confirm our data with FRET, which is also described in detail in the Materials and Methods chapter, which allows the visualization in the same cell of two putative interacting partners when they are within 10 nm distance. In our case, we chose the pair eGFP-mScarlet as fluorescent proteins, where eGFP acts as a donor while mScarlet is the acceptor. U2OS cells were transfected with ACE2-eGFP and TMEM16A-mScarlet or TMEM16F-mScarlet. 48H after transfection, slides were mounted and FRET was detected on a Nikon A1R confocal microscope. Image analysis was conducted with the Nikon NIS Element

software, as well as the pixFRET ImageJ plugin. We observed FRET in samples where the two proteins were co-transfected. We used mScarlet and eGFP as a negative control while the transfection of a construct with fused eGFP-mScarlet was used as a positive control (Fig.3a). Surprisingly, the amount of FRET in samples treated with niclosamide did not change, while a difference is observable in terms of signal localization (Fig. 3c). This could be attributed to the possibility that niclosamide augments the level of autophagy within the cells and blocks protein lysosomal degradation (Chai et al. 2020). This heightened autophagic activity may lead to the sequestration of proteins within intracellular vesicles. Importantly, due to their close proximity within these vesicles or shared microenvironments, FRET may still occur even if the proteins are not directly binding or interacting, given the micrometer-scale spatial constraints (approximately 0.2-2 µM). Again, the effects of niclosamide on proteins will be discussed in more detail in the following paragraphs.

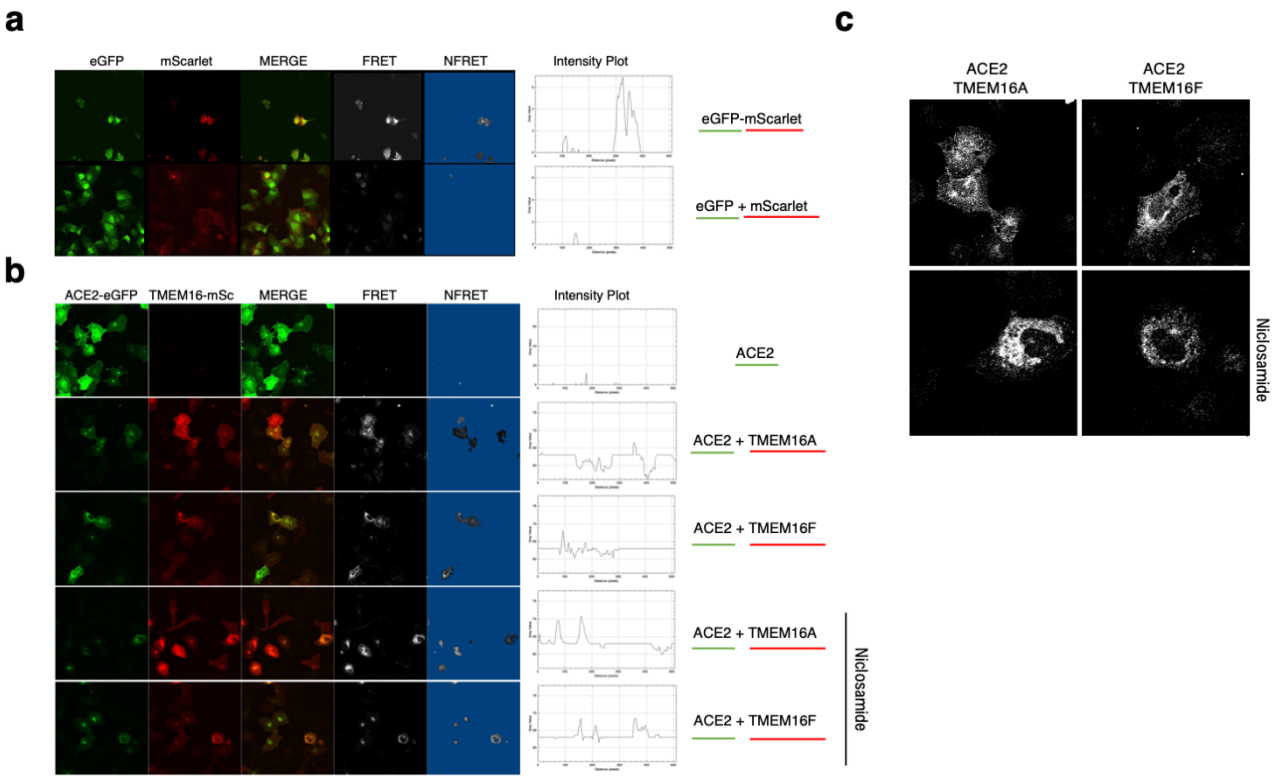

Figure 3: **Assessing ACE2-TMEM16A/TMEM16F interaction in FRET. a,b:** U2OS cells were transfected on 8-well slides with the different couples of fused proteins as indicated. Slides were mounted 48H post-transfection. “FRET” images are images acquired exciting eGFP (488 nm) and filtering mScarlet emission wavelength (594 nm). “FRET map” are images calculated with NIS Element software, normalizing the FRET on the intensity of the donor, and indicating the level of FRET

with different gradient colors, as indicated in the plot bar. While NFRET represents the level of FRET calculated through the PixFRET plugin of ImageJ, which is using the following formula:

I_{FRET} - BT_{DONOR} x I_{DONOR} - $BT_{ACCEPTOR}$ x $I_{ACCEPTOR}$ divided by the squared product of

I_{DONOR} x $I_{ACCEPTOR}$ and where I = intensity of fluorescence and BT = bleed through.

c. shows the differences in FRET signal localization between cells treated and untreated with niclosamide 5 μM.

In addition to these experiments, we took the opportunity of using the opensource software ColabFold for protein folding prediction. This software allowed us to predict the potential interaction site between ACE2 and TMEM16A/TMEM16F (Fig. 4a). These findings are in line with previous predictions kindly supplied by Dr. Sergio Pantano, where an interaction between the transmembrane helix of ACE2 and TMEM16s pore was suggested (Fig. 4b). In particular, ACE2 is known to act as a chaperone for the aminoacidic transporter B0AT1, which binds ACE2 on the transmembrane helix. The hypothesis of Dr. Pantano was that the same transmembrane helix could bind TMEM16s, being inserted into TMEM16s pores. Based on these predictions, we generated three mutated hACE2. All the mutations were punctiform on the helix, more precisely, we mutated Gly747 and Gly751 with, respectively, Isoleucine or Proline. In this way, we obtained ACE2Gly747Ile, ACE2Gly751Ile and ACE2Gly751Pro. Unfortunately, we did not see any decrease in terms of interaction with TMEM16A in co-IP (Fig. 4c) nor a decrease in syncytia formation (Fig. 4d) if transfected together with spike. From our new predictions (Fig. 4a) it seems that the interaction site could be slightly different, around AA804 for the interaction with TMEM16A and AA728 for the interaction with TMEM16F. Further investigations are required aiming at identifying the specific interaction site between the proteins.

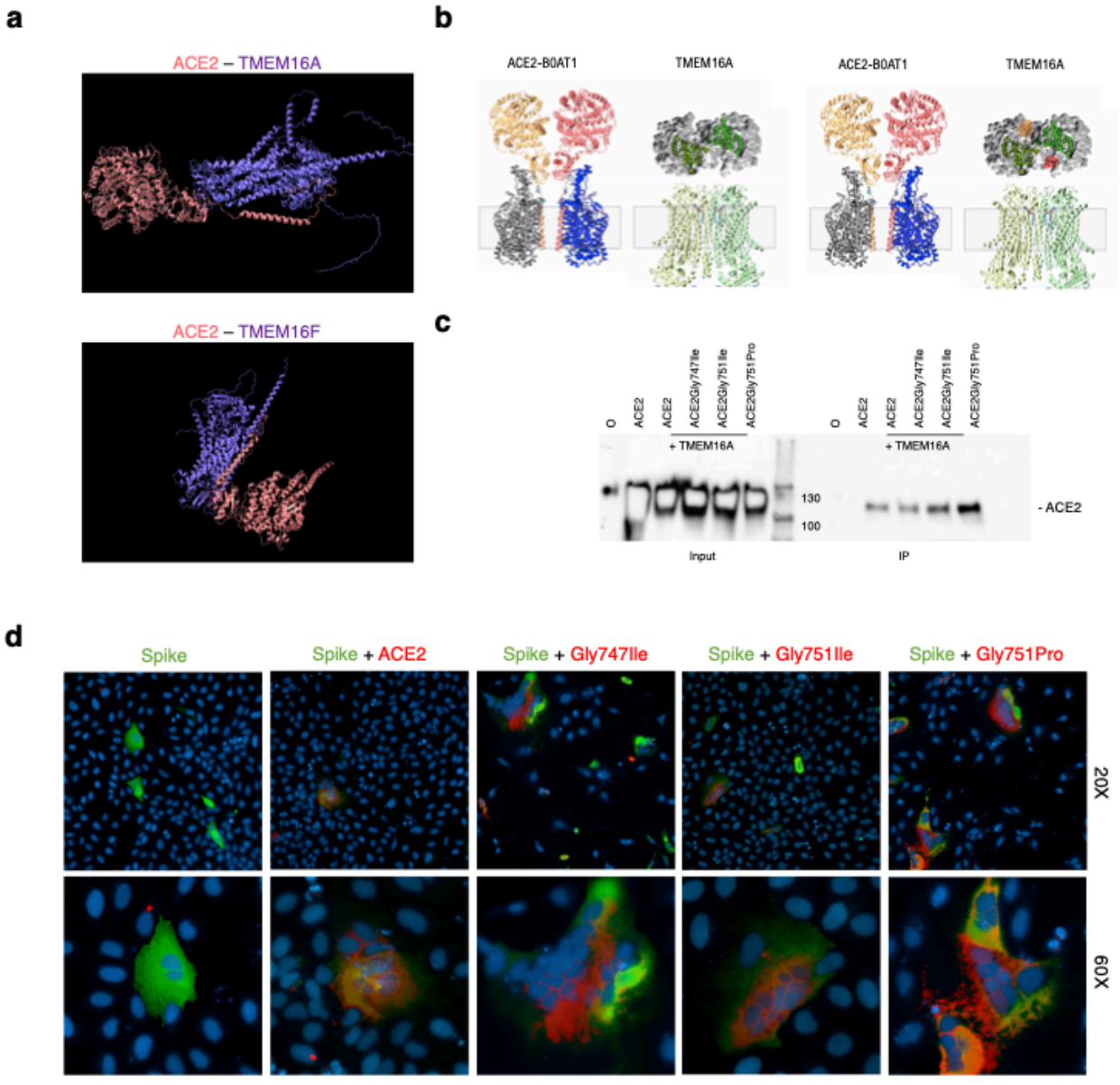

Figure 4: **Investigating the interaction site between ACE2 and TMEM16A/TMEM16F. a:** Interaction predictions generated with ColabFolb. (chiedi a Kazuki) ACE2 (pink) is interacting with TMEM16s (purple) on the C-terminal. b: Interaction model provided by Dr, Sergio Pantano. Both the images show, on the left ACE2 (orange and red) dimer interacting with the aminoacidic transporter B0AT1 (gray and blue) through the transmembrane helixes. On the right side of both images there is a representation of TMEM16A (green and light green), with a view from the top (top image) and from the front (image on the bottom). The right image shows how ACE2 helixes (orange and red dots) are supposed to interact with TMEM16A from top. c: coIP for TMEM16A in U2OS cells transfected with the indicated ACE2 mutants and TMEM16A. Cells were collected at 24H post-transfection. Input samples are found on the left side of the marker while the coimmunoprecipitates on the right. d: IF on U2OS cells transfected in duplicates in a 96 well plate. The images are showing the different expression of ACE2 mutants (red) and their ability of forming syncytia in combination with SPIKE (green).

TMEM16A and TMEM16F interact with spike

Investigating the interaction between ACE2 and TMEM16A/TMEM16F led us to wonder whether these two proteins bind spike too. Again, we decided to use co- immunoprecipitation and FRET.

To this aim, U2OS cells were transiently co-transfected with spike and either TMEM16A or TMEM16F. 24H post-transfection, the cells were eventually treated with niclosamide 5 μM for another 24H. 48H after transfection co-IP was performed with α-Flag agarose beads, targeting TMEM16A and TMEM16F. Again, we got indications of the interaction between spike and TMEM16s, with a stronger signal when TMEM16A was pulled down (Fig.5). Samples treated with niclosamide showed a reduction in terms of interaction. These findings align with Prof. Mauro Giacca's research, which highlighted niclosamide's ability to block the syncytia formation process by inhibiting TMEM16 family members.

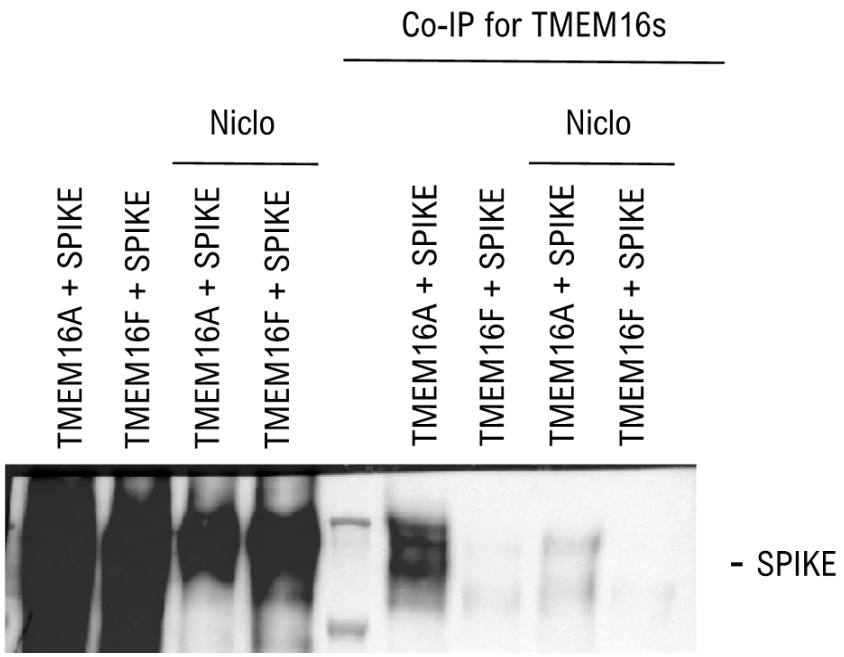

Figure 5: **Assessing spike-TMEM16A/TMEM16F interaction in co-IP.** U2OS cells were transiently transfected with the indicated plasmids and treated with niclosamide 5 μM for 24H. 48H post transfection coIP was performed on 800 μg of proteins with α-flag agarose beads. Samples were blotted for spike. Input samples are on the left side of the membrane while the flag immunoprecipitated samples are on the right side of the marker.

As far as FRET is concerned, U2OS cells were transfected with spike-eGFP construct and either TMEM16A-mScarlet or TMEM16F-mScarlet. 48H after transfection slides were mounted and FRET was detected on a Nikon AR1 confocal microscope. The analysis of the images was carried out with the Nikon NIS Element software, as well as the pixFRET ImageJ plugin. Again, we observed FRET in samples where the two proteins were co-transfected (Fig. 6b). We used mScarlet and eGFP as a negative control while a construct with eGFP- mScarlet as a positive control (Fig. 5a). Also in this case, the amount of FRET in samples treated with niclosamide did not change, getting a different FRET localization (Fig.6c).

Taking all the results together, in our experiments, we observed a reduced level of interaction between ACE2 and TMEM16s, and between TMEM16s and spike, if cells were treated with niclosamide. If we consider that spike binds TMEM16s to facilitate syncytia formation, and we are aware of ACE2 binding to spike for cellular entry, and we now suspect a potential interaction between TMEM16s and ACE2, it becomes plausible that niclosamide, by blocking TMEM16s, could influence the interaction between TMEM16s and either ACE2 or spike.

Moreover, ACE2, spike and TMEM16A/TMEM16F might be part of the same complex, and TMEM16A/TMEM16F might not only play a role in syncytia formation but also in the different steps of SARS-CoV-2 infection.

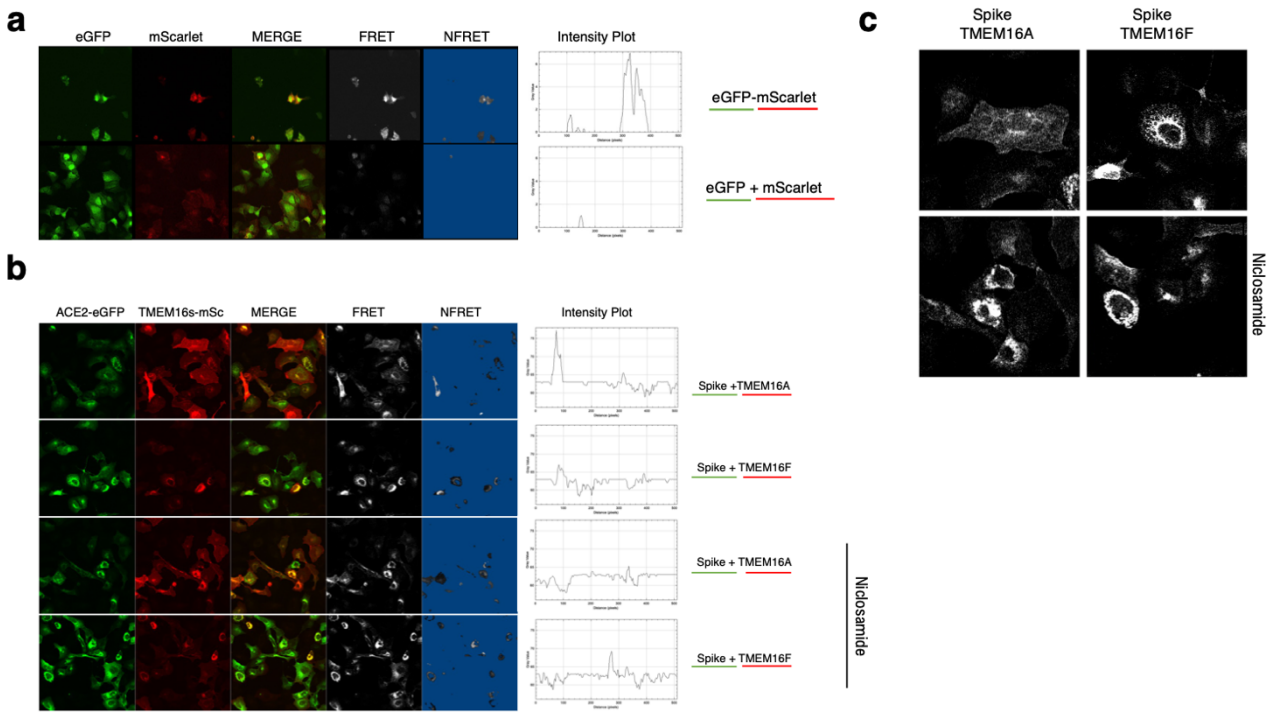

Figure 6: **Assessing SPIKE-TMEM16A/TMEM16F interaction in FRET. a,b:** U2OS cells were transfected on 8-well slides with the different couples of fused proteins as indicated. Slides were mounted 48H post-transfection. "FRET" images are images acquired exciting eGFP (488 nm) and filtering mSCARLET emission wavelength (594 nm). "FRET map" are images calculated with NIS Element software, normalizing the FRET on the intensity of the donor, and indicating the level of FRET with different gradient colors, as indicated in the plot bar. While NFRET represents the level of FRET calculated through the PixFRET plugin of ImageJ, which is using the following formula:

I_{FRET} - BT_{DONOR} x I_{DONOR} - $BT_{ACCEPTOR}$ x $I_{ACCEPTOR}$ divided by the squared product of

I_{DONOR} x $I_{ACCEPTOR}$ and where I = intensity of fluorescence and BT = bleed through.

c. shows the differences in FRET signal localization between cells treated and untreated with niclosamide 5 μM.

TMEM16A and TMEM16F lead to ACE2 degradation

While studying the interaction between ACE2 and TMEM16A/TMEM16F in U2OS cells, we noticed that, both in IF and WB, the co-transfection of ACE2 with TMEM16s led to lower levels of ACE2 (Fig. 7 a,b): Fig. 7a shows how the signal of ACE2 (green) in IF is decreased when cells were co-transfected with both ACE2 and TMEM16A. In particular, the effect of TMEM16A was much higher than that of TMEM16F (Fig. 7b). Of note, this result could be influenced by the different distribution of the two proteins (Fig. 7d): we noticed, in fact, that TMEM16A is more homogeneously distributed in the cell, mainly expressed on the cell surface, while

TMEM16F tends to localize in intracellular compartments, a finding that is in line with other studies reported in the literature (Ousingsawat et al., 2017). We confirmed the results through the knockdown of either TMEM16A or TMEM16F in VERO E6 cells (Fig. 7c). When silencing the TMEM16s, we observed an increase in ACE2 levels, indicating that TMEM16A and TMEM16F might be involved in ACE2 degradation.

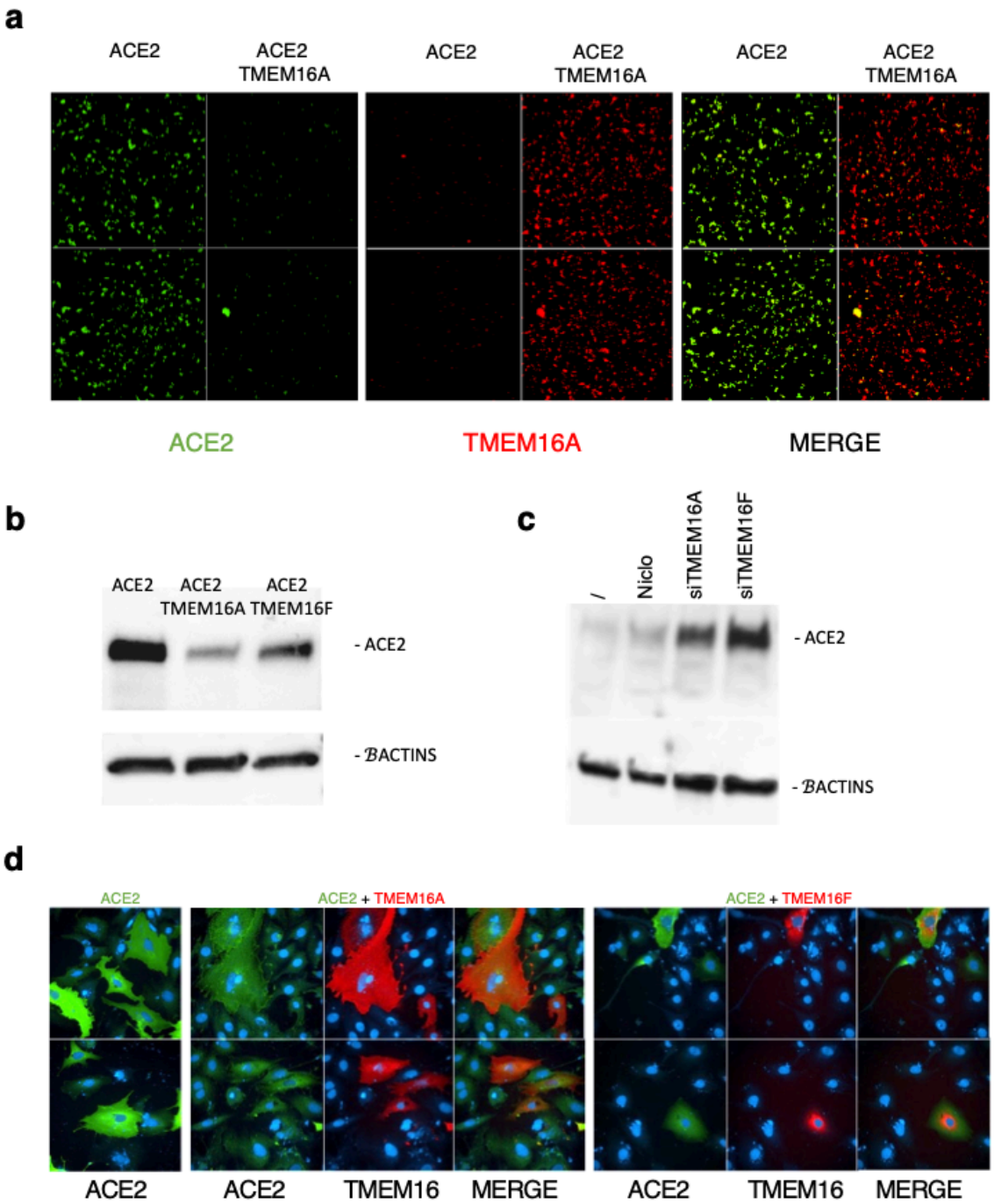

Figure 7: **TMEM16s lead to lower levels of ACE2.** In **a** U2OS cells were transfected in duplicates in a 96 well plate with the indicated plasmids. Duplicates of the samples are shown in column. **b:** U2OS cells were plated in a 6 well dish, transfected with the indicated plasmids. 48H post-transfection cells were collected and 10 ug of proteins were blotted for ACE2. **c:** Vero cells were plated in a 6 well dish, transfected with the indicated siRNAs or treated with niclosamide 5 μM for 24H. 48H post-transfection cells were collected and 25 ug of proteins were blotted for ACE2. **d** IF staining in U2OS cells showing the different levels of expression and distribution of ACE2 (green), TMEM16A (red), TMEM16F (red). Cells were grown on an 8 well slide, mounted and images acquired at the confocal microscope.

TMEM16A and TMEM16F are necessary for spike-driven ACE2 degradation

In literature, there are reports showing how spike determines both ACE2 downregulation and internalization and degradation through lysosomes (Gao et al. 2022; I et al. 2010; Lu et al. 2022). In our hands, spike expression leads to extremely low levels of ACE2 in U2OS, VERO and HEK293 cell lines (Fig. 8a). U2OS cells treated with niclosamide 5 μM for 24h, or transfected with siRNA for TMEM16A or TMEM16F show higher levels of ACE2 if co-transfected with spike (Fig. 8b). This indicates that TMEM16A and TMEM16F may be involved in ACE2 degradation caused by spike, which is in line with the finding of an interaction between spike and TMEM16A / TMEM16F.

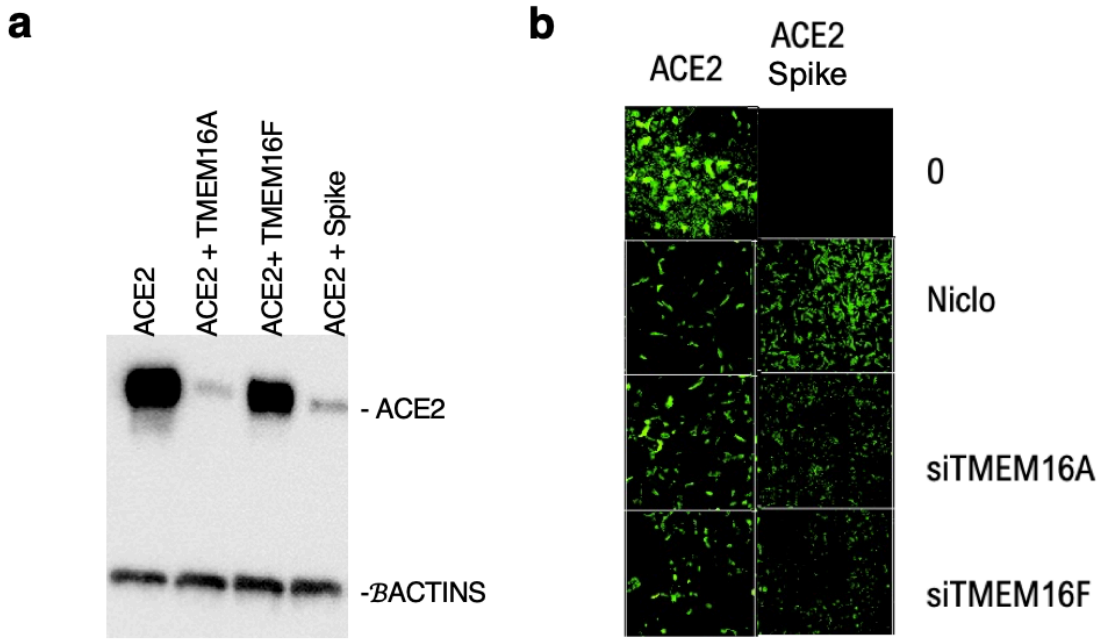

Figure 8: **TMEM16s are involved in SPIKE-driven ACE2 degradation. a:** WB for ACE2 showing the difference in its levels when U2OS are co-transfected with the indicated plasmids in a 6-well plate. Cells were collected 48H post-transfection and blotted for ACE2 (10 ug proteins). **b** IF showing how levels of ACE2 (green) are recovered when samples are treated with niclosamide 5 μM for 24H or transfected with siRNAs for TMEM16A and TMEM16F for 48H. Cells were first transfected in a 6-well plate with siRNAs 25nM in bulk, then split at 24H after and transfected in reverse in a 96 well plate with indicated plasmids.

TMEM16A and TMEM16F lead to ACE2 lysosomal degradation

Relying on the fact that spike determines ACE2 lysosomal degradation (Lu et al. 2022) and that TMEM16s interact with spike and decrease ACE2 levels, we hypothesized that the decreased levels of ACE2 observed when it is co-transfected with TMEM16A (and, to a lesser extent, with TMEM16F), could be due to lysosomal degradation.

To test this possibility, we first observed colocalization of ACE2 and lysosomes (LysoTracker) in the presence of TMEM16A in IF in U2OS cells transfected with eGFP-ACE2 and TMEM16A-mScarlet (Fig. 9a). In the same figure we also show the different distribution of ACE2 when it is alone, with TMEM16A, with spike, or both TMEM16A and spike.

We wanted to understand whether the degradation of ACE2 occurs in lysosomes. For this purpose, we used the well-known lysosome inhibitors bafilomycin (BafA1), trying different concentrations (50-200 nM) and different times of incubation (4-24H) and Chloroquine -CQ (50 μM). We successfully recovered levels of ACE2 pre-treating cells with lysosome inhibitors. To note, we first used a stable cell line of HEK293T expressing ACE2 (Fig. 9b1), which, once transfected with TMEM16A/TMEM16F, did not show a decrease of ACE2: this is probably due to the fact that the TMEM16s transfection efficiency is too low to detect ACE2 degradation. We repeated then the experiment in HEK293 wt (Fig. 9b2), co-transfecting both ACE2 and TMEM16A/TMEM16F or spike, and, despite levels of ACE2 in samples BafA1 treated is lower than the controls (BafA1 toxicity is suspected), we did not observe the same differences between the differently transfected samples as we did for the controls. We found that pre-treating cells with lysosome inhibitors for 4H played a critical role, as this pre-treatment allowed for the prevention of ACE2 degradation (Fig. 9b), although recovering ACE2 levels post-transfection proved to be challenging. As shown in Fig. 9d, U2OS cells transfected with ACE2 in combination with TMEM16A, TMEM16F, or spike, and subsequently treated with Bafilomycin (100 nm) or Chloroquine (50 μM) for 24H, added at 24H post-transfection, exhibited only a marginal increase in ACE2 levels (Fig. 9d). This increase, however, did not match the levels observed in ACE2-only transfected samples, nor did it reach the levels of the pre-treated samples (Figure 9b). In all cases, to prove drug efficiency, we performed a WB for LC3, which showed an increase in LC3-II, a marker of lysosomal inhibition (Fig. 9b,d). This observation may be attributed to the extended half-life of ACE2 and the timing of its maximum expression following transfection. To investigate this further, we performed a cycloheximide (CHX) assay, revealing the protein remarkable

stability for over 24H (Figure 9e). This suggests that ACE2 exhibits a lengthy turnover rate, and the 24H drug treatments may not suffice to achieve complete signal recovery. Unfortunately, extended drug treatments were not feasible due to associated toxicities. Another possibility is the fact that, being only transiently transfected, ACE2, if in combination with TMEM16s or spike, is degraded as soon as it starts to be produced. Hypothesizing that by 24H post-transfection the majority of ACE2 is produced and keeping in consideration its long half-life, ACE2 would be clearly detectable in cells for another 24H at least (so 48H post-transfection, the moment in which we were collecting all samples for the analysis). On the other hand, after 24H (the moment in which we were adding the drugs) there would not be more protein produced, so, even treating cells with lysosomes inhibitors, ACE2 would not be recoverable. We can probably assess this issue with a stable cells line expressing ACE2, but further investigations are needed.

Moreover, trying to exclude that the decrease of ACE2 levels we observed after co-transfecting ACE2 with TMEM16A, TMEM16F, was due to an inhibition of ACE2 transcription, we tested ACE2 mRNA levels in qPCR (Fig. 9g). Unfortunately, our results are uncertain: we did not find any significant difference in ACE2 expression levels with the simultaneous expression of either of the interactors, but a decrease in ACE2 mRNA levels is still observable, suggesting that its transcriptional level could be affected, even if not enough to justify the decrease observable in WB. Spike, as expected, show a significant reduction in ACE2 levels, confirming data found in literature (Gao et al. 2022).

On the other hand, we compared the behavior of ACE2 to Rec8, a meiotic recombination protein the degradation of which occurs through the proteasome, by IF experiments (Fig. 9c). We transfected in duplicate U2OS cells with Rec8 or ACE2 in combination with TMEM16A. We treated the cells with CHX (100 nm) for 3 and 6H, in combination with Bafilomycin (100 nm) or MG132 (10 μM). Again, we did not observe any recovery of ACE2 with MG132, differently from what occurs with Bafilomycin, which increased ACE2 levels. While Rec8 is visibly increasing with the MG132 treatment and there is no difference for the samples in which Bafilomycin was used.

A study by Dr. Umamaheswar Duvvuri and co-workers reported that TMEM16A increases the level of exocytosis in head and neck carcinoma (REF). We took into consideration the possibility of an increase of extracellular vesicles caused by TMEM16A. Thus, we performed a WB for ACE2 on the cell culture medium (Fig. 9d). Cells were grown for 6H in cell media without FBS (to avoid BSA altering protein quantification and WB run) and Phenol Red free

(to allow BCA quantification). In this case, we noticed a higher amount of soluble ACE2 (90 kDa) compared to the intracellular compartments, but in general, the levels of ACE2 reflected those of the intracellular compartment, leading us to also exclude this hypothesis.

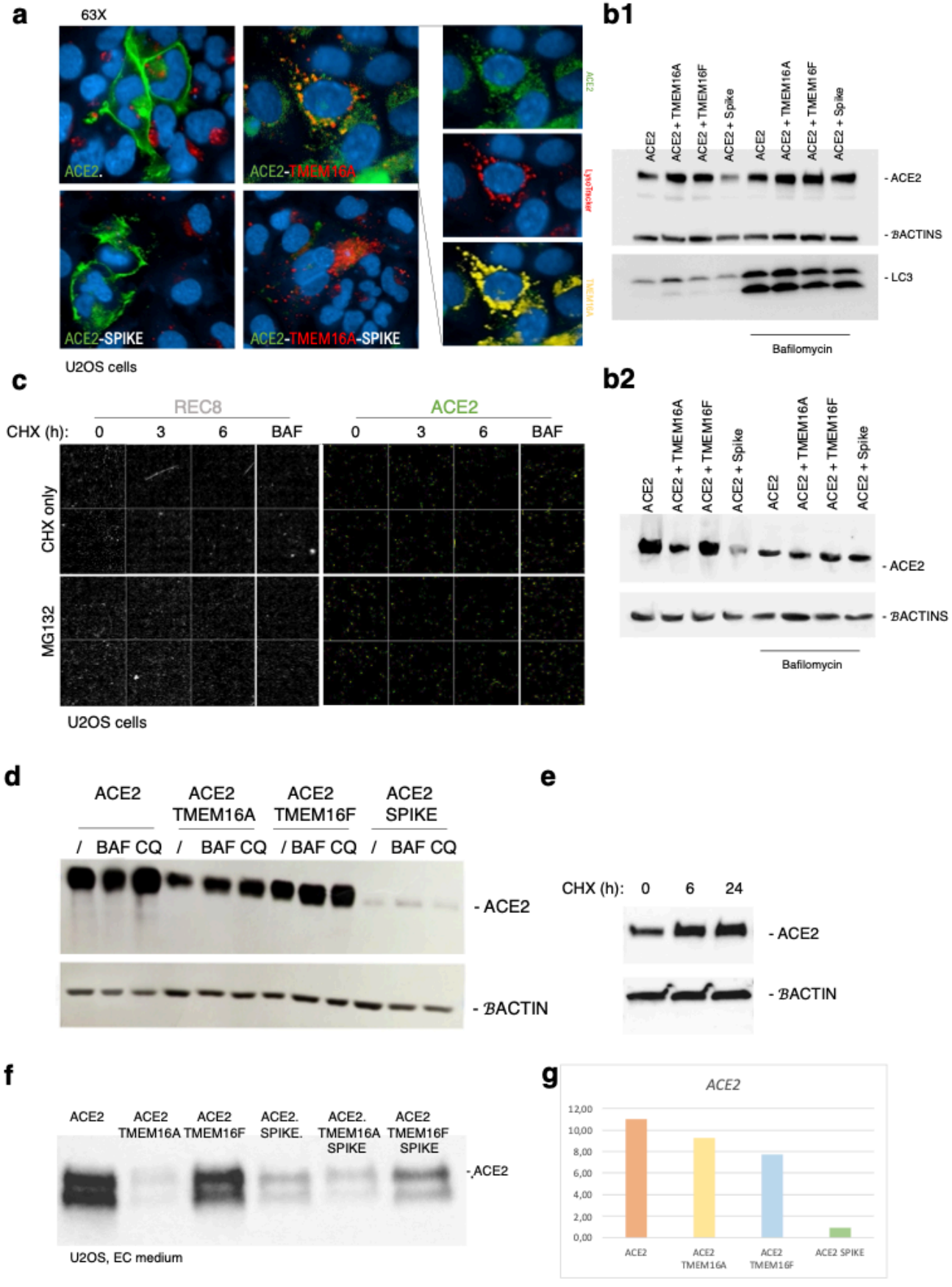
a
63X
ACE2.
ACE2-TMEM16A
ACE2-SPIKE
ACE2-TMEM16A-SPIKE
U2OS cells
b1
ACE2
ACE2 + TMEM16A
ACE2 + TMEM16F
ACE2 + Spike
- ACE2
- BACTINS
- LC3
Bafilomycin
b2
- ACE2
- BACTINS
Bafilomycin
c
REC8
ACE2
CHX (h): 0 3 6 BAF 0 3 6 BAF
CHX only
MG132
U2OS cells
d
ACE2
ACE2 TMEM16A
ACE2 TMEM16F
ACE2 SPIKE
/ BAF CQ / BAF CQ / BAF CQ / BAF CQ
- ACE2
- BACTIN
e
CHX (h): 0 6 24
- ACE2
- BACTIN
f
ACE2
ACE2 TMEM16A
ACE2 TMEM16F
ACE2. SPIKE.
ACE2. TMEM16A SPIKE
ACE2 TMEM16F SPIKE
-ACE2
U2OS, EC medium
g
ACE2
12,00
10,00
8,00
6,00
4,00
2,00
0,00
ACE2
ACE2 TMEM16A
ACE2 TMEM16F
ACE2 SPIKE

Figure 9: **TMEM16s lead to ACE2 lysosomal degradation. a:** U2OS cells were transfected with fused proteins: eGFP-ACE2 (green) and TMEM16A-mSCARLET (red) and/or spike. Moreover, cells were incubated for 1H before live acquisition with LysoTracker 75 μM. Of note, on the right side of the image we show the co-localization of both ACE2 (green) and TMEM16A (em 594 nm - yellow) with the LysoTracker (em 647 nm - red) signal. **b**: WB for of ACE2 in HEK293T. Cells were transfected in a 6 well plate with the indicated plasmids 4H after BafA1 100 nm (or DMSO only) pre-treatment. 24H post-transfection cells were collected, and 10 μg of proteins were blotted for ACE2 and LC3. **b1** shows a WB on cells which are stabling expressing ACE2, while b2 is showing a WB where HEK293T were transfected with both the indicated proteins. **c:** IF for REC8 (white) and ACE2 (green) in U2OS transfected in duplicates (in column) in a 96 well plate for 48H with ACE2 (green) or Rec8 (white), in combination with TMEM16A. Samples were then treated for 3 and 6H with Bafilomycin 100 nm or MG132 10 μM and stained. **d.** WB showing samples of U2OS cells transfected with the indicated plasmids in a 6 well plate, treated with Bafilomycin 100 nm or Chloroquine 50 μM for 24H. Drugs were added at 24H post-transfection and cells were collected at 48H post-transfection. **e.** Cycloheximide was admnistered to U2OS cells transfected with ACE2 at a concentration of 100 μg/mL 24H post transfection, for 6 or 24H, then cells were collected, and 10 μg proteins were blotted for ACE2. **f**. WB performed on 10 μg of extracellular proteins obtained from cell media of U2OS cells grown for 6H into a BSA and PhenolRed free medium. The medium was changed 24H post transfection. **g.** bar plot showing the quantification of ACE2 expression measured through TaqMan qPCR and normalized on GAPDH expression levels and expresses as -ddCT in samples transfected with ACE2 only (orange), ACE2 and TMEM16A (yellow), ACE2 and TMEM16F (light bluse) and ACE2 and spike (green).

Niclosamide increases ACE2 autophagy, but blocks TMEM16s and spike driven ACE2 degradation.

In the context of our study, a noteworthy observation related to the drug niclosamide, a known anthelmintic drug, which was demonstrated to block the formation of spike -driven syncytia by blocking TMEM16 family members (L. Braga et al., 2021). From the literature, we know that, on the one hand, niclosamide inhibits syncytia formation while, on the other, it increases autophagy and inhibitslysosomes (M. Li et al., 2013). We also observed the latter effect in Vero cells treated with niclosamide 5 μM for 24H (9b) which showed increased levels of the lipidated form of LC3 (LC3-II) in WB. Niclosamide also reduces the amount of ACE2 levels if transfected alone (Fig. 10 a,d), suggesting that ACE2 is probably internalized and degraded because of increased autophagy. This result is even more evident in a fractionation assay where whole protein extract from Vero cells was fractionated to separate proteins from different cell compartments (Fig. 10c): ACE2 is mainly on the cell membrane but, if samples are treated with niclosamide, ACE2 is not detectable on the membrane any longer. Interestingly, when ACE2 is co-transfected with TMEM16s or spike, and cells are treated with niclosamide, the levels of ACE2 are higher than in the untreated samples (Fig. 10d). Moreover, images taken at the confocal microscope (Fig. 10a) show that ACE2 recovered with niclosamide has a different cell localization compared to the controls and that, in general, cells display a different morphology (Fig. 10e), possibly caused by niclosamide toxicity.

The reasons underlying the phenomenon by which ACE2 is recovered with niclosamide when it is co-transfected with either spike or TMEM16A/F and degraded when ACE2 is expressed alone require further investigation. Taking all together, a possible explanation is the fact that, on the one hand, niclosamide activates autophagy by inhibiting mTORC1 (M. Li et al., 2013) and TMEM16A also regulates mTOR activity, inhibiting autophagy (S. Kulkarni et al., 2023), while, on the other hand, SPIKE leads to clathrin mediated internalization (followed by lysosomal degradation) of ACE2. If we now hypothesize that TMEM16s do the same, the pathway that niclosamide activates is different from the one through which ACE2 is degraded. Moreover, the timings for treatments and cell collection could play a key role in the experiments.

There are many questions still unsolved and the intricate interplay among these factors demands further exploration to uncover the underlying mechanisms.

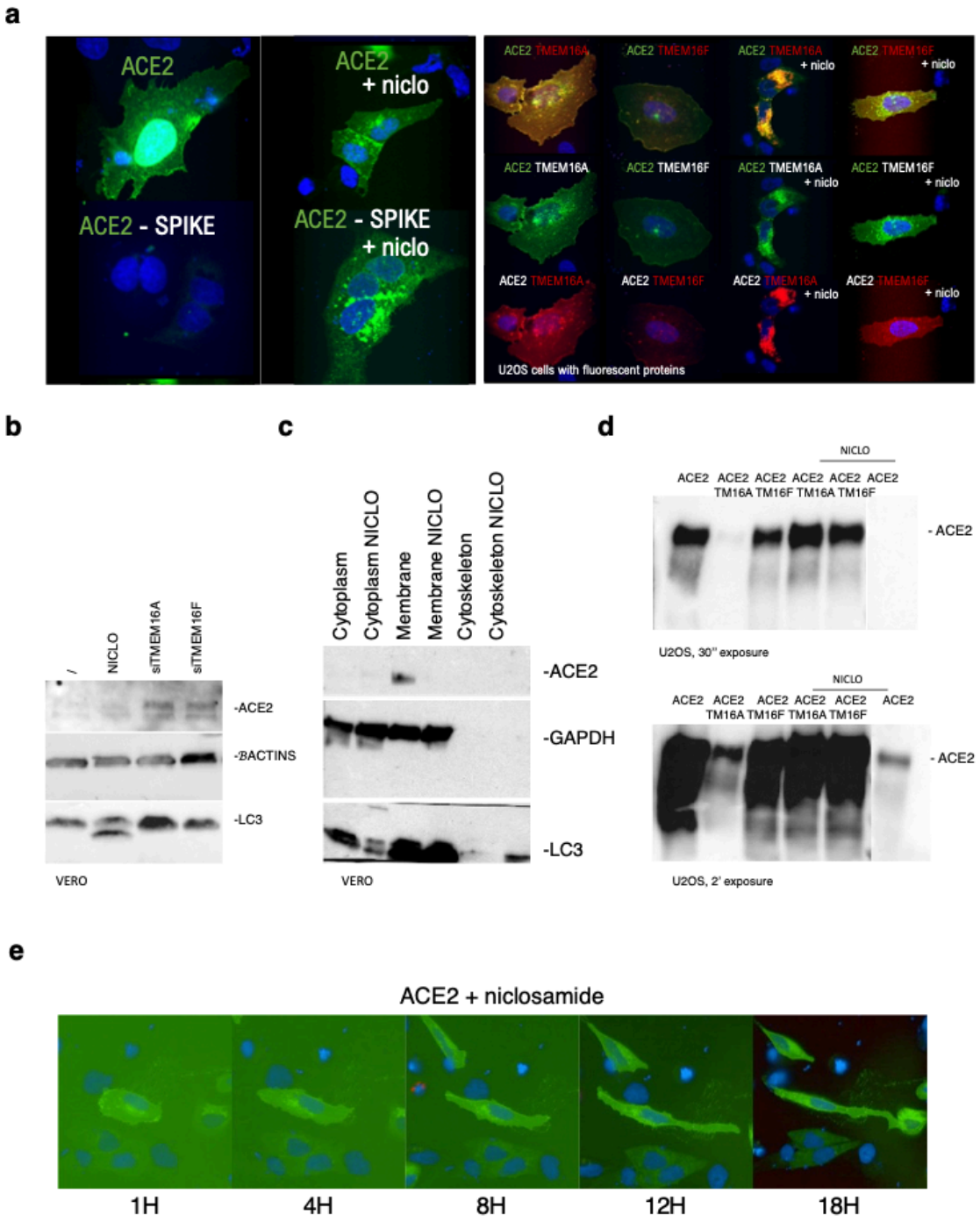

Figure 10: Niclosamide degrades ACE2 if alone and recovers ACE2 when it is co-transfected with S or TMEM16s. a: U2OS cells were transfected on an 8 well slides with the indicated proteins, treated with 5 μM niclosamide (or DMSO) for 24H and fixed 48H post-transfection, and images were acquired at the confocal microscope. **b** Niclosamide increases autophagy. **b.** WB performed on 20 μg of proteins from Vero cells treated for 24H with niclosamide 5 μM or transfected with siRNAs for TMEM16s for 48H. Membranes were blotted for ACE2 and LC3 II. **c.** WB on Vero cells samples fractionated into different cell compartments. Cells were treated with niclosamide 5 μM (or DMSO) for 24H. **d** WB on 10 ug of proteins from U2OS transfected with the indicated plasmids and treated with niclosamide 5 μM (or DMSO) for 24H. Cells were collected 48H post transfection and blotted for ACE2. The two images in **d** are representing the same WB, the upper one with shorter exposure while the bottom one with a longer exposure. **e**: Time lapse of U2OS cells expressing eGFP-ACE2 (green) treated with niclosamide 5 μM

CONCLUSIONS

COVID-19, short for Coronavirus Disease 2019, is an illness caused by the infection of the severe acute respiratory syndrome virus 2 (SARS-CoV-2). This virus was initially identified in November 2019 in Wuhan, Hubei Province, China, and subsequently spread worldwide, leading the World Health Organization (WHO) to declare it a global pandemic on March 11, 2020.

Common COVID-19 symptoms include fever, cough, shortness of breath, fatigue, muscle or body aches, headache, sore throat, loss of taste or smell, congestion or runny nose, nausea or vomiting, and diarrhea (Goyal et al., 2020). The severity of symptoms can vary, with potential complications including lung thrombosis (Levi et al. 2020), acute respiratory distress syndrome (ARDS) (Xu et al. 2020), abnormal activation of the inflammatory response (cytokine storm) and rapid deterioration of lung function characterized by alveolar edema (Edler et al. 2020; Jose et al., 2020).

The spike protein on SARS-CoV-2 (spike) plays a pivotal role in receptor attachment and host cell penetration binding angiotensin-converting enzyme 2 (ACE2) (Satarker and Nampoothiri 2020) leading to its tropism for tissues, where SARS-CoV-2 infection occurs, as well as its associated complications (Gkogkou et al. 2020; Hikmet et al. 2020).

Spike of SARS-CoV-2 possesses the remarkable ability to induce the formation of multinucleated giant cells known as syncytia, both in vitro and in vivo (Braga et al., 2021), process that is governed by a bi-arginine motif containing R682 and R685 within the polybasic S1/S2 cleavage site, a characteristic shared by the surface glycoproteins of many highly contagious viruses (Zhang et al., 2021).

Syncytia formation offers, in fact, advantages to viruses: it enables them to spread more rapidly within the host and syncytia can incorporate immune cells (Battles and McLellan 2019; Nardacci et al. 2015). In fact, it has been shown that these syncytia can readily internalize multiple lines of lymphocytes, forming typical cell-in-cell structures and ultimately leading to the death of internalized cells and contributing to the viral immune escape: a recent research by Sun et al. for example, identified a type of CD45 positive cell structure within the syncytia of COVID-19 patients, which were not present in mononucleated cells.

Moreover, it has been established that cells infected by SARS-CoV-2 express the Spike protein on their cell membrane following viral replication, allowing cells to fuse with neighboring cells expressing ACE2. Research has revealed that after ACE2 binds to spike, ACE2 undergoes internalization within the host cell via clathrin-mediated endocytosis and is subsequently degraded within lysosomes (Lu et al. 2022).

In 2020, Prof. Mauro Giacca and his research team published a study that highlighted the significance of TMEM16F, a calcium-dependent chloride channel and scramblase, in the formation of syncytia. In their study, they demonstrated that niclosamide, an antihelminthic drug renowned for its ability to block members of the TMEM16-Anoctamin family, can block the syncytia formation process, highlighting its potential role as a therapeutic drug for COVID19. To note, TMEM16s and niclosamide seem to have opposite effects on autophagy, both acting as, respectively, enhancer and inhibitor of mTORC1, leading to autophagy inhibition or increase (Fonseca et al. 2012; Kulkarni et al. 2023).

In our study we investigated the possible interaction between ACE2, TMEM16A/TMEM16F and spike, aiming at discovering new details of the SARS-CoV-2 infection process. We found that all proteins seem to interact, probably being part of the same protein complex, and in particular, we focused our attention on the interaction site between ACE2 and TMEM16s, which is likely involving ACE2 C-terminal domain and TMEM16s TM1-TM6 (Chai et al. 2020). In support of this hypothesis there is the fact niclosamide, small molecule which is known to block TMEM16s, is inserting into the Ca2+ pore and, in our hands, its treatment is reducing the interaction between ACE2 and TMEM16A/TMEM16F. Interestingly, we found that spike is interacting with TMEM16s and that niclosamide is reducing the level of interaction. Moreover, spike is known for leading to ACE2 lysosomal degradation through clathrin mediated endocytosis, but niclosamide, as well as TMEM16s knockdown, prevented the degradation, suggesting that TMEM16s could be involved and necessary for ACE2 internalization and degradation. On the other hand, we observed that TMEM16A and, to a lesser extent TMEM16F, lead to ACE2 lysosomal degradation and that, also in this case, niclosamide could prevent it. Intriguingly, niclosamide is reducing ACE2 levels if it is transfected alone. Here, we propose a working model (Fig. 11) where we assume that TMEM16s are causing ACE2 internalization through clathrin mediated endocytosis as spike does, we can explain these controversial effects of niclosamide hypothesizing the activation and degradation through different pathways in function of the presence/absence of TMEM16s and niclosamide: TMEM16s are inhibiting autophagy and promoting clathrin mediated endocytosis while

niclosamide is blocking TMEM16s on a specific site and promoting autophagy. We are proposing a model in which when ACE2 is alone is internalized through autophagy, while when ACE2 is transfected with TMEM16s (and without niclosamide), it is internalized through clathrin mediated endocytosis. When we are treating cells which are transfected with both ACE2 and TMEM16s, niclosamide could block the interaction site between ACE2 and TMEM16s, stopping clathrin mediated internalization. It is realistical to consider that the ability of TMEM16s of inhibiting autophagy could be not affected by niclosamide, allowing a recovery of ACE2 levels. Further investigations are required to understand this mechanism. Moreover, this model lacks in explaining why niclosamide could effectively recover ACE2 from spike -driven degradation even without TMEM16s overexpression.

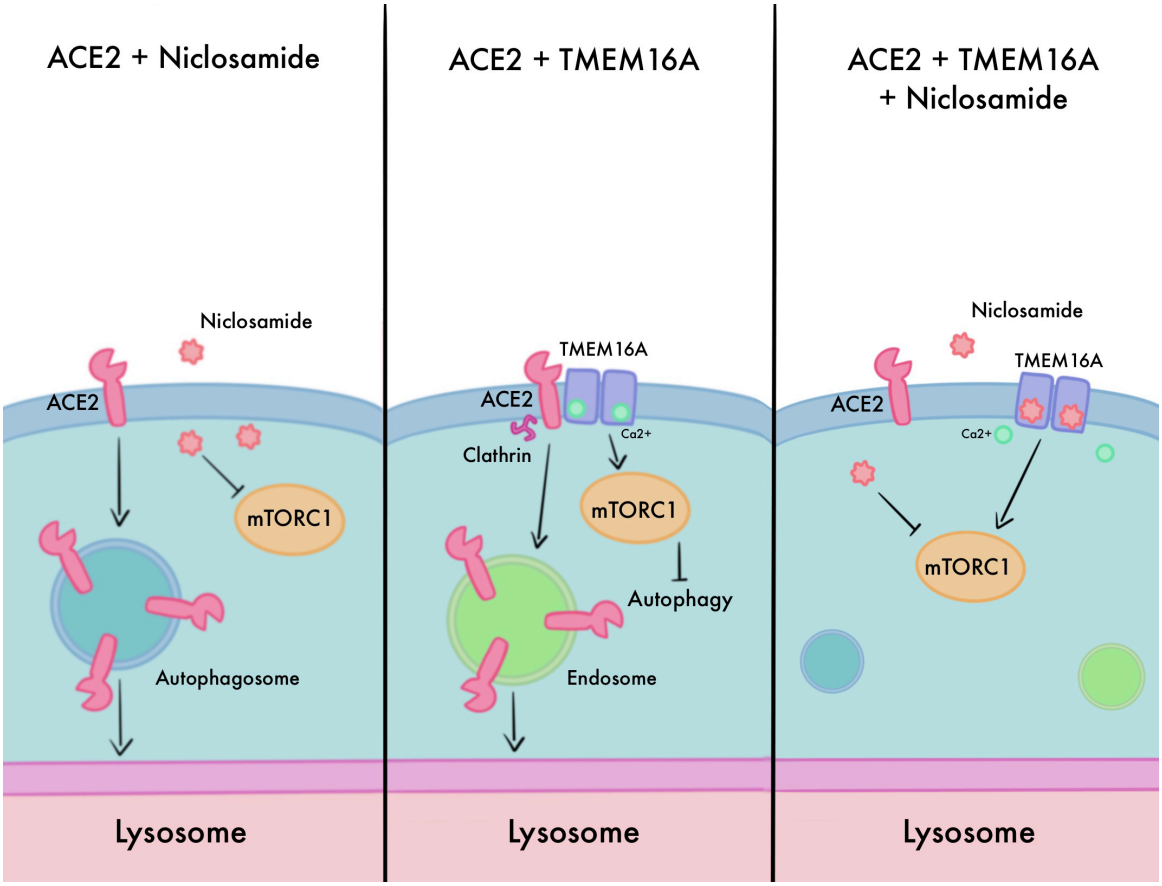

Figure 11: **Working Model explaining controversial effects of niclosamide on ACE2.** This figure shows the different behaviour of ACE2 in the different contexts. From the left: cells overexpressing ACE2 and treated with Niclosamide, overexpression of ACE2 and TMEM16A and overexpression of ACE2 and TMEM16A in combination with niclosamide treatment. When ACE2 is alone, niclosamide activates autophagy inhibiting mTOR, so ACE2 is internalized through autophagosomes and degraded. When ACE2 is overexpressed together with TMEM16A, TMEM16A is leading to ACE2 degradation through clathrin mediated endocytosis, ACE2 is then internalized by endosomes, while TMEM16A enhances mTOR activity inhibiting autophagy. Lastly, when ACE2 and TMEM16A are both overexpressed but cells are treated with niclosamide, TMEM16A and niclosamide have opposite effects on mTOR, so autophagy is not activated, while niclosamide

molecule is inhibiting ACE2-TMEM16A interaction and the internalization of ACE2 through clathrin mediated endocytosis does not occur.

Understanding the intricate molecular pathways underlying these interactions holds significant implications, not only from a physiological perspective, given the central role of ACE2 in the renin-angiotensin-aldosterone system (RAAS), but also in the context of potential future viral infections that utilize the same receptor. Unraveling these pathways opens up possibilities for new therapeutic targets that could aid in the prevention of severe symptoms associated with these pathologies.

AKNOWLEGMENTS

These three years have marked a profound period of transformation in my life. This journey has been both exciting and challenging, and I am acutely aware of how fortunate I have been to receive support from a remarkable group of people, without whom these experiences would have been significantly more difficult.

First and foremost, I want to thank Prof. Mauro Giacca, whose warm welcome into his lab and his inclusion in his team have left an indelible mark on my academic growth. These past two years have not only afforded me the chance to expand my knowledge but have also allowed me to work with exceptional individuals who have served as a constant source of inspiration and motivation.

I extend an immense thank you to my supervisor, Prof. Manola Comar, whose support has been instrumental in my academic and personal development providing me with the incredible opportunity to embark on a project abroad, a chance for which I am immensely grateful.

I would like to acknowledge Ilaria for her patience and unwavering support throughout this project. Her guidance has been invaluable in navigating the complexities of this research.

Lastly, I am deeply thankful to my parents, grandparents, and my brother, as well as my close friends in Trieste and London, all the people that supported me during this journey. Their consistent presence, willingness to listen, and their ability to make me laugh even in the most challenging moments gave me strength and they gifted me with light when everything seemed to be going awry.

From the depths of my heart, I extend my profound appreciation to each and every one of you.

BIBLIOGRAPHY

1. Adeline Heurich,a Heike Hofmann-Winkler,a Stefanie Gierer,a Thomas Liepold,b Olaf Jahn,b Stefan Pöhlmann. n.d. 'TMPRSS2 and ADAM17 Cleave ACE2 Differentially and Only Proteolysis by TMPRSS2 Augments Entry Driven by the Severe Acute Respiratory Syndrome Coronavirus Spike Protein'. Retrieved 1 June 2023 (https://journals.asm.org/doi/epub/10.1128/jvi.02202-13).
2. Agostinelli, Emilio, and Paolo Tammaro. 2022. 'Polymodal Control of TMEM16x Channels and Scramblases'. *International Journal of Molecular Sciences* 23(3):1580. doi: 10.3390/ijms23031580.
3. Aj, Verkleij, Zwaal Rf, Roelofsen B, Comfurius P, Kastelijn D, and van Deenen Ll. 1973. 'The Asymmetric Distribution of Phospholipids in the Human Red Cell Membrane. A Combined Study Using Phospholipases and Freeze-Etch Electron Microscopy'. *Biochimica et Biophysica Acta* 323(2). doi: 10.1016/0005-2736(73)90143-0.
4. Alsaadi, Entedar A. J., and Ian M. Jones. 2019. 'Membrane Binding Proteins of Coronaviruses'. *Future Virology* 14(4):275. doi: 10.2217/fvl-2018-0144.
5. Arndt, Melanie, Carolina Alvadia, Monique S. Straub, Vanessa Clerico Mosina, Cristina Paulino, and Raimund Dutzler. 2022. 'Structural Basis for the Activation of the Lipid Scramblase TMEM16F'. *Nature Communications* 13(1):1–17. doi: 10.1038/s41467-022-34497-x.
6. B, Korber, Fischer Wm, Gnanakaran S, Yoon H, Theiler J, Abfalterer W, Hengartner N, Giorgi Ee, Bhattacharya T, Foley B, Hastie Km, Parker Md, Partridge Dg, Evans Cm, Freeman Tm, de Silva Ti, McDanal C, Perez Lg, Tang H, Moon-Walker A, Whelan Sp, LaBranche Cc, Saphire Eo, and Montefiori Dc. 2020. 'Tracking Changes in SARS-CoV-2 Spike: Evidence That D614G Increases Infectivity of the COVID-19 Virus'. *Cell* 182(4). doi: 10.1016/j.cell.2020.06.043.
7. Bader, Michael. 2013. 'ACE2, Angiotensin-(1–7), and Mas: The Other Side of the Coin'. *Pflugers Archiv : European Journal of Physiology* 465(1). doi: 10.1007/s00424-012-1120-0.
8. Bagdonaite, Ieva, Andrew J. Thompson, Xiaoning Wang, Max Søgaard, Cyrielle Fougeroux, Martin Frank, Jolene K. Diedrich, I. I. I. John R. Yates, Ali Salanti, Sergey Y. Vakhrushev, James C. Paulson, and Hans H. Wandall. 2021. 'Site-Specific O-

Glycosylation Analysis of SARS-CoV-2 Spike Protein Produced in Insect and Human Cells'. *Viruses* 13(4). doi: 10.3390/v13040551.

9. Baranov, Maksim V., Frans Bianchi, Anastasiya Schirmacher, Melissa A. C. van Aart, Sjors Maassen, Elke M. Muntjewerff, Ilse Dingjan, Martin ter Beest, Martijn Verdoes, Samantha G. L. Keyser, Carolyn R. Bertozzi, Ulf Diederichsen, and Geert van den Bogaart. 2019. 'The Phosphoinositide Kinase PIKfyve Promotes Cathepsin-S-Mediated Major Histocompatibility Complex Class II Antigen Presentation'. *iScience* 11:160. doi: 10.1016/j.isci.2018.12.015.
10. Battles, Michael B., and Jason S. McLellan. 2019. 'Respiratory Syncytial Virus Entry and How to Block It'. *Nature Reviews Microbiology* 17(4):233–45. doi: 10.1038/s41579-019-0149-x.
11. Bayati, Armin, Rahul Kumar, Vincent Francis, and Peter S. McPherson. 2021. 'SARS-CoV-2 Infects Cells after Viral Entry via Clathrin-Mediated Endocytosis'. *The Journal of Biological Chemistry* 296. doi: 10.1016/j.jbc.2021.100306.
12. Benedetto, Roberta, Jiraporn Ousingsawat, Podchanart Wanitchakool, Yong Zhang, Michael J. Holtzman, Margarida Amaral, Jason R. Rock, Rainer Schreiber, and Karl Kunzelmann. 2017. 'Epithelial Chloride Transport by CFTR Requires TMEM16A'. *Scientific Reports* 7(1):1–13. doi: 10.1038/s41598-017-10910-0.
13. Benton, Donald J., Antoni G. Wrobel, Pengqi Xu, Chloë Roustan, Stephen R. Martin, Peter B. Rosenthal, John J. Skehel, and Steven J. Gamblin. 2020. 'Receptor Binding and Priming of the Spike Protein of SARS-CoV-2 for Membrane Fusion'. *Nature* 588(7837):327–30. doi: 10.1038/s41586-020-2772-0.
14. Breitling, Jörg, and Markus Aebi. 2013. 'N-Linked Protein Glycosylation in the Endoplasmic Reticulum'. *Cold Spring Harbor Perspectives in Biology* 5(8). doi: 10.1101/cshperspect.a013359.
15. Bretscher, Bretscher. 1972. 'Asymmetrical Lipid Bilayer Structure for Biological Membranes'. *Nature: New Biology* 236(61). doi: 10.1038/newbio236011a0.
16. Bricogne, Christopher, Michael Fine, Pedro M. Pereira, Julia Sung, Maha Tijani, Youxue Wang, Ricardo Henriques, Mary K. Collins, and Donald W. Hilgemann. 2019. 'TMEM16F Activation by Ca2+ Triggers Plasma Membrane Expansion and Directs PD-1 Trafficking'. *Scientific Reports* 9(1):1–13. doi: 10.1038/s41598-018-37056-x.
17. Brunaugh, Ashlee D., Hyojong Seo, Zachary Warnken, Li Ding, Sang Heui Seo, and Hugh D. C. Smyth. 2021. 'Development and Evaluation of Inhalable Composite

Niclosamide-Lysozyme Particles: A Broad-Spectrum, Patient-Adaptable Treatment for Coronavirus Infections and Sequalae'. *PLoS ONE* 16(2). doi: 10.1371/journal.pone.0246803.

18. C, Hartzell, Putzier I, and Arreola J. 2005. 'Calcium-Activated Chloride Channels'. *Annual Review of Physiology* 67. doi: 10.1146/annurev.physiol.67.032003.154341.
19. C, Paulino, Kalienkova V, Lam Akm, Neldner Y, and Dutzler R. 2017. 'Activation Mechanism of the Calcium-Activated Chloride Channel TMEM16A Revealed by Cryo-EM'. *Nature* 552(7685). doi: 10.1038/nature24652.
20. C, Zeng, Evans Jp, King T, Zheng Ym, Oltz Em, Whelan Spj, Saif Lj, Peeples Me, and Liu Sl. 2022. 'SARS-CoV-2 Spreads through Cell-to-Cell Transmission.' *Proceedings of the National Academy of Sciences of the United States of America* 119(1):e2111400119–e2111400119. doi: 10.1073/pnas.2111400119.
21. Callis, Judy. 2014. 'The Ubiquitination Machinery of the Ubiquitin System'. *The Arabidopsis Book / American Society of Plant Biologists* 12. doi: 10.1199/tab.0174.
22. Casler, Jason C., Effrosyni Papanikou, Juan J. Barrero, and Benjamin S. Glick. 2019. 'Maturation-Driven Transport and AP-1–Dependent Recycling of a Secretory Cargo in the Golgi'. *Journal of Cell Biology* 218(5):1582–1601. doi: 10.1083/jcb.201807195.
23. Cattin-Ortolá, Jérôme, Lawrence G. Welch, Sarah L. Maslen, Guido Papa, Leo C. James, and Sean Munro. 2021. 'Sequences in the Cytoplasmic Tail of SARS-CoV-2 Spike Facilitate Expression at the Cell Surface and Syncytia Formation'. *Nature Communications* 12. doi: 10.1038/s41467-021-25589-1.
24. Chai, Woei-Horng, Yi-Rong Li, Sheng-Hao Lin, Ya-Husan Chao, Cheng-Hsiung Chen, Po-Chiang Chan, and Ching-Hsiung Lin. 2020. 'Antihelminthic Niclosamide Induces Autophagy and Delayed Apoptosis in Human Non-Small Lung Cancer Cells *In Vitro* and *In Vivo*'. *Anticancer Research* 40(3):1405–17. doi: 10.21873/anticanres.14082.
25. Chan, Jasper Fuk-Woo, Kin-Hang Kok, Zheng Zhu, Hin Chu, Kelvin Kai-Wang To, Shuofeng Yuan, and Kwok-Yung Yuen. 2020. 'Genomic Characterization of the 2019 Novel Human-Pathogenic Coronavirus Isolated from a Patient with Atypical Pneumonia after Visiting Wuhan'. *Emerging Microbes & Infections* 9(1):221. doi: 10.1080/22221751.2020.1719902.
26. Chen, Wei, Jr Robert A. Mook, Richard T. Premont, and Jiangbo Wang. 2018. 'Niclosamide: Beyond an Antihelminthic Drug'. *Cellular Signalling* 41:89. doi: 10.1016/j.cellsig.2017.04.001.

27. Chen, Yang, Nan Zhang, Jie Zhang, Jiangtao Guo, Shaobo Dong, Heqiang Sun, Shuaixin Gao, Tingting Zhou, Min Li, Xueyuan Liu, Yaxin Guo, Beiwei Ye, Yingze Zhao, Tongqi Yu, Jianbo Zhan, Yongzhong Jiang, Catherine C. L. Wong, George F. Gao, and William J. Liu. 2022. 'Immune Response Pattern across the Asymptomatic, Symptomatic and Convalescent Periods of COVID-19'. *Biochimica et Biophysica Acta. Proteins and Proteomics* 1870(2):140736. doi: 10.1016/j.bbapap.2021.140736.
28. Chen, Yanjia, Xiaoyu Zhao, Hao Zhou, Huanzhang Zhu, Shibo Jiang, and Pengfei Wang. 2023. 'Broadly Neutralizing Antibodies to SARS-CoV-2 and Other Human Coronaviruses'. *Nature Reviews Immunology* 23(3):189–99. doi: 10.1038/s41577-022-00784-3.
29. Chen, Yi, Yao H, Zhang N, Wu J, Gao S, Guo J, Lu X, Cheng L, Luo R, Liang X, Wong Ccl, and Zheng M. 2021. 'Proteomic Analysis Identifies Prolonged Disturbances in Pathways Related to Cholesterol Metabolism and Myocardium Function in the COVID-19 Recovery Stage'. *Journal of Proteome Research* 20(7). doi: 10.1021/acs.jproteome.1c00054.
30. Chen, Yin-Yin, Han Hong, Yu-Ting Lei, Jia Zou, Yi-Ya Yang, and Li-Yu He. 2022. 'ACE2 Deficiency Exacerbates Obesity-Related Glomerulopathy through Its Role in Regulating Lipid Metabolism'. *Cell Death Discovery* 8(1):1–9. doi: 10.1038/s41420-022-01191-2.
31. Chuang, Huai-Chia, Chia-Hsin Hsueh, Pu-Ming Hsu, Rou-Huei Huang, Ching-Yi Tsai, Nai-Hsiang Chung, Yen-Hung Chow, and Tse-Hua Tan. 2022. 'SARS-CoV-2 Spike Protein Enhances MAP4K3/GLK-induced ACE2 Stability in COVID-19'. *EMBO Molecular Medicine* 14(9). doi: 10.15252/emmm.202215904.
32. Cooper, Geoffrey M. 2000. 'Protein Degradation'. in *The Cell: A Molecular Approach. 2nd edition*. Sinauer Associates.
33. Crottès, David, and Lily Yeh Jan. 2019. 'The Multifaceted Role of TMEM16A in Cancer'. *Cell Calcium* 82:102050. doi: 10.1016/j.ceca.2019.06.004.
34. Dang, Shangyu, Shengjie Feng, Jason Tien, Christian J. Peters, David Bulkley, Marco Lolicato, Jianhua Zhao, Kathrin Zuberbühler, Wenlei Ye, Lijun Qi, Tingxu Chen, Charles S. Craik, Yuh Nung Jan, Jr Daniel L. Minor, Yifan Cheng, and Lily Yeh Jan. 2017. 'Cryo-EM Structures of the TMEM16A Calcium-Activated Chloride Channel'. *Nature* 552(7685):426. doi: 10.1038/nature25024.
35. Danielsson, Jennifer, Jose Perez-Zoghbi, Kyra Bernstein, Matthew B. Barajas, Yi Zhang, Satish Kumar, Pawan K. Sharma, George Gallos, and Charles W. Emala. 2015.

'Antagonists of the TMEM16A Calcium-Activated Chloride Channel Modulate Airway Smooth Muscle Tone and Intracellular Calcium'. *Anesthesiology* 123(3):569. doi: 10.1097/ALN.0000000000000769.

36. Daniloski, Zharko, Tristan X. Jordan, Hans-Hermann Wessels, Daisy A. Hoagland, Silva Kasela, Mateusz Legut, Silas Maniatis, Eleni P. Mimitou, Lu Lu, Evan Geller, Oded Danziger, Brad R. Rosenberg, Hemali Phatnani, Peter Smibert, Tuuli Lappalainen, Benjamin R. tenOever, and Neville E. Sanjana. 2021. 'Identification of Required Host Factors for SARS-CoV-2 Infection in Human Cells'. *Cell* 184(1):92. doi: 10.1016/j.cell.2020.10.030.
37. Dikic, Ivan, Soichi Wakatsuki, and Kylie J. Walters. 2009. 'Ubiquitin-Binding Domains — from Structures to Functions'. *Nature Reviews Molecular Cell Biology* 10(10):659–71. doi: 10.1038/nrm2767.
38. Doyle, Laura M., and Michael Zhuo Wang. 2019. 'Overview of Extracellular Vesicles, Their Origin, Composition, Purpose, and Methods for Exosome Isolation and Analysis'. *Cells* 8(7). doi: 10.3390/cells8070727.
39. Drew Weissman, Mohamad Gabriel Alameh, Thushan de Silva, Paul Collini, Hailey Hornsby, Rebecca Brown, Celia C LaBlanche, Robert J Edwards, Laura Sutherland, Sampa Santra, Katayoun Mansouri, Sophie Gobeil, Charlene McDanal, Nobert Pardi, Nick Hengartner, Paulo J C Lin, Ying Tam, Pamela A Shaw, Mark G Lewis, Carsten Boesler, Ugur Sahin, Priyamvada Acharya, Barton F Haynes, Bette Korber, and David C Montefiori. 2021. 'D614G Spike Mutation Increases SARS CoV-2 Susceptibility to Neutralization'. *Cell Host & Microbe* 29(1):23-31.e4. doi: 10.1016/j.chom.2020.11.012.
40. Edler, Carolin, Ann Sophie Schröder, Martin Aepfelbacher, Antonia Fitzek, Axel Heinemann, Fabian Heinrich, Anke Klein, Felicia Langenwalder, Marc Lütgehetmann, Kira Meißner, Klaus Püschel, Julia Schädler, Stefan Steurer, Herbert Mushumba, and Jan-Peter Sperhake. 2020. 'Dying with SARS-CoV-2 Infection—an Autopsy Study of the First Consecutive 80 Cases in Hamburg, Germany'. *International Journal of Legal Medicine* 134(4):1275–84. doi: 10.1007/s00414-020-02317-w.
41. F, Morin, Kavian N, Nicco C, Cerles O, Chéreau C, and Batteux F. 2016. 'Niclosamide Prevents Systemic Sclerosis in a Reactive Oxygen Species-Induced Mouse Model'. *Journal of Immunology (Baltimore, Md. : 1950)* 197(8). doi: 10.4049/jimmunol.1502482.
42. Fang, Jin'e, Leqiang Sun, Guiqing Peng, Jia Xu, Rui Zhou, Shengbo Cao, Huanchun Chen, and Yunfeng Song. 2013. 'Identification of Three Antiviral Inhibitors against

Japanese Encephalitis Virus from Library of Pharmacologically Active Compounds 1280'. *PLoS ONE* 8(11). doi: 10.1371/journal.pone.0078425.

43. Fehr, Anthony R., and Stanley Perlman. 2015. 'Coronaviruses: An Overview of Their Replication and Pathogenesis'. *Coronaviruses* 1282:1–23. doi: 10.1007/978-1-4939-2438-7_1.
44. Feng, Shengjie, Cristina Puchades, Juyeon Ko, Hao Wu, Yifei Chen, Eric E. Figueroa, Shuo Gu, Tina W. Han, Brandon Ho, Tong Cheng, Junrui Li, Brian Shoichet, Yuh Nung Jan, Yifan Cheng, and Lily Yeh Jan. 2023. 'Identification of a Drug Binding Pocket in TMEM16F Calcium-Activated Ion Channel and Lipid Scramblase'. *Nature Communications* 14(1):1–12. doi: 10.1038/s41467-023-40410-x.
45. Feng Wei, Newbigging Am, Le C, Pang B, Peng H, Cao Y, Wu J, Abbas G, Song J, Wang Db, Cui M, Tao J, Tyrrell Dl, Zhang Xe, Zhang H, and Le Xc. 2020. 'Molecular Diagnosis of COVID-19: Challenges and Research Needs'. *Analytical Chemistry* 92(15). doi: 10.1021/acs.analchem.0c02060.
46. Figarola, James L., Jyotsana Singhal, Sharad Singhal, Jyotirmoy Kusari, and Arthur Riggs. 2018. 'Bioenergetic Modulation with the Mitochondria Uncouplers SR4 and Niclosamide Prevents Proliferation and Growth of Treatment-Naïve and Vemurafenib-Resistant Melanomas'. *Oncotarget* 9(97):36945. doi: 10.18632/oncotarget.26421.
47. Fonseca, Bruno D., Graham H. Diering, Michael A. Bidinosti, Kush Dalal, Tommy Alain, Aruna D. Balgi, Roberto Forestieri, Matt Nodwell, Charles V. Rajadurai, Cynthia Gunaratnam, Andrew R. Tee, Franck Duong, Raymond J. Andersen, John Orlowski, Masayuki Numata, Nahum Sonenberg, and Michel Roberge. 2012. 'Structure-Activity Analysis of Niclosamide Reveals Potential Role for Cytoplasmic pH in Control of Mammalian Target of Rapamycin Complex 1 (mTORC1) Signaling'. *The Journal of Biological Chemistry* 287(21):17530. doi: 10.1074/jbc.M112.359638.
48. Fountain, John H., Jasleen Kaur, and Sarah L. Lappin. 2023. 'Physiology, Renin Angiotensin System'. in *StatPearls [Internet]*. StatPearls Publishing.
49. G, Simmons, Gosalia Dn, Rennekamp Aj, Reeves Jd, Diamond Sl, and Bates P. 2005. 'Inhibitors of Cathepsin L Prevent Severe Acute Respiratory Syndrome Coronavirus Entry'. *Proceedings of the National Academy of Sciences of the United States of America* 102(33). doi: 10.1073/pnas.0505577102.
50. Gao, Xiang, Shengyuan Zhang, Jizhou Gou, Yanling Wen, Lujie Fan, Jian Zhou, Guangde Zhou, Gang Xu, and Zheng Zhang. 2022. 'Spike-Mediated ACE2 down-

Regulation Was Involved in the Pathogenesis of SARS-CoV-2 Infection'. *The Journal of Infection* 85(4):418. doi: 10.1016/j.jinf.2022.06.030.

51. Gennerich, Arne, and Ronald D. Vale. 2009. 'Walking the Walk: How Kinesin and Dynein Coordinate Their Steps'. *Current Opinion in Cell Biology* 21(1):59. doi: 10.1016/j.ceb.2008.12.002.
52. Gkogkou, Eirini, Grigoris Barnasas, Konstantinos Vougas, and Ioannis P. Trougakos. 2020. 'Expression Profiling Meta-Analysis of ACE2 and TMPRSS2, the Putative Anti-Inflammatory Receptor and Priming Protease of SARS-CoV-2 in Human Cells, and Identification of Putative Modulators'. *Redox Biology* 36. doi: 10.1016/j.redox.2020.101615.
53. Gomez-Navarro, Natalia, and Elizabeth Miller. 2016. 'Protein Sorting at the ER–Golgi Interface'. *The Journal of Cell Biology* 215(6):769. doi: 10.1083/jcb.201610031.
54. Goyal, Parag, Justin J. Choi, Laura C. Pinheiro, Edward J. Schenck, Ruijun Chen, Assem Jabri, Michael J. Satlin, Jr Thomas R. Campion, Musarrat Nahid, Joanna B. Ringel, Katherine L. Hoffman, Mark N. Alshak, Han A. Li, Graham T. Wehmeyer, Mangala Rajan, Evgeniya Reshetnyak, Nathaniel Hupert, Evelyn M. Horn, Fernando J. Martinez, Roy M. Gulick, and Monika M. Safford. 2020. 'Clinical Characteristics of Covid-19 in New York City'. *New England Journal of Medicine*. doi: 10.1056/NEJMc2010419.
55. H, Hofmann, Pyrc K, van der Hoek L, Geier M, Berkhout B, and Pöhlmann S. 2005. 'Human Coronavirus NL63 Employs the Severe Acute Respiratory Syndrome Coronavirus Receptor for Cellular Entry'. *Proceedings of the National Academy of Sciences of the United States of America* 102(22). doi: 10.1073/pnas.0409465102.
56. Han, Pengxun, Wenci Weng, Yinghui Chen, Yuchun Cai, Yao Wang, Menghua Wang, Hongyue Zhan, Changjian Yuan, Xuewen Yu, Mumin Shao, and Huili Sun. 2020. 'Niclosamide Ethanolamine Attenuates Systemic Lupus Erythematosus and Lupus Nephritis in MRL/Lpr Mice'. *American Journal of Translational Research* 12(9):5015.
57. Haßdenteufel, Sarah, Nicholas Johnson, Adrienne W. Paton, James C. Paton, Stephen High, and Richard Zimmermann. 2018. 'Chaperone-Mediated Sec61 Channel Gating during ER Import of Small Precursor Proteins Overcomes Sec61 Inhibitor-Reinforced Energy Barrier'. *Cell Reports* 23(5):1373. doi: 10.1016/j.celrep.2018.03.122.
58. Heald-Sargent, Taylor, and Tom Gallagher. 2012. 'Ready, Set, Fuse! The Coronavirus Spike Protein and Acquisition of Fusion Competence'. *Viruses* 4(4):557. doi:

10.3390/v4040557.

59. Herrero, Raquel, Gema Sanchez, and Jose Angel Lorente. 2018. 'New Insights into the Mechanisms of Pulmonary Edema in Acute Lung Injury'. *Annals of Translational Medicine* 6(2). doi: 10.21037/atm.2017.12.18.
60. Herring, Shawn, Jessica M. Oda, Jessica Wagoner, Delaney Kirchmeier, Aidan O'Connor, Elizabeth A. Nelson, Qinfeng Huang, Yuying Liang, Lisa Evans DeWald, Lisa M. Johansen, Pamela J. Glass, Gene G. Olinger, Aleksandr Ianevski, Tero Aittokallio, Mary F. Paine, Susan L. Fink, Judith M. White, and Stephen J. Polyak. 2021. 'Inhibition of Arenaviruses by Combinations of Orally Available Approved Drugs'. *Antimicrobial Agents and Chemotherapy* 65(4). doi: 10.1128/AAC.01146-20.
61. Hikmet, Feria, Loren Méar, Åsa Edvinsson, Patrick Micke, Mathias Uhlén, and Cecilia Lindskog. 2020. 'The Protein Expression Profile of ACE2 in Human Tissues'. *Molecular Systems Biology* 16(7). doi: 10.15252/msb.20209610.
62. Hl, Chiang, and Dice Jf. 1988. 'Peptide Sequences That Target Proteins for Enhanced Degradation during Serum Withdrawal'. *The Journal of Biological Chemistry* 263(14).
63. Hoffmann, Markus, Hannah Kleine-Weber, Simon Schroeder, Nadine Krüger, Tanja Herrler, Sandra Erichsen, Tobias S. Schiergens, Georg Herrler, Nai-Huei Wu, Andreas Nitsche, Marcel A. Müller, Christian Drosten, and Stefan Pöhlmann. 2020. 'SARS-CoV-2 Cell Entry Depends on ACE2 and TMPRSS2 and Is Blocked by a Clinically Proven Protease Inhibitor'. *Cell* 181(2):271. doi: 10.1016/j.cell.2020.02.052.
64. Huang, Yuan, Chan Yang, Xin-feng Xu, Wei Xu, and Shu-wen Liu. 2020. 'Structural and Functional Properties of SARS-CoV-2 Spike Protein: Potential Antivirus Drug Development for COVID-19'. *Acta Pharmacologica Sinica* 41(9):1141–49. doi: 10.1038/s41401-020-0485-4.
65. Hurley, James H. 2010. 'The ESCRT Complexes'. *Critical Reviews in Biochemistry and Molecular Biology* 45(6):463. doi: 10.3109/10409238.2010.502516.
66. I, Glowacka, Bertram S, Herzog P, Pfefferle S, Steffen I, Muench Mo, Simmons G, Hofmann H, Kuri T, Weber F, Eichler J, Drosten C, and Pöhlmann S. 2010. 'Differential Downregulation of ACE2 by the Spike Proteins of Severe Acute Respiratory Syndrome Coronavirus and Human Coronavirus NL63'. *Journal of Virology* 84(2). doi: 10.1128/JVI.01248-09.
67. I, Tanida, Ueno T, and Kominami E. 2008. 'LC3 and Autophagy'. *Methods in Molecular Biology (Clifton, N.J.)* 445. doi: 10.1007/978-1-59745-157-4_4.

68. J, Nylandsted, Gyrd-Hansen M, Danielewicz A, Fehrenbacher N, Lademann U, Høyer-Hansen M, Weber E, Multhoff G, Rohde M, and Jäättelä M. 2004. 'Heat Shock Protein 70 Promotes Cell Survival by Inhibiting Lysosomal Membrane Permeabilization'. *The Journal of Experimental Medicine* 200(4). doi: 10.1084/jem.20040531.
69. Jackson, Cody B., Michael Farzan, Bing Chen, and Hyeryun Choe. 2022. 'Mechanisms of SARS-CoV-2 Entry into Cells'. *Nature Reviews Molecular Cell Biology* 23(1):3–20. doi: 10.1038/s41580-021-00418-x.
70. Jackson, Laurelle, Hylton Rodel, Shi-Hsia Hwa, Sandile Cele, Yashica Ganga, Houriiyah Tegally, Mallory Bernstein, Jennifer Giandhari, Commit-Kzn Team, Bernadett I. Gosnell, Khadija Khan, Willem Hanekom, Farina Karim, Tulio de Oliveira, Mahomed-Yunus S. Moosa, and Alex Sigal. 2021. 'SARS-CoV-2 Cell-to-Cell Spread Occurs Rapidly and Is Insensitive to Antibody Neutralization'. *bioRxiv* 2021.06.01.446516. doi: 10.1101/2021.06.01.446516.
71. Jd, Brunner, Lim Nk, Schenck S, Duerst A, and Dutzler R. 2014. 'X-Ray Structure of a Calcium-Activated TMEM16 Lipid Scramblase'. *Nature* 516(7530). doi: 10.1038/nature13984.
72. Jennings, Benjamin C., Stuart Kornfeld, and Balraj Doray. 2021. 'A Weak COPI Binding Motif in the Cytoplasmic Tail of SARS-CoV-2 Spike Glycoprotein Is Necessary for Its Cleavage, Glycosylation, and Localization'. *Febs Letters* 595(13):1758. doi: 10.1002/1873-3468.14109.
73. Jiang, Fan, Jianmin Yang, Yongtao Zhang, Mei Dong, Shuangxi Wang, Qunye Zhang, Fang Fang Liu, Kai Zhang, and Cheng Zhang. 2014. 'Angiotensin-Converting Enzyme 2 and Angiotensin 1–7: Novel Therapeutic Targets'. *Nature Reviews Cardiology* 11(7):413–26. doi: 10.1038/nrcardio.2014.59.
74. Jin, Xin, Sihab Shah, Xiaona Du, Hailin Zhang, and Nikita Gamper. 2016. 'Activation of Ca2+-activated Cl– Channel ANO1 by Localized Ca2+ Signals'. *The Journal of Physiology* 594(1):19. doi: 10.1113/jphysiol.2014.275107.
75. Jocher, Georg, Vincent Grass, Sarah K. Tschirner, Lydia Riepler, Stephan Breimann, Tuğberk Kaya, Madlen Oelsner, M. Sabri Hamad, Laura I. Hofmann, Carl P. Blobel, Carsten B. Schmidt-Weber, Ozgun Gokce, Constanze A. Jakwerth, Jakob Trimpert, Janine Kimpel, Andreas Pichlmair, and Stefan F. Lichtenthaler. 2022. 'ADAM10 and ADAM17 Promote SARS-CoV-2 Cell Entry and Spike Protein-mediated Lung Cell Fusion'. *EMBO Reports* 23(6). doi: 10.15252/embr.202154305.

76. Jr, Fauver, Petrone Me, Hodcroft Eb, Shioda K, Ehrlich Hy, Watts Ag, Vogels Cbf, Brito Af, Alpert T, Muyombwe A, Razeq J, Downing R, Cheemarla Nr, Wyllie Al, Kalinich Cc, Ott Im, Quick J, Loman Nj, Neugebauer Km, Greninger Al, Jerome Kr, Roychoudhury P, Xie H, Shrestha L, Huang Ml, Pitzer Ve, Iwasaki A, Omer Sb, Khan K, Bogoch Ii, Martinello Ra, Foxman Ef, Landry Ml, Neher Ra, Ko Ai, and Grubaugh Nd. 2020. 'Coast-to-Coast Spread of SARS-CoV-2 during the Early Epidemic in the United States'. *Cell* 181(5). doi: 10.1016/j.cell.2020.04.021.
77. Jurgeit, Andreas, Robert McDowell, Stefan Moese, Eric Meldrum, Reto Schwendener, and Urs F. Greber. 2012. 'Niclosamide Is a Proton Carrier and Targets Acidic Endosomes with Broad Antiviral Effects'. *PLoS Pathogens* 8(10). doi: 10.1371/journal.ppat.1002976.
78. Kaushal, Jyoti B., Rakesh Bhatia, Ranjana K. Kanchan, Pratima Raut, Surya Mallapragada, Quan P. Ly, Surinder K. Batra, and Satyanarayana Rachagani. 2021. 'Correction: Kaushal et al. Repurposing Niclosamide for Targeting Pancreatic Cancer by Inhibiting Hh/Gli Non-Canonical Axis of Gsk3β. Cancers 2021, 13, 3105'. *Cancers* 13(22). doi: 10.3390/cancers13225591.
79. Kulkarni, Sucheta, Qin Li, Aatur D. Singhi, Silvia Liu, Satdarshan P. Monga, and Andrew P. Feranchak. 2023. 'TMEM16A Partners with mTOR to Influence Pathways of Cell Survival, Proliferation, and Migration in Cholangiocarcinoma'. *American Journal of Physiology-Gastrointestinal and Liver Physiology*. doi: 10.1152/ajpgi.00270.2022.
80. L, Huang, Yang M, Yuan Y, Li X, and Kuang E. 2017. 'Niclosamide Inhibits Lytic Replication of Epstein-Barr Virus by Disrupting mTOR Activation'. *Antiviral Research* 138. doi: 10.1016/j.antiviral.2016.12.002.
81. L, Premkumar, Segovia-Chumbez B, Jadi R, Martinez Dr, Raut R, Markmann A, Cornaby C, Bartelt L, Weiss S, Park Y, Edwards Ce, Weimer E, Scherer Em, Rouphael N, Edupuganti S, Weiskopf D, Tse Lv, Hou Yj, Margolis D, Sette A, Collins Mh, Schmitz J, Baric Rs, and de Silva Am. 2020. 'The Receptor Binding Domain of the Viral Spike Protein Is an Immunodominant and Highly Specific Target of Antibodies in SARS-CoV-2 Patients'. *Science Immunology* 5(48). doi: 10.1126/sciimmunol.abc8413.
82. Lambert, Daniel W., Mike Yarski, Fiona J. Warner, Paul Thornhill, Edward T. Parkin, A. Ian Smith, Nigel M. Hooper, and Anthony J. Turner. 2005. 'Tumor Necrosis Factor-α Convertase (ADAM17) Mediates Regulated Ectodomain Shedding of the Severe-Acute Respiratory Syndrome-Coronavirus (SARS-CoV) Receptor, Angiotensin-Converting

Enzyme-2 (ACE2)'. *The Journal of Biological Chemistry* 280(34):30113. doi: 10.1074/jbc.M505111200.

83. Laurent, Estelle M. N., Yorgos Sofianatos, Anastassia Komarova, Jean-Pascal Gimeno, Payman Samavarchi Tehrani, Dae-Kyum Kim, Hala Abdouni, Marie Duhamel, Patricia Cassonnet, Jennifer J. Knapp, Da Kuang, Aditya Chawla, Dayag Sheykhkarimli, Ashyad Rayhan, Roujia Li, Oxana Pogoutse, David E. Hill, Michael A. Calderwood, Pascal Falter-Braun, Patrick Aloy, Ulrich Stelzl, Marc Vidal, Anne-Claude Gingras, Georgios A. Pavlopoulos, Sylvie Van Der Werf, Isabelle Fournier, Frederick P. Roth, Michel Salzet, Caroline Demeret, Yves Jacob, and Etienne Coyaud. 2020. *Global BioID-Based SARS-CoV-2 Proteins Proximal Interactome Unveils Novel Ties between Viral Polypeptides and Host Factors Involved in Multiple COVID19-Associated Mechanisms*. *preprint*. Systems Biology. doi: 10.1101/2020.08.28.272955.
84. Le, Son C., Zhiguang Jia, Jianhan Chen, and Huanghe Yang. 2019. 'Molecular Basis of PIP2-Dependent Regulation of the Ca2+-Activated Chloride Channel TMEM16A'. *Nature Communications* 10. doi: 10.1038/s41467-019-11784-8.
85. Lee, Jin-Gu, Weiliang Huang, Hangnoh Lee, Joyce van de Leemput, Maureen A. Kane, and Zhe Han. 2021. 'Characterization of SARS-CoV-2 Proteins Reveals Orf6 Pathogenicity, Subcellular Localization, Host Interactions and Attenuation by Selinexor'. *Cell & Bioscience* 11. doi: 10.1186/s13578-021-00568-7.
86. Lee, Ming-Cheng, Yin-Kai Chen, Yih-Jen Hsu, and Bor-Ru Lin. 2020. 'Niclosamide Inhibits the Cell Proliferation and Enhances the Responsiveness of Esophageal Cancer Cells to Chemotherapeutic Agents'. *Oncology Reports* 43(2):549. doi: 10.3892/or.2019.7449.
87. Li, Haini, Ancheng Wu, Wuhui Zhu, Feng Hou, Shaoyun Cheng, Jinpeng Cao, Yufen Yan, Congxiao Zhang, and Zongtao Liu. 2019. 'Detection of ANO1 mRNA in PBMCs Is a Promising Method for GISTs Diagnosis'. *Scientific Reports* 9. doi: 10.1038/s41598-019-45941-2.
88. Li, Wenhui, Michael J. Moore, Natalya Vasilieva, Jianhua Sui, Swee Kee Wong, Michael A. Berne, Mohan Somasundaran, John L. Sullivan, Katherine Luzuriaga, Thomas C. Greenough, Hyeryun Choe, and Michael Farzan. 2003. 'Angiotensin-Converting Enzyme 2 Is a Functional Receptor for the SARS Coronavirus'. *Nature* 426(6965):450. doi: 10.1038/nature02145.
89. Li, Zhong, Jimin Xu, Yuekun Lang, Xiaoyu Fan, Lili Kuo, Lianna D'Brant, Saiyang Hu,

Subodh Kumar Samrat, Nicole Trudeau, Anil M. Tharappel, Natasha Rugenstein, Cheri A. Koetzner, Jing Zhang, Haiying Chen, Laura D. Kramer, David Butler, Qing-Yu Zhang, Jia Zhou, and Hongmin Li. 2020. 'JMX0207, a Niclosamide Derivative with Improved Pharmacokinetics, Suppresses Zika Virus Infection Both In Vitro and In Vivo'. *ACS Infectious Diseases* 6(10):2616. doi: 10.1021/acsinfecdis.0c00217.

90. Liu, Xiaonan, Sini Huuskonen, Tuomo Laitinen, Taras Redchuk, Mariia Bogacheva, Kari Salokas, Ina Pöhner, Tiina Öhman, Arun Kumar Tonduru, Antti Hassinen, Lisa Gawriyski, Salla Keskitalo, Maria K. Vartiainen, Vilja Pietiäinen, Antti Poso, and Markku Varjosalo. 2021. 'SARS-CoV-2–Host Proteome Interactions for Antiviral Drug Discovery'. *Molecular Systems Biology* 17(11). doi: 10.15252/msb.202110396.
91. Liu, Yang, Jianying Liu, Kenneth S. Plante, Jessica A. Plante, Xuping Xie, Xianwen Zhang, Zhiqiang Ku, Zhiqiang An, Dionna Scharton, Craig Schindewolf, Steven G. Widen, Vineet D. Menachery, Pei-Yong Shi, and Scott C. Weaver. 2022. 'The N501Y Spike Substitution Enhances SARS-CoV-2 Infection and Transmission'. *Nature* 602(7896):294–99. doi: 10.1038/s41586-021-04245-0.
92. Lu Yi, Qingwei Zhua, Douglas M. Foxa, Carol Gaoa, Sarah A. Stanleya, and Kunxin Luo. 2022. 'SARS-CoV-2 down-Regulates ACE2 through Lysosomal Degradation'. *SARS-CoV-2 down-Regulates ACE2 through Lysosomal Degradation* 33.
93. Lu, Yi, Qingwei Zhu, Douglas M. Fox, Carol Gao, Sarah A. Stanley, and Kunxin Luo. 2022. 'SARS-CoV-2 down-Regulates ACE2 through Lysosomal Degradation'. *Molecular Biology of the Cell* 33(14). doi: 10.1091/mbc.E22-02-0045.
94. M, Donoghue, Hsieh F, Baronas E, Godbout K, Gosselin M, Stagliano N, Donovan M, Woolf B, Robison K, Jeyaseelan R, Breitbart Re, and Acton S. 2000. 'A Novel Angiotensin-Converting Enzyme-Related Carboxypeptidase (ACE2) Converts Angiotensin I to Angiotensin 1-9'. *Circulation Research* 87(5). doi: 10.1161/01.res.87.5.e1.
95. M, Huang, Zeng S, Qiu Q, Xiao Y, Shi M, Zou Y, Yang X, Xu H, and Liang L. 2016. 'Niclosamide Induces Apoptosis in Human Rheumatoid Arthritis Fibroblast-like Synoviocytes'. *International Immunopharmacology* 31. doi: 10.1016/j.intimp.2015.11.002.
96. Ma, Ma, Gao F, Chen Q, Xuan X, Wang Y, Deng H, Yang F, and Yuan L. 2020. 'ACE2 Modulates Glucose Homeostasis through GABA Signaling during Metabolic Stress'. *The Journal of Endocrinology* 246(3). doi: 10.1530/JOE-19-0471.

97. Marcel Levi, Jecko Thachil, Toshiaki Iba, and Jerrold H Levi. 2020. 'Coagulation Abnormalities and Thrombosis in Patients with COVID-19'. *The Lancet Haematology* 7(6):e438–40. doi: 10.1016/S2352-3026(20)30145-9.

98. Matsuyama, S., N. Nagata, K. Shirato, M. Kawase, F. Takeda, and F. Taguchi. 2010. 'Efficient Activation of the Severe Acute Respiratory Syndrome Coronavirus Spike Protein by the Transmembrane Protease TMPRSS2'. *Journal of Virology* 84(24). doi: 10.1128/JVI.01542-10.

99. Mayor, Satyajit, and Richard E. Pagano. 2007. 'Pathways of Clathrin-Independent Endocytosis'. *Nature Reviews Molecular Cell Biology* 8(8):603–12. doi: 10.1038/nrm2216.

100. Mettlen, Marcel, Ping-Hung Chen, Saipraveen Srinivasan, Gaudenz Danuser, and Sandra L. Schmid. 2018. 'Regulation of Clathrin-Mediated Endocytosis'. *Annual Review of Biochemistry* 87:871. doi: 10.1146/annurev-biochem-062917-012644.

101. Millet, Jean Kaoru, François Kien, Chung-Yan Cheung, Yu-Lam Siu, Wing-Lim Chan, Huiying Li, Hiu-Lan Leung, Martial Jaume, Roberto Bruzzone, Joseph S. Malik Peiris, Ralf Marius Altmeyer, and Béatrice Nal. 2012. 'Ezrin Interacts with the SARS Coronavirus Spike Protein and Restrains Infection at the Entry Stage'. *PLoS ONE* 7(11). doi: 10.1371/journal.pone.0049566.

102. Miner, Kent, Katja Labitzke, Benxian Liu, Paul Wang, Kathryn Henckels, Kevin Gaida, Robin Elliott, Jian Jeffrey Chen, Longbin Liu, Anh Leith, Esther Trueblood, Kelly Hensley, Xing-Zhong Xia, Oliver Homann, Brian Bennett, Mike Fiorino, John Whoriskey, Gang Yu, Sabine Escobar, Min Wong, Teresa L. Born, Alison Budelsky, Mike Comeau, Dirk Smith, Jonathan Phillips, James A. Johnston, Joseph G. McGivern, Kerstin Weikl, David Powers, Karl Kunzelmann, Deanna Mohn, Andreas Hochheimer, and John K. Sullivan. 2019. 'Drug Repurposing: The Anthelmintics Niclosamide and Nitazoxanide Are Potent TMEM16A Antagonists That Fully Bronchodilate Airways'. *Frontiers in Pharmacology* 10. doi: 10.3389/fphar.2019.00051.

103. Mm, Ma, Gao M, Guo Km, Wang M, Li Xy, Zeng Xl, Sun L, Lv Xf, Du Yh, Wang Gl, Zhou Jg, and Guan Yy. 2017. 'TMEM16A Contributes to Endothelial Dysfunction by Facilitating Nox2 NADPH Oxidase-Derived Reactive Oxygen Species Generation in Hypertension'. *Hypertension (Dallas, Tex.: 1979)* 69(5). doi: 10.1161/HYPERTENSIONAHA.116.08874.

104. Moreno-Layseca, Paulina, Niklas Z. Jäntti, Rashmi Godbole, Christian Sommer,

Guillaume Jacquemet, Hussein Al-Akhrass, James R. W. Conway, Pauliina Kronqvist, Roosa E. Kallionpää, Leticia Oliveira-Ferrer, Pasquale Cervero, Stefan Linder, Martin Aepfelbacher, Henrik Zauber, James Rae, Robert G. Parton, Andrea Disanza, Giorgio Scita, Satyajit Mayor, Matthias Selbach, Stefan Veltel, and Johanna Ivaska. 2021. 'Cargo-Specific Recruitment in Clathrin- and Dynamin-Independent Endocytosis'. *Nature Cell Biology* 23(10):1073–84. doi: 10.1038/s41556-021-00767-x.

105. Mostafa, Ahmed, Ahmed Kandeil, Yaseen A. M. M. Elshaier, Omnia Kutkat, Yassmin Moatasim, Adel A. Rashad, Mahmoud Shehata, Mokhtar R. Gomaa, Noura Mahrous, Sara H. Mahmoud, Mohamed GabAllah, Hisham Abbas, Ahmed El Taweel, Ahmed E. Kayed, Mina Nabil Kamel, Mohamed El Sayes, Dina B. Mahmoud, Rabeh El-Shesheny, Ghazi Kayali, and Mohamed A. Ali. 2020. 'FDA-Approved Drugs with Potent In Vitro Antiviral Activity against Severe Acute Respiratory Syndrome Coronavirus 2'. *Pharmaceuticals* 13(12). doi: 10.3390/ph13120443.

106. Mp, Wilkie, Hubert Td, Boogaard Ma, and Birceanu O. 2019. 'Control of Invasive Sea Lampreys Using the Piscicides TFM and Niclosamide: Toxicology, Successes & Future Prospects'. *Aquatic Toxicology (Amsterdam, Netherlands)* 211. doi: 10.1016/j.aquatox.2018.12.012.

107. Mulcahy, Laura Ann, Ryan Charles Pink, and David Raul Francisco Carter. 2014. 'Routes and Mechanisms of Extracellular Vesicle Uptake'. *Journal of Extracellular Vesicles* 3. doi: 10.3402/jev.v3.24641.

108. N, Wu, Cernysiov V, Davidson D, Song H, Tang J, Luo S, Lu Y, Qian J, Gyurova Ie, Waggoner Sn, Trinh Vq, Cayrol R, Sugiura A, McBride Hm, Daudelin Jf, Labrecque N, and Veillette A. 2020. 'Critical Role of Lipid Scramblase TMEM16F in Phosphatidylserine Exposure and Repair of Plasma Membrane after Pore Formation'. *Cell Reports* 30(4). doi: 10.1016/j.celrep.2019.12.066.

109. Naqvi, Ahmad Abu Turab, Kisa Fatima, Taj Mohammad, Urooj Fatima, Indrakant K. Singh, Archana Singh, Shaikh Muhammad Atif, Gururao Hariprasad, Gulam Mustafa Hasan, and Md Imtaiyaz Hassan. 2020. 'Insights into SARS-CoV-2 Genome, Structure, Evolution, Pathogenesis and Therapies: Structural Genomics Approach'. *Biochimica et Biophysica Acta. Molecular Basis of Disease* 1866(10):165878. doi: 10.1016/j.bbadis.2020.165878.

110. Nardacci, R., J. L. Perfettini, L. Grieco, D. Thieffry, G. Kroemer, and M. Piacentini. 2015a. 'Syncytial Apoptosis Signaling Network Induced by the HIV-1 Envelope

Glycoprotein Complex: An Overview'. *Cell Death & Disease* 6(8):e1846–e1846. doi: 10.1038/cddis.2015.204.

111. Nardacci, R., J. L. Perfettini, L. Grieco, D. Thieffry, G. Kroemer, and M. Piacentini. 2015b. 'Syncytial Apoptosis Signaling Network Induced by the HIV-1 Envelope Glycoprotein Complex: An Overview'. *Cell Death & Disease* 6(8):e1846–e1846. doi: 10.1038/cddis.2015.204.

112. Neuhof, Andrea, Melissa M. Rolls, Berit Jungnickel, Kai-Uwe Kalies, and Tom A. Rapoport. 1998. 'Binding of Signal Recognition Particle Gives Ribosome/Nascent Chain Complexes a Competitive Advantage in Endoplasmic Reticulum Membrane Interaction'. *Molecular Biology of the Cell* 9(1):103. doi: 10.1091/mbc.9.1.103.

113. Neuman, Benjamin W., Brian D. Adair, Craig Yoshioka, Joel D. Quispe, Gretchen Orca, Peter Kuhn, Ronald A. Milligan, Mark Yeager, and Michael J. Buchmeier. 2006. 'Supramolecular Architecture of Severe Acute Respiratory Syndrome Coronavirus Revealed by Electron Cryomicroscopy'. *Journal of Virology* 80(16):7918. doi: 10.1128/JVI.00645-06.

114. O, Wiese, Zemlin Ae, and Pillay Ts. 2021. 'Molecules in Pathogenesis: Angiotensin Converting Enzyme 2 (ACE2)'. *Journal of Clinical Pathology* 74(5). doi: 10.1136/jclinpath-2020-206954.

115. Oh, Uhtaek, and Jooyoung Jung. 2016. 'Cellular Functions of TMEM16/Anoctamin'. *Pflugers Archiv* 468:443. doi: 10.1007/s00424-016-1790-0.

116. P, Andrews, Thyssen J, and Lorke D. 1982. 'The Biology and Toxicology of Molluscicides, Bayluscide'. *Pharmacology & Therapeutics* 19(2). doi: 10.1016/0163-7258(82)90064-x.

117. P, Shah, Canziani Ga, Carter Ep, and Chaiken I. 2021. 'The Case for S2: The Potential Benefits of the S2 Subunit of the SARS-CoV-2 Spike Protein as an Immunogen in Fighting the COVID-19 Pandemic'. *Frontiers in Immunology* 12. doi: 10.3389/fimmu.2021.637651.

118. Pereira, Naveen L., Ferhaan Ahmad, Mirnela Byku, Nathan W. Cummins, Alanna A. Morris, Anjali Owens, Sony Tuteja, and Sharon Cresci. 2021. 'COVID-19: Understanding Inter-Individual Variability and Implications for Precision Medicine'. *Mayo Clinic Proceedings* 96(2):446. doi: 10.1016/j.mayocp.2020.11.024.

119. Pinto, Dora, Maximilian M. Sauer, Nadine Czudnochowski, Jun Siong Low, M. Alejandra Tortorici, Michael P. Housley, Julia Noack, Alexandra C. Walls, John E.

Bowen, Barbara Guarino, Laura E. Rosen, Julia di Iulio, Josipa Jerak, Hannah Kaiser, Saiful Islam, Stefano Jaconi, Nicole Sprugasci, Katja Culap, Rana Abdelnabi, Caroline Foo, Lotte Coelmont, Istvan Bartha, Siro Bianchi, Chiara Silacci-Fregni, Jessica Bassi, Roberta Marzi, Eneida Vetti, Antonino Cassotta, Alessandro Ceschi, Paolo Ferrari, Pietro E. Cippà, Olivier Giannini, Samuele Ceruti, Christian Garzoni, Agostino Riva, Fabio Benigni, Elisabetta Cameroni, Luca Piccoli, Matteo S. Pizzuto, Megan Smithey, David Hong, Amalio Telenti, Florian A. Lempp, Johan Neyts, Colin Havenar-Daughton, Antonio Lanzavecchia, Federica Sallusto, Gyorgy Snell, Herbert W. Virgin, Martina Beltramello, Davide Corti, and David Veesler. 2021. 'Broad Betacoronavirus Neutralization by a Stem Helix–Specific Human Antibody'. *Science*. doi: 10.1126/science.abj3321.

120. Prasad, Prasad, Cerikan B, Stahl Y, Kopp K, Magg V, Acosta-Rivero N, Kim H, Klein K, Funaya C, Haselmann U, Cortese M, Heigwer F, Bageritz J, Bitto D, Jargalsaikhan S, Neufeldt C, Pahmeier F, Boutros M, Yamauchi Y, Ruggieri A, and Bartenschlager R. 2023. 'Enhanced SARS-CoV-2 Entry via UPR-Dependent AMPK-Related Kinase NUAK2'. *Molecular Cell* 83(14). doi: 10.1016/j.molcel.2023.06.020.

121. Q, Ji, Guo S, Wang X, Pang C, Zhan Y, Chen Y, and An H. 2019. 'Recent Advances in TMEM16A: Structure, Function, and Disease'. *Journal of Cellular Physiology* 234(6). doi: 10.1002/jcp.27865.

122. R, Papp, Nagaraj C, Zabini D, Nagy Bm, Lengyel M, Skofic Maurer D, Sharma N, Egemnazarov B, Kovacs G, Kwapiszewska G, Marsh Lm, Hrzenjak A, Höfler G, Didiasova M, Wygrecka M, Sievers Lk, Szucs P, Enyedi P, Ghanim B, Klepetko W, Olschewski H, and Olschewski A. 2019. 'Targeting TMEM16A to Reverse Vasoconstriction and Remodelling in Idiopathic Pulmonary Arterial Hypertension'. *The European Respiratory Journal* 53(6). doi: 10.1183/13993003.00965-2018.

123. R, Yan, Zhang Y, Li Y, Xia L, Guo Y, and Zhou Q. 2020. 'Structural Basis for the Recognition of SARS-CoV-2 by Full-Length Human ACE2'. *Science (New York, N.Y.)* 367(6485). doi: 10.1126/science.abb2762.

124. Reily, Colin, Tyler J. Stewart, Matthew B. Renfrow, and Jan Novak. 2019. 'Glycosylation in Health and Disease'. *Nature Reviews Nephrology* 15(6):346–66. doi: 10.1038/s41581-019-0129-4.

125. Rensong Ye and Zhenwei Liu. 2020. 'ACE2 Exhibits Protective Effects against LPS-Induced Acute Lung Injury in Mice by Inhibiting the LPS-TLR4 Pathway'.

Experimental and Molecular Pathology 113. doi: 10.1016/j.yexmp.2019.104350.

126. Ricardo Jose. 2020. 'COVID-19 Cytokine Storm: The Interplay between Inflammation and Coagulation'. *The Lancet Respiratory Medicine* 8(6):e46–47. doi: 10.1016/S2213-2600(20)30216-2.

127. Runwal, Gautam, Eleanna Stamatakou, Farah H. Siddiqi, Claudia Puri, Ye Zhu, and David C. Rubinsztein. 2019. 'LC3-Positive Structures Are Prominent in Autophagy-Deficient Cells'. *Scientific Reports* 9(1):1–14. doi: 10.1038/s41598-019-46657-z.

128. Saad, Mabroka H., Raied Badierah, Elrashdy M. Redwan, and Esmail M. El-Fakharany. 2021. 'A Comprehensive Insight into the Role of Exosomes in Viral Infection: Dual Faces Bearing Different Functions'. *Pharmaceutics* 13(9). doi: 10.3390/pharmaceutics13091405.

129. Samavarchi-Tehrani, Payman, Hala Abdouni, James D. R. Knight, Audrey Astori, Reuben Samson, Zhen-Yuan Lin, Dae-Kyum Kim, Jennifer J. Knapp, Jonathan St-Germain, Christopher D. Go, Brett Larsen, Cassandra J. Wong, Patricia Cassonnet, Caroline Demeret, Yves Jacob, Frederick P. Roth, Brian Raught, and Anne-Claude Gingras. 2020. *A SARS-CoV-2 – Host Proximity Interactome*. *preprint*. Systems Biology. doi: 10.1101/2020.09.03.282103.

130. Sanda, Miloslav, Lindsay Morrison, and Radoslav Goldman. 2021. 'N and O Glycosylation of the SARS-CoV-2 Spike Protein'. *Analytical Chemistry* 93(4):2003. doi: 10.1021/acs.analchem.0c03173.

131. Sandrin Belouzard, Victor C. Chu, and Gary R. Whittaker. 2009. 'Activation of the SARS Coronavirus Spike Protein via Sequential Proteolytic Cleavage at Two Distinct Sites'. *Proceedings of the National Academy of Sciences of the United States of America* 106(14). doi: 10.1073/pnas.0809524106.

132. Santini, Francesca, Michael S. Marks, and James H. Keen. 1998. 'Endocytic Clathrin-Coated Pit Formation Is Independent of Receptor Internalization Signal Levels'. *Molecular Biology of the Cell* 9(5):1177. doi: 10.1091/mbc.9.5.1177.

133. Satarker, Sairaj, and Madhavan Nampoothiri. 2020. 'Structural Proteins in Severe Acute Respiratory Syndrome Coronavirus-2'. *Archives of Medical Research* 51(6):482. doi: 10.1016/j.arcmed.2020.05.012.

134. Schmidt, Oliver, and David Teis. 2012. 'The ESCRT Machinery'. *Current Biology* 22(4):R116. doi: 10.1016/j.cub.2012.01.028.

135. Schoeman, Dewald, and Burtram C. Fielding. 2019. 'Coronavirus Envelope

Protein: Current Knowledge'. *Virology Journal* 16. doi: 10.1186/s12985-019-1182-0.

136. Schubert, Desirée, Marie-Christine Klein, Sarah Hassdenteufel, Andrés Caballero-Oteyza, Linlin Yang, Michele Proietti, Alla Bulashevska, Janine Kemming, Johannes Kühn, Sandra Winzer, Stephan Rusch, Manfred Fliegauf, Alejandro A. Schäffer, Stefan Pfeffer, Roger Geiger, Adolfo Cavalié, Hongzhi Cao, Fang Yang, Yong Li, Marta Rizzi, Hermann Eibel, Robin Kobbe, Amy L. Marks, Brian P. Peppers, Robert W. Hostoffer, Jennifer M. Puck, Richard Zimmermann, and Bodo Grimbacher. 2018. 'Plasma Cell Deficiency in Humans with Heterozygous Mutations in SEC61A1'. *The Journal of Allergy and Clinical Immunology* 141(4):1427. doi: 10.1016/j.jaci.2017.06.042.

137. Shajahan, Asif, Nitin T. Supekar, Anne S. Gleinich, and Parastoo Azadi. 2020. 'Deducing the N- and O-Glycosylation Profile of the Spike Protein of Novel Coronavirus SARS-CoV-2'. *Glycobiology* 30(12):981. doi: 10.1093/glycob/cwaa042.

138. Sokolowska, Milena. 2020. 'Outsmarting SARS-CoV-2 by Empowering a Decoy ACE2'. *Signal Transduction and Targeted Therapy* 5(1):1–3. doi: 10.1038/s41392-020-00370-w.

139. Sr, Tipnis, Hooper Nm, Hyde R, Karran E, Christie G, and Turner Aj. 2000. 'A Human Homolog of Angiotensin-Converting Enzyme. Cloning and Functional Expression as a Captopril-Insensitive Carboxypeptidase'. *The Journal of Biological Chemistry* 275(43). doi: 10.1074/jbc.M002615200.

140. Stukalov, Alexey, Virginie Girault, Vincent Grass, Ozge Karayel, Valter Bergant, Christian Urban, Darya A. Haas, Yiqi Huang, Lila Oubraham, Anqi Wang, M. Sabri Hamad, Antonio Piras, Fynn M. Hansen, Maria C. Tanzer, Igor Paron, Luca Zinzula, Thomas Engleitner, Maria Reinecke, Teresa M. Lavacca, Rosina Ehmann, Roman Wölfel, Jörg Jores, Bernhard Kuster, Ulrike Protzer, Roland Rad, John Ziebuhr, Volker Thiel, Pietro Scaturro, Matthias Mann, and Andreas Pichlmair. 2021. 'Multilevel Proteomics Reveals Host Perturbations by SARS-CoV-2 and SARS-CoV'. *Nature* 594(7862):246–52. doi: 10.1038/s41586-021-03493-4.

141. Su, Siyuan, Jianfeng Chen, Ying Wang, Lilly M. Wong, Zhichuan Zhu, Guochun Jiang, and Pengda Liu. 2021. 'Lenalidomide Downregulates ACE2 Protein Abundance to Alleviate Infection by SARS-CoV-2 Spike Protein Conditioned Pseudoviruses'. *Signal Transduction and Targeted Therapy* 6. doi: 10.1038/s41392-021-00608-1.

142. Suliman, Mohammed A., Zhenxing Zhang, Heya Na, Ailton L. L. Ribeiro, Yu

Zhang, Bachir Niang, Abdu Salim Hamid, Hua Zhang, Lijie Xu, and Yunfei Zuo. 2016. 'Niclosamide Inhibits Colon Cancer Progression through Downregulation of the Notch Pathway and Upregulation of the Tumor Suppressor miR-200 Family'. *International Journal of Molecular Medicine* 38(3):776. doi: 10.3892/ijmm.2016.2689.

143. Sun, Xiaoyu, Chunyan Yi, Yuanfei Zhu, Longfei Ding, Shuai Xia, Xingchen Chen, Mu Liu, Chenjian Gu, Xiao Lu, Yadong Fu, Shuangfeng Chen, Tianlong Zhang, Yaguang Zhang, Zhuo Yang, Liyan Ma, Wangpeng Gu, Gaowei Hu, Shujuan Du, Renhong Yan, Weihui Fu, Songhua Yuan, Chenli Qiu, Chen Zhao, Xiaoyan Zhang, Yonghui He, Aidong Qu, Xu Zhou, Xiuling Li, Gary Wong, Qiang Deng, Qiang Zhou, Hongzhou Lu, Zhiyang Ling, Jianping Ding, Lu Lu, Jianqing Xu, Youhua Xie, and Bing Sun. 2022. 'Neutralization Mechanism of a Human Antibody with Pan-Coronavirus Reactivity Including SARS-CoV-2'. *Nature Microbiology* 7(7):1063–74. doi: 10.1038/s41564-022-01155-3.

144. Sy, Park, Kim Jy, Choi Jh, Kim Jh, Lee Cj, Singh P, Sarkar S, Baek Jh, and Nam Js. 2019. 'Inhibition of LEF1-Mediated DCLK1 by Niclosamide Attenuates Colorectal Cancer Stemness'. *Clinical Cancer Research : An Official Journal of the American Association for Cancer Research* 25(4). doi: 10.1158/1078-0432.CCR-18-1232.

145. Takei, Kohji, Vladimir I. Slepnev, Volker Haucke, and Pietro De Camilli. 1999. 'Functional Partnership between Amphiphysin and Dynamin in Clathrin-Mediated Endocytosis'. *Nature Cell Biology* 1(1):33–39. doi: 10.1038/9004.

146. Tang, Xiaopeng, Mengli Yang, Zilei Duan, Zhiyi Liao, Lei Liu, Mingqian Fang, Gan Wang, Hongqi Liu, Jingwen Xu, Zhiye Zhang, Lian Yang, Xudong Zhao, Xiaozhong Peng, and Ren Lai. n.d. 'Transferrin Receptor Is Another Receptor for SARS-CoV-2 Entry'.

147. Teng, Felicia Yu Hsuan, Ya Wang, and Bor Luen Tang. 2001. 'The Syntaxins'. *Genome Biology* 2(11):reviews3012.1. doi: 10.1186/gb-2001-2-11-reviews3012.

148. Tian, Fang, Bei Tong, Liang Sun, Shengchao Shi, Bin Zheng, Zibin Wang, Xianchi Dong, and Peng Zheng. 2021. 'N501Y Mutation of Spike Protein in SARS-CoV-2 Strengthens Its Binding to Receptor ACE2'. *eLife*. Retrieved 5 October 2023 (https://elifesciences.org/articles/69091).

149. Tian, Wenmin, Delin Li, Nan Zhang, Guijie Bai, Kai Yuan, Haixia Xiao, Feng Gao, Yang Chen, Catherine C. L. Wong, and George Fu Gao. 2021. 'O-Glycosylation Pattern of the SARS-CoV-2 Spike Protein Reveals an "O-Follow-N" Rule'. *Cell Research*

31(10):1123. doi: 10.1038/s41422-021-00545-2.

150. Tian, Wenmin, Nan Zhang, Ronghua Jin, Yingmei Feng, Siyuan Wang, Shuaixin Gao, Ruqin Gao, Guizhen Wu, Di Tian, Wenjie Tan, Yang Chen, George Fu Gao, and Catherine C. L. Wong. 2020. 'Immune Suppression in the Early Stage of COVID-19 Disease'. *Nature Communications* 11. doi: 10.1038/s41467-020-19706-9.

151. Turk, Vito, Veronika Stoka, Olga Vasiljeva, Miha Renko, Tao Sun, Boris Turk, and Dušan Turk. 2012. 'Cysteine Cathepsins: From Structure, Function and Regulation to New Frontiers'. *Biochimica et Biophysica Acta. Proteins and Proteomics* 1824(1):68. doi: 10.1016/j.bbapap.2011.10.002.

152. V'kovski, Philip, Annika Kratzel, Silvio Steiner, Hanspeter Stalder, and Volker Thiel. 2021. 'Coronavirus Biology and Replication: Implications for SARS-CoV-2'. *Nature Reviews Microbiology* 19(3):155–70. doi: 10.1038/s41579-020-00468-6.

153. Walls, Alexandra C., Young-Jun Park, M. Alejandra Tortorici, Abigail Wall, Andrew T. McGuire, and David Veesler. 2020. 'Structure, Function, and Antigenicity of the SARS-CoV-2 Spike Glycoprotein'. *Cell* 181(2):281-292.e6. doi: 10.1016/j.cell.2020.02.058.

154. Wang, Yu-Ming, Jeng-Wei Lu, Chang-Chi Lin, Yuan-Fan Chin, Tzong-Yuan Wu, Liang-In Lin, Zheng-Zong Lai, Szu-Cheng Kuo, and Yi-Jung Ho. 2016. 'Antiviral Activities of Niclosamide and Nitazoxanide against Chikungunya Virus Entry and Transmission'. *Antiviral Research* 135:81. doi: 10.1016/j.antiviral.2016.10.003.

155. Wang, Zhan, Junyi Ren, Jinxiu Du, Huan Wang, Jia Liu, and Guiling Wang. 2022. 'Niclosamide as a Promising Therapeutic Player in Human Cancer and Other Diseases'. *International Journal of Molecular Sciences* 23(24). doi: 10.3390/ijms232416116.

156. Watanabe, Yasunori, Joel D. Allen, Daniel Wrapp, Jason S. McLellan, and Max Crispin. 2020. 'Site-Specific Glycan Analysis of the SARS-CoV-2 Spike'. *Science (New York, N.y.)* 369(6501):330. doi: 10.1126/science.abb9983.

157. Weed, Darin J., and Anthony V. Nicola. 2017. 'Herpes Simplex Virus Membrane Fusion'. *Advances in Anatomy, Embryology, and Cell Biology* 223:29. doi: 10.1007/978-3-319-53168-7_2.

158. Wei C, Wan L, Yan Q, Wang X, Zhang J, Yang X, Zhang Y, Fan C, Li D, Deng Y, Sun J, Gong J, Yang X, Wang Y, Wang X, Li J, Yang H, Li H, Zhang Z, Wang R, Du P, Zong Y, Yin F, Zhang W, Wang N, Peng Y, Lin H, Feng J, Qin C, Chen W, Gao Q, Zhang R, Cao Y, and Zhong H. 2020. 'HDL-Scavenger Receptor B Type 1 Facilitates

SARS-CoV-2 Entry'. *Nature Metabolism* 2(12). doi: 10.1038/s42255-020-00324-0.

159. Wl, Wu, Chiang Cy, Lai Sc, Yu Cy, Huang Yl, Liao Hc, Liao Cl, Chen Hw, and Liu Sj. 2022. 'Monoclonal Antibody Targeting the Conserved Region of the SARS-CoV-2 Spike Protein to Overcome Viral Variants'. *JCI Insight* 7(8). doi: 10.1172/jci.insight.157597.

160. World healh Organisation (WHO) COVID19 Dashboard. n.d. 'Transmission of SARS-CoV-2: Implications for Infection Prevention Precautions'. Retrieved 13 September 2023 (https://www.who.int/news-room/commentaries/detail/transmission-of-sars-cov-2-implications-for-infection-prevention-precautions).

161. Wu, Aiping, Yousong Peng, Baoying Huang, Xiao Ding, Xianyue Wang, Peihua Niu, Jing Meng, Zhaozhong Zhu, Zheng Zhang, Jiangyuan Wang, Jie Sheng, Lijun Quan, Zanxian Xia, Wenjie Tan, Genhong Cheng, and Taijiao Jiang. 2020. 'Genome Composition and Divergence of the Novel Coronavirus (2019-nCoV) Originating in China'. *Cell Host & Microbe* 27(3):325. doi: 10.1016/j.chom.2020.02.001.

162. Wu, Bin, and Wei Guo. 2015. 'The Exocyst at a Glance'. *Journal of Cell Science* 128(16):2957. doi: 10.1242/jcs.156398.

163. Wu, Chang-Jer, Jia-Tsrong Jan, Chi-Min Chen, Hsing-Pang Hsieh, Der-Ren Hwang, Hwan-Wun Liu, Chiu-Yi Liu, Hui-Wen Huang, Su-Chin Chen, Cheng-Fong Hong, Ren-Kuo Lin, Yu-Sheng Chao, and John T. A. Hsu. 2004. 'Inhibition of Severe Acute Respiratory Syndrome Coronavirus Replication by Niclosamide'. *Antimicrobial Agents and Chemotherapy* 48(7):2693. doi: 10.1128/AAC.48.7.2693-2696.2004.

164. Wu, Fan, Su Zhao, Bin Yu, Yan-Mei Chen, Wen Wang, Zhi-Gang Song, Yi Hu, Zhao-Wu Tao, Jun-Hua Tian, Yuan-Yuan Pei, Ming-Li Yuan, Yu-Ling Zhang, Fa-Hui Dai, Yi Liu, Qi-Min Wang, Jiao-Jiao Zheng, Lin Xu, Edward C. Holmes, and Yong-Zhen Zhang. 2020. 'A New Coronavirus Associated with Human Respiratory Disease in China'. *Nature* 579(7798):265. doi: 10.1038/s41586-020-2008-3.

165. Wysocki, Jan, David I. Ortiz-Melo, Natalie K. Mattocks, Katherine Xu, Jessica Prescott, Karla Evora, Minghao Ye, Matthew A. Sparks, Syed K. Haque, Daniel Batlle, and Susan B. Gurley. 2014. 'ACE2 Deficiency Increases NADPH-mediated Oxidative Stress in the Kidney'. *Physiological Reports* 2(3). doi: 10.1002/phy2.264.

166. Xiao, Fengxia, Joseph Zimpelmann, Samih Agaybi, Susan B. Gurley, Lawrence Puente, and Kevin D. Burns. 2014. 'Characterization of Angiotensin-Converting Enzyme 2 Ectodomain Shedding from Mouse Proximal Tubular Cells'. *PLoS ONE* 9(1).

doi: 10.1371/journal.pone.0085958.

167. Xiaomiao Zhang, Jian Zheng, Yunqi Yan, Zheng Ruan, Su Yijiang, Jin Wang, Haihua Huang, Yi Zhang, Wenjie Wang, Jinjue Gao, Yifan Chi, Xiaoqian Lu, and Zhenwei Liu. 2019. 'Angiotensin-Converting Enzyme 2 Regulates Autophagy in Acute Lung Injury through AMPK/mTOR Signaling'. *Archives of Biochemistry and Biophysics* 672. doi: 10.1016/j.abb.2019.07.026.

168. Xu, Jimin, Judith Berastegui-Cabrera, Marta Carretero-Ledesma, Haiying Chen, Yu Xue, Eric A. Wold, Jerónimo Pachón, Jia Zhou, and Javier Sánchez-Céspedes. 2021. 'Discovery of a Small Molecule Inhibitor of Human Adenovirus Capable of Preventing Escape from the Endosome'. *International Journal of Molecular Sciences* 22(4). doi: 10.3390/ijms22041617.

169. Xu, Jimin, Pei-Yong Shi, Hongmin Li, and Jia Zhou. 2020. 'Broad Spectrum Antiviral Agent Niclosamide and Its Therapeutic Potential'. *ACS Infectious Diseases* 6(5):909. doi: 10.1021/acsinfecdis.0c00052.

170. Xu, Zhe, Lei Shi, Yijin Wang, Jiyuan Zhang, Lei Huang, Chao Zhang, Shuhong Liu, Peng Zhao, Hongxia Liu, Li Zhu, Yanhong Tai, Changqing Bai, Tingting Gao, Jinwen Song, Peng Xia, Jinghui Dong, Jingmin Zhao, and Fu-Sheng Wang. 2020. 'Pathological Findings of COVID-19 Associated with Acute Respiratory Distress Syndrome'. *The Lancet. Respiratory Medicine* 8(4):420. doi: 10.1016/S2213-2600(20)30076-X.

171. Y, Liu, Zhang H, Men H, Du Y, Xiao Z, Zhang F, Huang D, Du X, Gamper N, and Zhang H. 2019. 'Volume-Regulated Cl- Current: Contributions of Distinct Cl- Channels and Localized Ca2+ Signals'. *American Journal of Physiology. Cell Physiology* 317(3). doi: 10.1152/ajpcell.00507.2018.

172. Yadati, Tulasi, Tom Houben, Albert Bitorina, and Ronit Shiri-Sverdlov. 2020. 'The Ins and Outs of Cathepsins: Physiological Function and Role in Disease Management'. *Cells* 9(7). doi: 10.3390/cells9071679.

173. Yang, Huanghe, Andrew Kim, Tovo David, Daniel Palmer, Taihao Jin, Jason Tien, Fen Huang, Tong Cheng, Shaun R. Coughlin, Yuh Nung Jan, and Lily Yeh Jan. 2012. 'TMEM16F Forms a Ca2+-Activated Cation Channel Required for Lipid Scrambling in Platelets during Blood Coagulation'. *Cell* 151(1):111–22. doi: 10.1016/j.cell.2012.07.036.

174. Yang, Quan, Jinyao Zhao, Dan Chen, and Yang Wang. 2021. 'E3 Ubiquitin

Ligases: Styles, Structures and Functions'. *Molecular Biomedicine* 2. doi: 10.1186/s43556-021-00043-2.

175. Yao, Hangping, Yutong Song, Yong Chen, Nanping Wu, Jialu Xu, Chujie Sun, Jiaxing Zhang, Tianhao Weng, Zheyuan Zhang, Zhigang Wu, Linfang Cheng, Danrong Shi, Xiangyun Lu, Jianlin Lei, Max Crispin, Yigong Shi, Lanjuan Li, and Sai Li. 2020. 'Molecular Architecture of the SARS-CoV-2 Virus'. *Cell* 183(3):730. doi: 10.1016/j.cell.2020.09.018.

176. Yaqin, Yaqin, Cai Chen, Junru Pan, Junfa Xu, Zhi-Guang Zhou, and Cong-Yi Wang. 2012. 'The Ubiquitin Proteasome Pathway (UPP) in the Regulation of Cell Cycle Control and DNA Damage Repair and Its Implication in Tumorigenesis'. *International Journal of Clinical and Experimental Pathology* 5(8):726.

177. Yavuz, Serap ŞİMŞEK, and İpek KOMŞUOĞLU Çelikyurt. 2021. 'An Update of Anti-Viral Treatment of COVID-19'. *Turkish Journal of Medical Sciences* 51(7):3372. doi: 10.3906/sag-2106-250.

178. Yd, Yang, Cho H, Koo Jy, Tak Mh, Cho Y, Shim Ws, Park Sp, Lee J, Lee B, Kim Bm, Raouf R, Shin Yk, and Oh U. 2008. 'TMEM16A Confers Receptor-Activated Calcium-Dependent Chloride Conductance'. *Nature* 455(7217). doi: 10.1038/nature07313.

179. Yeung, Man Lung, Jade Lee Lee Teng, Lilong Jia, Chaoyu Zhang, Chengxi Huang, Jian-Piao Cai, Runhong Zhou, Kwok-Hung Chan, Hanjun Zhao, Lin Zhu, Kam-Leung Siu, Sin-Yee Fung, Susan Yung, Tak Mao Chan, Kelvin Kai-Wang To, Jasper Fuk-Woo Chan, Zongwei Cai, Susanna Kar Pui Lau, Zhiwei Chen, Dong-Yan Jin, Patrick Chiu Yat Woo, and Kwok-Yung Yuen. 2021. 'Soluble ACE2-Mediated Cell Entry of SARS-CoV-2 via Interaction with Proteins Related to the Renin-Angiotensin System'. *Cell* 184(8):2212. doi: 10.1016/j.cell.2021.02.053.

180. Yim, Willa Wen-You, and Noboru Mizushima. 2020. 'Lysosome Biology in Autophagy'. *Cell Discovery* 6(1):1–12. doi: 10.1038/s41421-020-0141-7.

181. Yu, Kuai, Tao Jiang, YuanYuan Cui, Emad Tajkhorshid, and H. Criss Hartzell. 2019. 'A Network of Phosphatidylinositol 4,5-Bisphosphate Binding Sites Regulates Gating of the Ca2+-Activated Cl– Channel ANO1 (TMEM16A)'. *Proceedings of the National Academy of Sciences of the United States of America* 116(40):19952. doi: 10.1073/pnas.1904012116.

182. Zhai, Yujia, Fei Sun, Xuemei Li, Hai Pang, Xiaoling Xu, Mark Bartlam, and Zihe

Rao. 2005. ‘Insights into SARS-CoV Transcription and Replication from the Structure of the Nsp7–Nsp8 Hexadecamer’. *Nature Structural & Molecular Biology* 12(11):980. doi: 10.1038/nsmb999.

183. Zhang, Jialin, Wenyu Yang, Sawrab Roy, Heidi Liu, R. Michael Roberts, Liping Wang, Lei Shi, and Wenjun Ma. 2023. ‘Tight Junction Protein Occludin Is an Internalization Factor for SARS-CoV-2 Infection and Mediates Virus Cell-to-Cell Transmission’. *Proceedings of the National Academy of Sciences* 120(17):e2218623120. doi: 10.1073/pnas.2218623120.

184. Zhang, Ling, Li Zhou, Linlin Bao, Jiangning Liu, Hua Zhu, Qi Lv, Ruixue Liu, Wei Chen, Wei Tong, Qiang Wei, Yanfeng Xu, Wei Deng, Hong Gao, Jing Xue, Zhiqi Song, Pin Yu, Yunlin Han, Yu Zhang, Xiuping Sun, Xuan Yu, and Chuan Qin. 2021. ‘SARS-CoV-2 Crosses the Blood–Brain Barrier Accompanied with Basement Membrane Disruption without Tight Junctions Alteration’. *Signal Transduction and Targeted Therapy* 6(1):1–12. doi: 10.1038/s41392-021-00719-9.

185. Zhang, Lizhou, Cody B. Jackson, Huihui Mou, Amrita Ojha, Haiyong Peng, Brian D. Quinlan, Erumbi S. Rangarajan, Andi Pan, Abigail Vanderheiden, Mehul S. Suthar, Wenhui Li, Tina Izard, Christoph Rader, Michael Farzan, and Hyeryun Choe. 2020. ‘SARS-CoV-2 Spike-Protein D614G Mutation Increases Virion Spike Density and Infectivity’. *Nature Communications* 11(1):1–9. doi: 10.1038/s41467-020-19808-4.

186. Zhang, Yuanyuan, Renhong Yan, and Qiang Zhou. 2022. ‘ACE2, B0AT1, and SARS-CoV-2 Spike Protein: Structural and Functional Implications’. *Current Opinion in Structural Biology* 74:102388. doi: 10.1016/j.sbi.2022.102388.

187. Zz, Shi, Shang L, Jiang Yy, Hao Jj, Zhang Y, Zhang Tt, Lin Dc, Liu Sg, Wang Bs, Gong T, Zhan Qm, and Wang Mr. 2013. ‘Consistent and Differential Genetic Aberrations between Esophageal Dysplasia and Squamous Cell Carcinoma Detected by Array Comparative Genomic Hybridization’. *Clinical Cancer Research : An Official Journal of the American Association for Cancer Research* 19(21). doi: 10.1158/1078-0432.CCR-12-3753.